Article type: Progress Report

Title: Self-assembled α-cyanostilbenes for advanced functional materials

*Marta Martínez-Abadía, Raquel Giménez [*] and M. Blanca Ros **

Dr. M. Martínez-Abadía,[a] Dr. Raquel Giménez, Prof. M. Blanca Ros
Instituto de Ciencia de Materiales de Aragón (ICMA), Departamento de Química Orgánica - Facultad de Ciencias, Universidad de Zaragoza - CSIC, 50009 Zaragoza, Spain.
E-mail: rgimenez@unizar.es, bros@unizar.es
[a] Current address: POLYMAT, University of the Basque Country UPV/EHU. Avenida de Tolosa 72, E-20018 Donostia-San Sebastian, Spain

Keywords: aggregation-induced emission, self-assembly, liquid crystals, nanoaggregates, gels

Abstract

In the specific context of condensed media, the significant and increasing recent interest in the α-cyanostilbene (CS) motif [–Ar–CH=C(CN)–Ar–] is relevant. These compounds have shown remarkable optical features in addition to interesting electrical properties, and hence they are recognized as very suitable and versatile options for the development of functional materials. This progress report is focused on current and future use of CS structures and molecular assemblies with the aim of exploring and developing for the next generations of functional materials. A critical selection of illustrative materials that contain the CS motif, including relevant sub-families such as the dicyanodistyrylbenzene (DCS) and 2,3,3-triphenylacrylonitrile (TPAN) shows how, driven by the self-assembly of CS blocks, a variety of properties, effects and possibilities for practical applications can be offered to the scientific community, through different rational routes for the elaboration of advanced materials. A survey is provided on the research efforts directed towards promoting the self-assembly of the solid state (polycrystalline solids, thin films and single crystals), liquid crystals, nanostructures and gels with multi-stimuli responsiveness, and applications for sensors, OLED, OFET, solar cell materials or bioimaging purposes.

1. Introduction

Functional organic materials now constitute an extremely active and breakthrough research area in which numerous proposals, achievements and challenges are converging and inspiring the best interdisciplinarity specialists in all aspects of materials science, including chemistry, physics, engineering, biology and nanotechnology. In these projects π-conjugated materials are widely used due to their structural diversity and unique optical and photophysical properties, which are intensified to achieve multiresponse systems. In particular, organic luminophores have shown great potential for applications in hot areas such as organic optoelectronic/photonic devices, sensors, photoswitches or bioimaging.[1]

In condensed media, many efficient π-conjugated luminophores suffer from a pronounced weakening of their luminescence, known as aggregation (or concentration) quenching,[2] and this limits their applications. In contrast, some compounds with specific structures are luminescent in the condensed phase or at high concentrations due to favorable effects that occur in the solid state.[3] From the broad variety of organic structures proposed and tested as luminescent platforms in condensed media, it is worth highlighting the significant recent interest in the α-cyanostilbene (CS) motif [–Ar–CH=C(CN)–Ar–] (Figure 1). These compounds have shown remarkable optical features in addition to interesting electrical properties, and hence they are recognized as a very suitable and versatile options for the development of functional materials. Interesting reviews dedicated to highlight relevant properties of CS have been published,[4] in addition it has been cited in recent work covering luminescent materials,[5] and this has fostered a large number of further studies and applications.

The aim of this progress report is to highlight well-stated and attractive recent results on CS-based supramolecular functional and smart materials as well as to stimulate further research activity in this area. This analysis will focus on representative self-assembled functional materials that contain the α-cyanostilbene (CS) backbone, with attention also paid to relevant

sub-families such as the dicyanodistyrylbenzenes (DCS), which consist of symmetrical 'outer' or 'inner' dicyano-substitution in the vinylene units, and the 2,3,3-triphenylacrylonitrile (TPAN) moiety (Figure 1). We will consider a critical selection of illustrative examples that show how, driven by the self-assembly of CS blocks, a variety of properties, effects and more importantly possibilities for practical applications can be offered to the scientific community, with different rational routes for the development of advanced functional materials. The general considerations on structural aspects, properties and phenomena, which commonly characterize CS-containing materials, will be discussed first. Our survey will then cover research efforts directed towards promoting the self-assembly of the key structural units covered in this report, namely the solid state, dealing with polycrystalline solids, thin films and single crystals, liquid crystals, nanostructures and gels with multi-stimuli responsiveness, and applications for sensors, organic light-emitting diodes (OLEDs), organic field effect transistors (OFETs), solar cell materials or bioimaging applications. The conclusion of the work will consider some assumptions and personal perspectives on the future judicious use of CS structures to explore and develop technological and biological applications for the next generations of functional materials.

2. General considerations

CS is of interest as a building block for functional materials due to several features. One advantage of CS materials is their straightforward synthesis. The preparation usually requires a benzaldehyde and an acetonitrile precursor, both of which are readily accessible chemical synthons. Moreover, the CS structure is tunable by substitution in either the aromatic rings or the double bond, thus allowing a wide variety of structural designs.

As far as molecular materials are concerned, the optical properties of CS in solution derive from their chemical structure. The absorption and emission spectra, optical bandgap, radiative rates and other photophysical parameters can be modulated by extension of the π-conjugated

structure, the electronic character of the functional groups, and steric factors that determine the planarity and effective conjugation length. The cyano group has steric effects on the stilbene backbone and isolated molecules in dilute solution are significantly non-planar with a low rotational energy barrier. The majority of CS compounds have low photoluminescent (PL) quantum yields (QY) in liquid solution due to high non-radiative rates, which are a consequence of torsionally induced deactivation processes. Moreover, as the cyano group has electron-withdrawing character, its combination with donor moieties has led to donor-aceptor (D-A) molecules with intramolecular charge transfer (ICT) behavior.[4b, 6]

In condensed media, the optical and photophysical properties are usually different from those in solution due to intermolecular interactions that affect the conformation and relative arrangement of the molecules and to restrictions imposed by the solid state, such as high viscosity or inhomogeneities. As a consequence, intermolecular coupling of electronic transition dipole moments (excitonic coupling), reduction of torsionally induced non-radiative deactivation processes, and migration of excitation energy to distortions or impurity traps can all occur. The consequence is that the PL wavelength and QY in the solid state are a balance of numerous factors and they are difficult to predict. In this respect, the work of Park and Gierschner revealed some structure/property relationships for CS (in particular for the DCS family) based on the correlation of molecular structure, packing arrangements from single crystal structural data and the resulting optical and photophysical properties.[4b] Arrangements such as herringbone or stacks with different degrees of π-overlap have been observed in the crystal structures, and these have been related to photophysical data from relaxed excitons (structured emission) or excimer emission (red-shifted and unstructured).

In this respect, CS has yielded fascinating luminescent properties in solid state, as they can show aggregation-induced enhanced emission (AIEE) or aggregation induced emission (AIE), yielding materials with high applicability in their condensed states as they circumvent the unfavorable aggregation (or concentration) caused quenching (ACQ). Although both, AIEE

and AIE, refer to the increased emission in the assembled state, they must be distinguished by the exciton coupling feature. The AIEE phenomenon, as defined by Park and coworkers and found in CS materials,[4a, 7] is the synergistic combination of aggregation-induced planarization and specific favorable intermolecular interactions (such as *J*-aggregation) that allow the emission enhancement. Apart from that, some bulky CS molecules, e.g. TPAN derivatives, belong to the class of materials named by Tang and coworkers as "AIEgens" (compounds with aggregation induced emission (AIE) properties), as authors propose that solid-state PL enhancement is only derived from restricted intramolecular rotational motion (RIR).[5g, 8]

As a further complication, organic materials have a soft nature due to the kinds of intermolecular interactions (supramolecular weak interactions such as H-bonding, π-stacking, van der Waals forces or other secondary interactions), so CS materials may have several types of molecular packing (crystalline polymorphs, liquid crystal phases, nanoaggregates with diverse morphologies), thus leading to a complex scenario in which each arrangement exhibits different optical properties. This means that the photophysical properties of different CS self-assemblies could be tuned in response to a variety of external stimuli, such as heat, light, pressure, solvents, pH or ions. Besides, CS shows photochemical activity and it can undergo *Z/E* isomerization of the double carbon-carbon bond or [2+2]-cycloaddition reactions, which lead to photoproducts that change the composition of the material. The investigation of this photoreactivity and the associated changes in properties has evolved into an interesting topic for the development of novel photoswitchable systems,[9] as discussed in this report.

3. Solid-state: Polycrystalline powders, single crystals and thin films

Tailored molecular structures derived from the CS backbone have generated interesting functionality, mainly due to their high solid-state PL. In the following sections, attention will be paid to this relevant property in several solid matter systems: polycrystalline powders,

single crystals and thin films. Studies are mainly focused on responsive emission switching under several stimuli in the powder, single crystals for laser emission, or nanometer-thick thin films for emissive layers in organic light-emitting diode (OLED) devices. In addition, non-luminescent properties such as interesting electronic properties for charge transport for organic field effect transistor (OFET) devices or solar cells have been identified. It is intended to analyze the main studies undertaken on CS-based materials in these three different systems in an effort to shed some light on their real possibilities for applications. This section is organized with the aim of grouping the studies by molecular design and, where possible, by highlighting the supramolecular organizations or mechanisms that underly a given property.

3.1. Polycrystalline powders

Polycrystalline powders of CS-based small molecules are easily obtained from pristine samples and they show interesting fluorescence properties that respond to several stimuli, such as crystallization condition, temperature, pressure, light, solvents, etc., and provide a reversible multi-stimuli response. Potential applications, such as in sensors, displays, or optical storage, have been envisaged. The required properties for optimum performance are high solid-state PLQY, emission dependence on molecular arrangements, and the possibility of altering the molecular packing with high contrast color change. All of these properties can be achieved with CS compounds due to their efficient emission in solid state (QY up to almost unity has been reported) and the twist elasticity in their crystal arrangements. This allows the easy disturbance of the initial solid-state structure and leads to a change in fluorescence.

The first report on stimuli-responsive PL was published by Weder's group in 2002. They observed changes in the excimer emission of methoxy-substituted DCSs by heating, by varying concentration[10] or by deformation in polymer films.[11] In 2008 the same group reported a reversible color change with rod-like DCSs terminated with long alkoxy terminal

tails[12] (**C18-YB** and **C12-YB**) (Figure 2A). These molecules in powder showed blue fluorescence and this is consistent with a solid state without excimer emission. Moreover, at RT this phase could be transformed by grinding or pressing into another crystalline polymorph that emitted in green. The pressed materials were stable over time, but the change was reversible, with **C18-YB** converted from green to blue upon heating at 130 °C. Powder X-ray diffraction (PXRD) data confirmed a partial transformation between two different crystalline forms, with the pressed form dominated by excimer emission.

Since that time, the number of reports on CS-based compounds whose PL properties in powder samples can be changed mechanically has grown considerably and this is a subject of increasing interest.[5f, 5h, 13] The general term mechanofluorochromism (MCF) is adopted in this progress report to denote the property in which fluorescence color can be transformed upon grinding, shearing or pressing. In CS MCF materials a reversible color change is commonly observed and recovery is achieved by thermal annealing, vapor fuming or high pressure release (particularly referred to mechanoresponsive luminescent materials). In addition to color change, off/on luminescence switching by mechanical input has also been obtained.

In this respect, DCS compounds with alkoxy[14] or thiomethyl[15] terminal substituents similar to Weder's compounds also showed an emission change under pressure or upon grinding, and these revert when heating is applied. However, a different behavior was evident depending on the position of the CN groups in the structure (symmetrically inner or outer substitution) due to the influence of the conjugation length and solid-state packing. Park and co-workers reported an interesting study on an inner cyano-substituted compound with butyloxy terminal groups **DBDCS** (Figure 2B) and they identified AIEE behavior and two polymorphs that emit in blue (B) or green (G).[14a] Photophysical data together with analysis of the single crystal structure of the green polymorph (G) allowed the phase transition pathways and their spectroscopic implications to be elucidated. In the crystal structure of the G-phase the

molecule was in a planar conformation and formed sheets with intermolecular CH…N and CH…O secondary interactions. Antiparallel coupling of the local dipoles kinetically stabilizes a structure with rather moderate excitonic coupling but efficient excimer formation. The change to the B-phase, which is more thermodynamically stable, was proposed to comprise a smooth slip of the molecular sheets to give a head-to-tail arrangement of the local dipoles. In this arrangement the excimer formation is diminished, while excitonic interactions increase substantially. This change between supramolecular structures is easily obtained by annealing (G to B), pressing (B to G), and vapor fuming (B to G), which serve in combination to provide a rewritable fluorescent optical recording medium. The analogous compound without substituents, **BDCS**, shows similar behavior but with a unidirectional blue-to-green transformation upon heating or grinding,[16] but a reversible change under a critical pressure.[17] These phenomena are also reported to arise from the molecules adjusting from a twisted conformation to a more compact planar conformation.

Interestingly, while alkoxy-DCS with additional 2,5-dimethoxy-substitution in the central aromatic ring do not give MCF properties,[12] multicolor luminescence has been achieved by terminating the alkoxy chains with aromatic groups such as tolyloxy or phenoxy, which play an important role in the supramolecular organizations. Terminal tolyloxy units make the material crystallize in four polymorphs with different emission spectra (green, yellow, orange, and red-orange polycrystalline powders) (Figure 2C). In the crystalline structure of the orange polymorph the tolyl groups interdigitate with the DCS moiety. All polymorphs can be converted to a largely amorphous state with orange emission by mechanical grinding, thus giving five different emissive states.[18] It was discovered that the presence of phenoxy substitution allowed MCF to be temperature-dependent as it shows a yellow to reddish-orange change at RT and a yellow to yellowish-green change at 100 °C.[19] The behavior at ambient temperature is caused by a mechanically induced phase transition from a crystalline to an amorphous solid in which the dye molecules form excimers, whereas at elevated temperature

the blue-shift is ascribed to a crystal-crystal phase transition. More recently, with the aim of translating MCF to self-supported objects that can be moulded into various shapes, terminal ureido-4-pyrimidone groups have been used to form novel hydrogen-bonded supramolecular polymers (Figure 2D) with multicolor thermo- and mechanoresponsive properties.[20]

Another class of stimuli-responsive CS are those substituted with CF_3 groups. The CF_3 moiety is known to produce tightly packed structures due to the formation of specific intermolecular interactions such as C–F…H and C–F…π, thus adding to the π-stacking of the aromatic part and dipolar interactions introduced by the CN group.[21] As a consequence, unique behaviors have been found such as the induction of fluorescence blue-shift upon application of mechanical force[22] (contrary to the usual red-shift behavior) or the development of materials with fluorescence off/on switching by shearing.[23]

Park *et al*. discovered a fluorescent turn-on with asymmetrically CF_3-substituted compounds in which a close antiparallel π-stacking of molecules was promoted. The molecule **CN(L)-TrFMBE** (Figure 3A) did not show luminescence either in solution or as a crystalline powder but it became highly blue emissive under UV light irradiation or mechanical shearing [23a] due to a lateral displacement of the molecules either by mechanical or light stimuli, which distort the tight π-stacking. Irradiation with light was effective because the molecules were topologically situated to favor a photochemical reaction known as a [2+2]-cycloaddition. The expanded volume of the photoproduct formed, i.e., a sigma-dimer, produced an 'internal shear' that displaced adjacent molecules and distorted their packing, thus resulting in enhanced fluorescence emission at the cost of frustrated cycloadditions. The process was reversible as the sigma-dimers could be broken by heating, thus restoring the tight packing and consequently the non-fluorescent state.

A different mechanism to obtain off-on luminescence switching was elegantly achieved by controlling mechanically the rate of electron transfer in a donor-acceptor-donor triad.[23b] In

this case, a CF_3-substituted DCS, which has acceptor character, was bound to two carbazole units *via* a flexible spacer to give the molecule **m-BHDCS** (Figure 3B). The thermodynamically stable crystal phase led to a charge transfer state that was not fluorescent (QY = 7×10^{-5}), but grinding destroyed the packing and led to a metastable amorphous phase with orange-red emission at 600 nm (QY = 0.09). Annealing or vapor fuming recovered the off state, so a rewritable medium with a high contrast ratio and high stability over time was fabricated. The incorporation of a nitrogen atom in the carbazole unit (harmane unit) (Figure 3C) gave the triad **m-BHHDCS**, which has additional acidochromic properties that work in an orthogonal fashion, thus providing a material that could distinguish two different signals in both the writing and reading processes.[23c]

Terminal halogen substitution has also been studied with varied success. CS with fluoro substitution and phenothiazine luminescent units show MCF properties[24] with red-shifted emission whereas other halogen groups (Cl, Br) did not give rise to this property. Two isomeric C_3-symmetric molecules with a bromo terminal group (Figure 3D) were found to exhibit MCF, whereas unsubstituted compounds did not show this behavior.[25] Upon grinding, the isomer with inner CN groups, **α-BPAN-Br**, exhibited substantial quenching of bluish green emission, which represents a case of fluorescence turn-off, while the one with CN groups in the outer position, **β-BPAN-Br**, showed a color change from bluish green to deep blue. This behavior was ascribed to transitions between ordered and disordered phases enabled by the weak intermolecular interactions and the different degrees of molecular torsion, which were calculated to be higher in the former compound. The initial emission of each molecule was restored by exposure to an organic solvent vapor.

Another series of molecules that warrant special attention in this survey due to their stimuli-responsive properties are those where CS is conjugated to tri- or diphenylamine (BPA or TPA) groups. As CS has electron-acceptor character and BPA or DPA are well-known donor moieties, the molecules may exhibit donor-acceptor characteristics (push-pull effect,

eventually generating low-lying intramolecular charge transfer (ICT) states). In addition, the bulky and non-planar shape of the BPA and TPA facilitate phase transformations that usually occur in MCF materials. Zhang's group has explored some basic structures,[26] among which only **α-CN-TPA** (Figure 4A) with CN groups near the diphenylamine unit is able to switch from almost no fluorescence in the blue region to sky-blue as consequence of crystal-crystal transitions. The isomeric molecule (**β-CN-TPA**) did not show MCF properties on grinding as the original solid was not disturbed. However, hydrostatic pressure caused a gradual green to red variation of up to 135 nm due to the forced increase in intermolecular interactions, as observed by Raman spectroscopy (Figure 4B).[27] On the other hand, structural variation of the conjugated core by changing to a CN group in the terminal position (**pCN-TPA**) increases the donor/acceptor character of the molecule and leads to clear ICT properties in solution. In this case multicolored fluorescence switching from green to red, with a huge 111 nm variation while keeping the variation of the QY small (from 0.46 to 0.32), was observed under simple grinding or under hydrostatic pressure (Figure 4C). During the process a gradual change from crystal to amorphous took place and this was accompanied by a transformation of the emissive states from the local excited state to the red-shifted ICT state.[28] Among all the TPA-containing molecules, interesting multifunctional materials were obtained by a design strategy that relied on a cruciform, i.e., rigid X-shaped molecules with donors and acceptors situated on two crossed axes. The new molecules showed high QY in powder and the values were higher than those in solution. The emission of the original powder originated from the molecules with a twisted geometry. A sharp color change under mechanical stimuli from yellow to green-yellow to reddish-orange both in absorption and emission was observed for **DCS-TPA** (with emission shifts up to 70 nm) (Figure 4D). In this case, although some amorphization occurred after grinding the semicrystalline powder, a phase transformation was probably not responsible for such a noticeable change but rather a conformational change of the molecule from a twisted geometry to a planar conformation, which allowed the extension

of conjugation and enhancement of ICT.[29] In addition, as TPA is an electroactive unit, electrochromic films with multiple colors (green, red, gray and blue) and high contrast were prepared by electrochemical deposition on ITO electrodes. Carbazole-terminated DCS is another conjugated D-A-D molecule that was reported to show a reversible color change from green to yellow under a grinding/fuming or grinding/annealing cycle. Interestingly, the green single crystal could sense external pressure from 1 atm to 9.21 GPa accompanied by color changes from green to red with high reversibility and reproducibility.[30]

The AIE concept, as named by Tang,[5g] has been implemented in CS materials through the triphenylacrylonitrile (TPAN) unit (Figure 1). TPAN has in the solid state a propeller or twisted conformation that impedes close stacking and this helps to prevent detrimental excimer emission. Possible additional CH…π interactions help to rigidify their non-planar structures, which in turn decreases non-radiative rates and leads to QY emission in solid state. Moreover, these void-like structures are deformable and tend to give easy distortion, which makes them interesting candidates for stimuli-responsive materials. In fact TPAN molecules can exhibit rich behavior such as polymorphism and multi-stimuli fluorescence switching by thermal, mechanical, or vapor stimuli.[31] A modular analysis proved useful to analyze and interpret the complex structure/luminescence relationship in highly twisted TPAN conjugated molecules in which polymorphism is due to slight differences in molecular torsional angles and sparse π-stackings.[32] The combination of propeller-like TPAN with bulky DPA donors gave rise to D-A molecules with efficient emission in the powder and high contrast MCF. Zhang's group has been prolific in synthesizing this class of AIE-ICT dyes,[33] which can show quantum yields up to 100% in the as-obtained powder form – a value that is rarely found in D-A molecules. The powders of **TPATPAN** showed MCF with high contrast, changing from blue to yellow (up to 78 nm) and then reverting upon heating or solvent fuming (Figure 4E).[33a] The proposed mechanism is an induced molecular planarization by mechanical force that increased the conjugation length and produced a red-shift in the

emission. More recently, the **TPATPAN** molecule has been combined with a rhodamine B derivative to form a binary blend in solid state that shows three color switching (blue-yellow-red) under 365 nm irradiation by grinding (Figure 4F).[34] In contrast, more extended conjugated molecules with TPAN and arylamine in an A-D-D-A configuration (**BPA2TPAN** or **PNA2TPAN**) [35] show poorer properties. These compounds are yellow or yellowish-orange powders with high thermal stability but with lower QY (around 0.47) and MCF change arising from a crystal-to-amorphous change with lower contrast to an orange color proposed to come from excimer emission. The acceptor TPAN has also been conjugated with donor N-alkylcarbazole in different structural designs.[36] Architectures such as **Cz1TPAN**[36b] (Figure 4G) give powders with QY values as high as 0.75 and reversible green to yellow MCF with the same characteristics as other ICT-AIE dyes. The crystalline network collapses under mechanical stimulus to give an amorphous phase in which it is assumed that some interactions are destroyed and molecules are forced to adopt a less twisted conformation, thus increasing the ICT that produces the red-shifted emission. Similar combinations with donor N-phenylcarbazole[37] or pyrenoimidazole (a sterically hindered pyrene that overcomes its tendency to π-stacking)[38] yielded powders with reversible MCF from blue to green.

Following the same strategy for the design of molecules with twisted conformations to allow crystal structures with loose packing that is slideable by mechanical force to give amorphization, the basic CS unit has recently been combined with other bulky groups such as tetraphenylvinyl[39] or tetraphenylimidazole.[40] These compounds also show dual fluorescence switching as powders by mechanical force or vapor fuming.

In conclusion, CSs give excellent performance as fluorescent materials in powder form. A full color range and multicolor luminescence variation has been achieved with high QY and high contrast color changes by mechanical input due to the easy perturbation of their molecular arrangements. A crystal-to-crystal transformation or an amorphization process accounted for the MCF property of the as-obtained polycrystalline powders. In rod-like dyes (‘basic’ CS or

DCS family) the polar cyano group (dipole moment 3.75 D) plays an important role in organizing the molecules as supramolecular stacking architectures with different degrees of local dipole coupling. As a consequence, luminescence variations are related to changes in excimer/exciton coupling. In D-A bulky dyes or TPAN-derived molecules the mechanical stimulus usually brings a conformational change that leads to ICT enhancement.

Future interesting work would include the structural design of novel AIE-ICT dyes that combine high QY and predictable color variation in order to prepare 'materials on demand' for sensory applications that do not require a complex processing, i.e., from the as-synthesized powder state.

3.2. Single crystals

High quality single crystals have been obtained with compounds of the DCS family. The crystals exhibit higher QY than the powder form due to low trap concentrations, a characteristic that makes crystals potential candidates for spectrally narrowed emission behavior such as amplified spontaneous emission (ASE) and/or laser emission (LE) (Table 1). The first reports on ASE were carried out on the phenyl-substituted DCS, **CN-DPDSB**, which could be crystallized to give high-quality crystals with blue emission and a QY of 0.8, in contrast to the low efficiency found in solution.[41] ASE at 470 nm with very low threshold values was reported.[42] In addition, the crystal showed well-balanced bipolar carrier-transport characteristics that make it a promising candidate for organic laser diodes.[43]

Ma's group studied single crystals of 'naked DCS' with CN groups in the outer position, **CN-DSB**, and reported green electroluminescence,[44] ASE with a low threshold [45], waveguiding and very high and balanced ambipolar transport, which is of great importance for organic light-emitting transistor (OLET) devices.[46] Interestingly, these authors deduced that the presence of the electronegative CN groups favors the formation of high quality tubular crystals that consist of molecular sheets stabilized through CN..H and organized by CH…π

interactions to give a herringbone arrangement without detrimental π-stacks. Moreover, the authors observed that the CN group interacts with Au electrodes in OFET devices, which is beneficial for charge mobility. The same group prepared single crystals of DCS flanked with bulky DPA end-groups such as **CNDPASDB**. This material shows a self-organized uniaxial orientation of the molecules with strong polarized self-waveguided emission in the yellow region and ASE with low thresholds.[47] In addition, **CNDPASDB** showed two-photon absorption properties that were used for excitation with 800 nm light for up-conversion lasers.[48] The analog **TPCNDSB** with the same terminal substitution also showed substantial two-photon absorption properties and this allowed ASE under one-photon and two-photon excitation for single crystals.[49]

Park and Gierschner's group explored the stimulated emission properties of highly emissive crystals of alkoxy-substituted DCSs with different substitution patterns to provide wide-range color tuning.[50] Only packings with low π-overlap show spontaneous or stimulated emission narrowing, such as **α-MODCS**, which has a *J*-type packing arrangement and showed emission at 495 nm with a QY of 0.66, or **β-DBDCS**, which arranges in a weak *H*-type aggregation that shows emission at 490 nm with a QY of 0.84. **β-DBDCS** showed ASE in crystalline films and lasing oscillations in thermally evaporated platelet-like single crystals. Laser emission at 482 nm was collected from the crystal edge when optically pumped along the longest side, with a threshold value that was comparable to the lowest reported in molecular crystals to date. In another significant study the dialkylamino-terminated molecule **DBADCS** was crystallized in elongated platelet single crystals with a high QY of 0.69 and *J*-aggregation. ASE and random lasing were obtained upon excitation at 355 nm, whereas excitation at 532 nm gave a single-mode stimulated emission at 581 nm. This behavior was attributed to stimulated resonance Raman scattering (SRRS) of the vibration mode at 1567 cm^{-1} corresponding to the in-plane stretch of vinylene units.[51] In addition, a combination of

2,5-dimethoxy-substituents in the central DCS-structure with dialkylamino terminal tails provided a D-A-D-A-D motif that is a viable strategy to produce a red-shifted fluorescence in order to achieve bright solid-sate deep red/near IR emission.[52]

Interestingly, CF_3 substitution was beneficial for crystal processing. A compound substituted with four electron-defficient CF_3 groups, **CN-TFPA**, had two polymorphs with different emissions (blue or green) and only the blue one exhibited ASE in a crystalline film, but single crystals of suitable size for study could not be obtained.[53] In addition, the blue phase could be grown with a dense and well-ordered terrace structure by a simple solution process, which allowed the fabrication of OFET devices with electron mobilities up to 0.55 $cm^2\ V^{-1}\ s^{-1}$.[54] This compound cocrystallized with a tetramethyl-substituted distyrylbenzene, **4M-DSB**, to form a D-A system with the unusual property of showing a charge transfer band with high luminescence due to a combination of factors (high oscillator strength, dense packing that yielded low internal conversion and good quality crystals with low exciton trapping).[55] Single crystal OFETs prepared by a solvent vapor annealing process showed ambipolar transport, with average mobilities along the long crystal axis of $4.3 \times 10^{-3}\ cm^2\ V^{-1}\ s^{-1}$ and $5.4 \times 10^{-2}\ cm^2\ V^{-1}\ s^{-1}$ for hole and electron mobility, respectively.[56a] More recently, a new 2:1 donor (D):acceptor (A) mixed-stacked charge-transfer (CT) cocrystal comprising isometrically structured dicyanodistyrylbenzene-based D and A molecules have shown balanced ambipolar charge transport and interesting OLET performance.[56b] Besides, a CF_3-substituted compound with thiophene rings, **Me-4-TFPTA**, formed a single crystalline nanosheet with one of the highest electron mobility values of all n-type semiconducting materials ($7.8\ cm^{-1}\ V^{-1}\ s^{-1}$) that was stable at room temperature. The processing conditions proved crucial to obtain such high values, as solvated nanosheets showed electron mobilities two orders of magnitude higher than non-solvated 1D structures. [57] In other set of studies Joo's group reported optical waveguiding in single crystalline microplates of similar DCS

compounds with CF_3 groups and additional bromo-substituents and they identified waveguiding of various Raman modes.[58]

In conclusion, single crystals of DCSs with high luminescence efficiency and high quality have been reported and they show great potential as the gain medium for solid state lasers under one-photon and two-photon excitation (up-conversion lasers) and promise for electrically pumped lasers due to their excellent charge carrier mobilities. Nevertheless, to obtain packings with little π-overlap is crucial for the occurrence of stimulated emission. Finally, it is worth mentioning the easy processing of CF_3-substituted DCS crystals with very high charge mobilities for OFET devices.

3.3. Thin films

A wide variety of CS-based compounds have been processed as thin films either in neat form, in blends with other functional matrices, or mixed with inert polymers for a variety of applications. Among them, remarkable results have been reported for films with multicolored emission and color switching for optical storage based on their known stimuli-responsive properties.[11, 14a, 23c, 59] Extensive work has been carried out on optoelectronic applications such as OLEDs, solar cells (either dye-sensitized solar cells, DSSCs, or bulk-heterojunction, BHJ) and OFETs, which are reviewed below.

CS-based materials have been widely used as the emitting layer in PLED/OLED devices due to their electroluminescence. Either vapor deposition techniques (usually for small molecules) or spin-coating from solvents (mainly for polymers) provide the required good quality nanometer-thin film for these devices, which generally show high fluorescent QY and electroluminescence with similar characteristics. Since the discovery of electroluminescence in the conjugated polymer poly(*p*-phenylenevinylene) (**PPV**),[60] structural variations consisting of the attachment of electron-withdrawing cyano groups onto the vinylene linker (**CN-PPV**) have been studied. These changes resulted in red-shifted emission and higher

electron affinity, thus allowing the use of cathode metals with higher work function and improved stability of the devices. In fact, **CN-PPV** showed a red color emission with high efficiency (4%).[61] Since then, a broad range of **CN-PPV** derivatives have been synthesized. Particular attention should be paid to the preparation of well-defined oligomers with the aim of gaining a better understanding of the physical properties in relation to structural variations and to relate structural aspects of the solid state, such as molecular conformation and packing, with the photophysical properties of the film.[10, 62] As an example, the electronic properties of CS-based conjugated polymers were tuned by copolymerization of cyanostilbene segments with benzene, fluorene or binaphthyl units[63] that reduce the effective conjugation length and stacking. These copolymers were blue-emitting materials and their emission in thin films was narrow and only red-shifted by 6–11 nm in comparison with their fluorescence in solution. Non-optimized devices with the fluorene polymer showed an external quantum efficiency (EQE) of 0.2% in an ambient atmosphere in double layer configuration prepared by spin-coating. Several recent reports on CS-polymeric materials have focused on white electroluminescence (WOLED). Dalimba *et al*.[64] reported white electroluminescence with CIE coordinate values (0.32, 0.35) very close to those of white light (0.33, 0.33) for a conjugated polymer containing 3,4-didodecyloxythiophene donor units and 1,3,4-oxadiazole modified by CS units as the electron-acceptor. The CS moiety lowers the LUMO level and enhances the charge transfer along the polymer chain, thus reducing the bandgap energy of the polymer and the threshold operating voltage of the device. The electroluminescence spectra were broad, with maxima at 514 nm and a white color at a driving voltage of 14 V. Another way to achieve white emission is to combine blue and yellow/orange emitting materials. In this respect, one strategy has involved the coating of a blue LED with a yellow emitting poly(lactide) containing amino-DCS.[65] In a different study Somanathan *et al*. prepared several conjugated polymers based on the copolymerization of **FBTPAN** and 9,9-dihexylfluorene monomers at different feed ratios (Figure 5).[66] Thin films of copolymers

showed different fluorescence, with a gradual red-shift from blue to yellow observed on increasing the **FBPAN** feed ratio. This change was attributed to an energy transfer from the fluorene segments to the **FBPAN** moieties. Investigation of the supramolecular structures of the films showed different assemblies, which were 'flower-shaped' for the 0.5 composition and hollow spherical for feed ratios of 10, 25 and 50. The copolymer with the 0.5 composition showed bright white fluorescence with a QY as high as 0.80 and pure white electroluminescence with CIE coordinates (0.32, 0.31), which are very close to those of standard white light emission (0.33, 0.33).

Low molecular weight molecules/small oligomers that may allow good processability and improved OLED performance have been obtained on using thin films prepared by vacuum deposition. In this respect, a high thermal stability is recommended for processing at high temperatures in order to avoid decomposition of the material. In terms of the compounds studied, the rational molecular design combines the electron transport properties of the CS unit with known hole transport moieties in a conjugated skeleton, so as to obtain active films with a balanced electron flow. Hole transport moieties such as triphenylene,[67] carbazole,[68], DPA/TPA,[33, 35, 68c, 69] (bisdimethylamino)terphenyl,[70] tetrahydroquinoline,[71] or benzothiazine[68c] were incorporated. Representative examples of device configurations and performances are provided in Table 2. Yellow colored OLEDs have been mainly obtained in multilayer devices in either neat or in doped-layer configurations. TPA-derivatives show high luminance and CN substitution in the outer position gave rise to better performance than inner substitution in similar devices.[69e] Interestingly, several approaches toward white emission have been considered with doped films and it is worth highlighting the performance of a solution-processed WOLED that combines the yellow-orange emitting compound **CN-DPADSB** with a blue emitting dendrimer as the active layer.[69d]

As far as solar cell applications are concerned, CS molecules with convenient anchoring groups (COOH, OH or anhydride) have been adsorbed onto TiO_2 surfaces to act as dyes in

DSSCs. CS is used as a π-linker in the structure of dye. In particular, Sharma's group synthesized several 4-nitro-CS dyes and evaluated the photovoltaic responses of DSSCs with different structures and anchoring groups. The basic system, [72] the dimer,[73] or the material combined with porphyrin,[74] TPA,[75] or pyran[76] have been studied and efficiencies of up to 5.8% have been achieved. A-D-A systems with DPA or carbazole and cyanoacrylic acid gave efficiencies up to 2.37%.[77]

With respect to BHJ solar cells, CS units have been incorporated either in the electron acceptor or in the electron donor materials that are blended to form a D-A heterojunction. Most BHJ solar cells use fullerene acceptors. In this respect, new fullerene electron acceptors have been designed by adding CS as a substituent. Sharma's group has been productive in this field and they have reported the modification of **PCBM**[78],[79] and **PC70CBM**[80] with nitro-CS to increase the LUMO level to obtain broader and stronger absorption spectra. As a result, the cells performed better than standard **PCBM** cells under the same conditions (4.23% vs 2.93% for **PCBM** and 4.88% vs 3.23% for **PC70CBM**). Other structural modifications involved substitution of the **bis-PCBM** dyad with two nitro-CS moieties, which led to an increase in the absorption by incorporation of an additional light-harvesting unit that initially showed superior efficiency to the traditional acceptor **PCBM** in blends with **P3HT**.[81] Interestingly, **PCBM** modification with the trioctyloxy-CS group[82] showed that the CS units were responsible for forming a blended film with **P3HT** that exhibited a well-defined microstructure without the need for any additional treatment. It has been claimed that BHJ devices show an excellent power conversion energy (PCE) of 4.2%. However, a new fullerene acceptor that incorporated a nitro-CS in conjuction with dialkylfluorene had poor solubility and device efficiency was not improved.[83]

Another type of BHJ solar cell contains the CS group as a π-linker in the structure of a polymeric donor. In this respect, conjugated polymers in which the CN group had been placed in different positions were evaluated as donors in BHJ solar cells using **PC70BM** as the

acceptor.[84] The CN group improved the efficiency of devices that contained thiophene or thiophene/triphenylamine conjugated polymers.[85]

Small molecules that contain a nitro-CS group in dimeric form,[86] or combined with TPA,[87] benzobisthiadiazole and thienothiadiazole,[88] phthalimide,[89] pyrrole and carbazole[90] or diketopyrrolopyrrole,[91] have been found to act as donors in BHJ with fullerene as the acceptor and PCE values in the range 0.6–4.1% have been obtained.

In a similar way, Li's group has explored novel donors with D-A-D structures using CS as the linker between TPA and benzoxadiazole, benzothiadiazole, diketopyrrolopyrrole or isoindigo and they obtained PCE values up to 4.9 %.[92] The effect of the linkage was analyzed[92b] and it was concluded that CS leads to a higher open circuit voltage (V_{oc}) due to the lower HOMO values. In another comparison study the inclusion of CS led to an increase in hole mobility, lower HOMO and increased crystallinity in films that provided BHJ solar cells with a superior efficiency compared with non-cyano analogs.[92d]

Perhaps the most interesting possibility for CS-derived compounds is to act as novel acceptors in non-fullerene BHJ solar cells. Mathews' group studied the influence of the position of the CN groups in two isomeric **CN-OPVs** and found evidence for charge transfer in a 3:1 blend with **MEH-PPV**, which exhibited a PCE of only 0.05% due to the poor film morphology.[93]

More recently, Park's group reported novel electron acceptors for solution-processed BHJ solar cells by incorporating naphthalimide groups in a DCS derivative. The resulting films formed from blends with low molecular weight donors[94] or polymeric donors[95] showing well intermixed film morphology, balanced charge transport and a maximum PCE 7.6 %,[95c] (Figure 6) which is among the highest observed in non-fullerene polymer solar cells and providing great potential to exceed fullerene-based devices.

Finally, important results for CS-based materials have been reported for thin film transistor (TFT) devices. [54, 96] Although this is a relatively unexplored field, it has been shown that CF_3-substituted DCS molecules show excellent properties as n-type semiconductors for

OFETs (Table 3), with electron mobilities as high as 2.14 $cm^2 V^{-1} s^{-1}$ obtained.[96c] These compounds have several advantages. Firstly, they have low LUMO values (–3.6 eV to –4.1 eV) to achieve good electron injection and air stability. Secondly, they form high quality smooth films and this facilitates contact with the electrodes. Thirdly, molecules can be deposited by thermal evaporation methods in the correct orientation (edge-on orientation with π-stacking parallel to the substrate surface) to facilitate charge hopping on substrates with in-plane source and drain electrodes, and finally the tight packing also prevents oxidants from penetrating into the π-conjugated cores, thus increasing their lifetime. In addition, crystalline films with high electron mobilities can be prepared by the solvent evaporation crystal growth technique.[54]

4. Liquid crystals

Liquid crystal (LC) organizations are unique self-assemblies that combine the characteristics of both liquid and crystalline states, such as mobility and anisotropy, respectively.[97] These simultaneous properties make LCs functional stimuli-responsive soft materials,[98] which are mainly known for their electrooptic response in display applications. Moreover, the incorporation of additional properties in LC phases, such as fluorescence,[99] is of great interest because such light-emitting LCs could find several applications in anisotropic OLEDs, simplified LC displays, chemosensors, optical memory or polarized organic lasers. Nevertheless, it is very difficult to incorporate luminescent moieties in LC molecules while retaining the mesomorphic behavior by keeping intermolecular interactions without leading to aggregation quenching (ACQ). In this respect, the CS-motif represents a good strategy to maintain the liquid crystalline and emitting properties. Furthermore, as CS-based molecules are sensitive to different stimuli, additional responsive properties can be imparted to these liquid crystals.

Two main approaches towards CS-LCs have been described and these involve either doping an LC matrix with a CS dye[100] or the design of an appropriate CS molecule tailored to show LC phases. In the latter case, an attractive variety of liquid crystalline organizations have been obtained to date. With a focus on classical liquid crystals, nematic[10, 12, 14d, 101] and smectic[10, 12, 14b, 14d, 101b, 101g, 102] mesophases from typical rod-like molecules, as well as columnar liquid crystalline organizations[103] with different molecular designs, have been described. Both low molecular weight compounds and macromolecules (homopolymers,[101d, 101e, 102a] homopolymers doped with a CS-LC,[101o] copolymers,[104] or even H-bonded supramolecular polymers)[101j, 105] have been used with success. On following common liquid crystal molecular design trends, CS[101f, 102b] or DCS[10, 12, 14b, 14d, 101a, 101n] structures with a reduced number of terminal flexible chains (alkoxy- or alkyl-tails) as lateral substituents or combined with amino,[102c, 106] carboxylic acid or ester[107] groups have allowed the synthesis of rod-like molecules that form nematic or smectic phases. However, it should be noted that CSs with less common molecular structures, such as six-arm star-shaped cyclotriphosphazenes,[101k, 101l] dimers,[101c, 101g-i, 102d] or even carbazole derivatives,[37a] assembled in a similar manner to give *calamitic* mesophases. On the other hand, more crowded CS[103b] and DCS[103a] structures surrounded by six alkoxy chains or incorporating one or two cyanostilbene moities as a side chain[103c] on a triphenylene core are able to induce columnar mesophases by filling space. Additionally, in recent years the novel bent-core liquid crystal phases have also been obtained with CSs and these materials show either polar smectic or columnar phases, as described by our group.[107-108]

The initial reports in this area concerned basic studies on the synthesis and liquid crystalline properties of the new compounds. However, nowadays the CS-based liquid crystal field is gaining more interest and mesomorphic advanced functional materials that incorporate this structural motif are very appealing due to their special responses to external stimuli and electronic properties within an ordered assembly.

In 2008 Weder's group[12] discovered that **C18-YB** (Figure 2A), in addition to MCF in the crystal state, formed a thermochromic liquid crystal phase with yellow luminescent emission in the nematic phase and blue emission in the smectic mesophase and several stimuli-responsive CS-LCs have been reported.

For example, **GDCS** (Figure 7A) is a phasmidic molecule with six terminal alkoxy chains and it shows AIEE properties of thermochromism and semiconductivity.[103a] This compound exhibited a columnar hexagonal liquid crystal phase at room temperature with moderate quantum yield (QY = 0.25) and green emission, in contrast to the crystal state, which had a yellow luminescence and higher quantum yield (QY = 0.45). Interestingly, this fluid assembly allowed uniaxially aligned and fluorescent (LC and crystalline) microwires to be obtained by using the micromolding in capillaries (MIMIC) method, thus providing electrical conductivities in both the LC (0.8×10^{-5} S cm^{-1}) and the crystalline (3.9×10^{-5} S cm^{-1}) phases comparable to those of the well-known organic semiconductor **P3HT** (6.7×10^{-5} S cm^{-1}).

Light-driven liquid crystalline materials have now become a hot topic due to their potential applications in optics, photonics, and nanotechnology, amongst other possibilities.[109] In this respect, the CS unit has been identified as being suitable for photoresponsive materials due to the possibility of C=C bond photoisomerization. There are several examples that show how this phenomenon occurs easily in a fluid phase such as the liquid crystal state or a liquid solution.[14d, 102b] This strategy has been applied to produce several CS-LCs that undergo *Z/E*-isomerization, interestingly giving rise to modulation of their emissive properties[102b, 106a] and to photoinduced phase transitions[14d, 103b] in a similar way to azobenzene-materials but, in contrast to the latter, with almost no thermal back isomerization. In this respect, Park's group explored the possibility of *Z/E*-photochange in neat samples for the fabrication of surface relief gratings (SRG), similar to those described for azobenzene-based LCs, using a mesogenic polycatenar CS (**GCS**) (Figure 7B).[103b] **GCS** formed a Col_h mesophase from 31.9 to 11.3 °C with a strong tendency to crystallize in a tetragonal arrangement close to room

temperature. The authors exploited this isothermal crystallization and succeeded in fabricating highly fluorescent micropatterns in crystalline films based on a photo-triggered crystal-to-LC phase transition that led to a mass flow and SRG formation. Even at a small photon dose (150 mJ cm^{-2}), high diffraction efficiency (<30%) and rapid SRG formation (within 150 s) with a high surface modulation of nearly 200% were claimed.

The molecule **Z-CN-APHP**[106a] (Figure 7C), which formed an enantiotropic smectic mesophase between 80 and 112 °C on heating, changed its emission from green to blue upon irradiation of the LC phase (90 °C) for 2 hours, with a concomitant QY decrease from 0.195 to 0.092 due to the photoisomerization process. Taking advantage of this response, **CN-APHP** was dispersed in a liquid crystal matrix to promote electrically switchable fluorescence. Upon irradiation, the starting rod-like *Z*-isomer transformed into the *E*-isomer, which has a bent conformation that is not compatible with LCs, thus inducing phase separation. In the field-off state there were numerous randomly oriented LC domains, which strongly scattered the incident light, and this maximized the chance of the photons finding fluorescent molecules in their path. However, in the field-on state, the LC molecules were oriented along the electric field and this produced lower fluorescence intensity.

Also based on photoisomerization in a LC matrix, the first chiral fluorescent photoswitchable liquid crystal has recently been reported and was used to construct an optically tunable reflective-photoluminescent cholesteric liquid crystal (LC) device.[100c] In this target two chiral DCSs were used as chiral-photoactive dopants to induce a photo-response in the cholesteric mesophase (Figure 8). The photo-induced *Z/E*-isomerization of the DCS-dopant induced a dramatic variation in the helical twisting power, which in turn allowed a spectral reflection shift of more than 1500 nm in the cholesteric LC. In addition, the emissive activity of the DCS-dopant made this kind of chiral photoswitch a suitable candidate for reflective-photoluminescent cholesteric liquid crystalline devices in which the emissive properties could be readily adjusted upon UV irradiation.

Remarkably, in contrast to azobenzene-LCs, photoisomerization is not the only suitable process claimed for CS-LCs because a [2+2]-cycloaddition photoprocess could be also expected, even though it is less commonly reported.[23a] The first attempts to investigate the potential of this photoprocess in liquid crystalline phases was addressed by our group. Focused on rod-like structures, we recently studied two DCS derivatives (**DSC14** and **DCS4**) that showed nematic and smectic mesophases.[14d] Besides thermo-, mechano- and vapochromism, these compounds revealed an interesting photoreactivity in the liquid crystal state as they gave rise to *Z/E*-photoisomerization and [2+2]-photocycloaddition reactions, which caused phase transitions, while the crystal phase was stable towards photoirradiation. The more compact lamellar packing meant that the cycloaddition process was favored in the smectic mesophase.

In the search for alternative CS-luminophore mesogenic assemblies our group also recently described two new families of CS-LCs.[102d, 107-108] These compounds were characterized and distinguished by either a rigid [107-108] or a flexible bent-core.[102d] Interestingly, flexible compounds **FD4** and **FD14**, which consist of two rod-like CS-structures linked by an odd-methylene spacer (flexible dimers), dramatically hinder the stabilization of mesophases due to conformational freedom when compared to rigid bent-core structures. Nevertheless, this freedom enhanced their stimuli-responsive properties and thermochromism was observed with high QYs (up to 0.43) in crystalline phases and significant photochemical activity at room temperature (cycloaddition). This photoactivity in bulk led to an efficient and fast luminescence modulation from green to blue emission with potential for writing applications.[102d] On the other hand, compounds with a rigid 3,4'-biphenylene bent-core assemble into very compact and different bent-core mesophases, such as columnar, polar smectic C, dark-conglomerate and B_6 phases, by simply varying the number of CS units, the position of the cyano group on the C=C bond or the terminal chain lengths.[107-108] However, a

liquid crystalline assembly was not obtained when DCS units were incorporated in the bent core structure[14d] because of the strong intermolecular interactions in the solid assemblies. Interestingly, some of these rigid-bent core CSs, isomers **β-B** and **α-B**, assembled into switchable antiferroelectric and ferroelectric organizations and this allowed light-driven modulation of the macroscopic polarization.[108b] However, depending on the position of the CN group, upon mesophase irradiation different photochemical changes occurred, namely a *Z/E*-isomerization for compound **α-B** and a [2+2]-cycloaddition for **β-B** (Figure 9), and these in turn led to different courses for polarization light-driven modulation. In the case of the isomerization, a very fast and time-stable change in the polar order occurred (**α-B**), while cycloaddition gradually caused a controlled variation in the polarization with recovery by heating the sample at 240 °C (**β-B**).

Subsequent results on CS-LCs have opened up new and attractive prospects for interesting applications. For example, different CS-based liquid crystal materials have been proposed for photonic band-edge laser devices by using DCS as dyes in a chiral nematic phase[101n] or for light-emitting liquid crystal displays based on LC matrices doped with CS and DCS.[100d, 104-105] Furthermore, nematic liquid crystalline elastomer microactuators[100b] that showed simultaneous thermomechanical deformation and photoluminescence (PL) emission variations have been described, as liquid crystalline composite polymeric films with directional MCF behavior.[101o] Nevertheless, taking into account the high photochemical activity imparted by the CS moiety in the liquid crystal state, in our opinion special care and confirmation in this respect is a prerequisite for reproducible results and future implementation of CS-LC materials in devices.

5. Nanostructures

Work at the nanoscale offers a variety of extremely attractive physical properties, chemical performance and applications with wide-ranging potential. Materials and technologies based

on size, controlled morphologies and structured organizations at nanodimensions have had an enormous impact in strategic areas of materials science or biomedicine where nanometer magnitudes matter.

In the route to functional nanomaterials, CSs undoubtedly have outstanding properties due to the characteristics highlighted above, such as an easy synthetic approach, design-modulated properties, and photoreactivity, amongst others. In addition to these wide-ranging possibilities for molecular design, the rod-like core, almost planar structure and π-conjugated features provide an outstanding ability for self-assembly. As well as the crystalline arrays, thin-films and mesophases discussed previously, self-assembly and self-organization processes either in bulk, in the presence of solvents or on surfaces have provided a substantial number of functional nanostructures in recent years. In this section, we explore representative results published to date and highlight appealing trends and progress in self-assembly, preparative strategies and properties of CS-based nanoaggregates and outline prospects for their applications.

A large number of CSs, from simple small molecules to more complex designs including polymers, are suitable for assembly to provide nano-sized aggregates, as proven by TEM and/or DLS techniques in many cases. However, the shape of the aggregates either strongly limits or opens up the potential of these materials and, in this respect, a broad range of morphologies has been achieved from CS-assemblies. Solid spherical nanoparticles[15b, 26a, 68c, 110] or hollow ones without or with holes,[66, 111] fibrillar organizations with variable widths with non-twisted[22b, 112] or helical torsions[113], rod- or needle-shaped objects,[15b, 39, 114] nanotubes[65, 115] and other less common shapes[66] have been described. Furthermore, both micellar[116] and vesicular[115c, 117] formations have been differentiated, particularly in aqueous media. On the other hand, both amorphous[26b] and crystalline[16a, 118] molecular packings form the nanoscale structures.

Interesting and diverse strategies have been reported to stabilize the CS-nanoaggregates, such as crosslinking,[119] or modification of the pristine qualities of nanoagregates. Different factors are appropriate to affect and control the size and shape of assemblies and these include temperature,[15b] the preparation procedure, changes in molecular design or external stimuli. For example, by keeping the emissive CS-motif, the incorporation of appropriate flexible lateral substituents,[110c] changing the slab-size of block-polymers,[66] or through host-guest complexation[112b, 117c] it is possible to govern successfully the morphology of nanoparticles. On the other hand, chirality seems to affect the self-assembly process and leads to shape differences in the aggregates initiated by chiral recognition.[111, 112g] Taking into account the unique *Z/E*-isomerization in the CS-structure, one aspect that warrants a special mention is the morphology or size variations as ordered hierarchical self-assembled structures in the *Z*-form could be converted into disordered systems by changing the compound to the *E*-form. Thus, upon irradiation (254 nm), helical nanofibers can become non-chiral fibers[113b] or spheres,[113c] vesicles can fuse together to generate branched and capped nanotubes[115c] (Figure 10A) or disordered aggregates,[117d] and vesicles from CS-compounds could shrink to form smaller and non-emissive systems triggered by photoreaction[117c] (Figure 11A).

The majority of the CS-based nanoassemblies described to date have been prepared by standard methodologies (precipitation, emulsification, sonication, or encapsulation procedures) or by *in situ* generation procedures (in a solid-matrix, in aqueous media, during the synthetic reaction, etc.), which are normally determined by the final use of the material. However, it should be pointed out that remarkable attempts to innovate synthetic and preparative aspects of the assembly of CS-molecules are well documented and these will be discussed below. Depending on the experimental process, aggregates in colloidal solution or suspensions, or matrix-dispersions can be achieved. Interestingly, some experimental methods, such as emission spectroscopy[120] or fluorescence microscopy, that exploit the emissive

abilities of CS-blocks have allowed the observation and control of the assembly processes[121] and enabled the interactions in the assemblies to be evaluated.[117a]

Undoubtedly a common and attractive feature of mainstream CS-nanoassemblies that has been promoted or pursued by researchers is the manifestation of AIE or AIEE effects, which lead to fluorescent aggregates. Interestingly, key-working tools mediated by light emissive processes are accessible in this way. As a simple example, colloidal solutions of fluorescent organic nanoparticles (FONs) could provide a broad range of emission colors. Furthermore, by choosing the appropriate CS-molecule, usually including TPA units, a full color palette could be obtained through molecular aggregation by either changing the solvent polarity through red- or blue-shifted absorption or emissive variations[117b, 122] or with the appropriate solvent/non-solvent ratios.[26a, 27, 29b, 39, 110k, 123]

As in the case of thin films, the distinctive *Z/E*-photoisomerization of the CS-unit has also been employed for adaptable light-emitting systems,[117c, 117d] some of which provide white-light-emitting materials.[113c, 118c] For example, Zhu *et al*.[118c] reported nanocrystalline **QDs (CdSe570@1)** prepared by grafting a CS-dye onto the CdSe-QD, which upon irradiation showed a blue emission band either in suspension or when dispersed in a PMMA matrix. The emitted light fused with the complementary yellow emission generated from the QD core to provide an apparent white light emission that was stable for several days after the irradiation source was removed. In another example, a naphthalimide-containing CS reported by Zhao and co-workers[113c] was able to exhibit a dual-fluorescence feature. The material showed a hypsochromic shift and markedly strengthened emission in the blue spectral region upon the photoisomerization, which gradually overhelmed the green fluorescence of the naphthalimide unit (Figure 10B).

It has been revealed that the intramolecular charge transfer from donor/acceptor (D-A) groups, the strength of these groups, the character of the conjugated bridge, the planarity of the chromophores, and the dimensionality of the charge-transfer network are issues that affect

multi-photon absorption activity. Therefore, an attractive range of excitation wavelengths can be used for fluorescence generation. As previously mentioned, the CS-core is suitable to connect within a molecule electron-donor and/or acceptor structures and, hence, in addition to looking for AIE and AIEE responses, CSs, DCSs and TPANs are applicable in the route to molecules with large two- or three-photon absorption cross-sections, which have been extensively explored for applications in three-dimensional fluorescence imaging, optical data storage, photodynamic therapy, optical power limiting, three-dimensional microfabrication or up-converted lasers. A selection of references for two-photon absorption (2PA) or three-photon absorption (3PA) cross-section values of these compounds are gathered in Table 4. Most of these examples are either CS-[110c, 110k, 124] or DCS-type cores[68c, 110b, 110d, 114c, 116b, 123a, 125] coupled to TPA structures. Fluorescence imaging has proven to be an indispensable and versatile tool in tracking and understanding complex biological environments both *in vivo* and *in vitro*. In this respect, fluorescence in the far-red/near-infrared (FR/NIR) region is even more attractive to avoid overlap with fluorescence of endogenous cell components and to improve the emitted light in thick samples. Of particular significance are the fluorescent dyes with both emission and excitation in the NIR (NIR-to-NIR) range, which have recently emerged as a new generation of nanoprobes for bioimaging. Interestingly, a number of CSs have been reported to be suitable for these purposes. [112b, 116a, 122b, 126] It is worth highlighting the first organic fluorophore-based nanoaggregates suitable for bioimaging in the NIR region using 3PA, as reported by Mandal *et al*.,[110c] successful probes for blood vasculature imaging,[110d] and FONs that enter cells and localize to the mitochondria specifically (Figure 12C).[127]

In vitro and *in vivo* imaging has motivated the majority of the aforementioned studies in the search for suitable fluorescent monitors through one- or multi-photon absorption to obtain advantages over conventional fluorescence visualizing techniques, such as increased penetration depth, lower tissue autofluorescence, and reduced photo-damage and

photobleaching, which would be particularly useful for imaging tissues and animals. In this direction, CS-FONs have been successfully evaluated and they are suitable for local detection using different types of cells: MCF-7,[110c, 110d] A549 lung carcinoma cells,[110h, 110i, 128] HepG2[123a, 124b] and U2OS[123a] cell lines, HEK293 healthy[110c] and HeLa cell lines.[110c, 112b, 117b]

Interestingly, an alternative strategy for tuning fluorescence emission spectra that has also been explored for CS-nanoassemblies is by fluorescence resonance energy transfer (FRET) combining two emitter systems. Thus, fluorescence of CS-FONs has been precisely modulated by the ratio of distance between the donor and acceptor components in systems considered for different applications (Figure 13A).[59b, 116f, 129]

Low molecular weight compounds have generally been proposed to target light-emission effects by forcing the assembly of CS-structures, as demonstrated by the information discussed here. However, for practical applications polymers have well-known advantages and it should be pointed out that CS-polymers are attracting a great deal of attention in this respect. Molecular designs and working strategies towards the assembly of this family of compounds are clearly driven by applications, especially when aqueous media are required. A survey of this area is presented below.

- *Towards self-assembly in aqueous media:* Steady aggregations in water are certainly a strategic task when considering applications. Water is the most common, cheap and green solvent and it is crucial to success for biopurposes. In this regard, CS-motifs have been identified by many authors as very attractive and worthwhile structures on the road to emission-based applications in bioenvironments and aqueous media. Water-assisted aggregation has been highlighted as a common method to form nanoobjects, and generally percentages higher than 50% of water, as a poor solvent, helps to build nanoaggregates with a wide variety of CS-compounds. Interestingly, changing the volume ratio of water is one of the

most general approaches to achieve the assembly process and to control the nanoshape,[113b, 117c, 117d, 123a, 125a, 130] the dimensions of vesicles[115c] and the hole-size of nanosphere surfaces.[111] This methodology has been applied to the self-assembly of both small molecules and CS-polymers, thus supporting their great potential due to suitable intramolecular nanosegregation processes. For example, Sherwood *et al*.[131] worked on previously mentioned **CN-PPVs** and showed that aggregates of long-chain oligomers had broad and red-shifted emission spectra and relatively long emission lifetimes, which are characteristics of excimer states. For intermediate chain lengths, dual monomer-like (green) and excimer-like (red) emission could be observed. Likewise, the presence of bulky isopropyl groups in dialkylsilylene-[4,4-divinyl(cyanostilbene)] copolymers led to significantly enhanced QY upon aggregation.[132] Poly(3-caprolactone) (**I-PCL**) and poly(D,L-lactide) (**I-PLA**) incorporating a DCS-motif were reported by Jia *et al*.[65] and these had enhanced luminogen-block emission by aggregation. Qiu *et al.* [133] described an efficient polymerization route for the *in situ* generation of AIE-active polymers (**PTPANs**) by palladium-catalyzed polyarylcyanation of diynes, which provided emission-tuned polymeric fluorescent organic nanoparticles (PFON) from green to yellow.

Nevertheless, alternative strategies have been proposed with the aim of promoting, controlling and stabilizing the molecular self-assembly and self-organization of CS-based compounds in aqueous channels, both by designing amphiphilic-CSs and by sufactant-assisted aggregations of common CSs.

Suitable molecular designs that lead to molecules with an amphiphilic structure are rather staighfoward. There are a number of interesting reports that address the design, synthesis and supramolecular formation of nanomicelles or nanovesicles in water, by providing a hydrophobic/hydrophilic balance. The CS-moiety acts as a hydrophobic block, while several water-friendly groups have been incorporated to interact with water. Besides obtaining nano-aggregates, the aim of achieving more intense emission upon self-assembly has led to

numerous proposals for investigations on both low molecular weight compounds and polymers.

This is the case of systems with side-chain glycopolymers, which were studied by Lim *et al*.[126a] containing hydrophilic glycol chitosan as a bio-backbone and a tricyanostilbene derivative as a hydrophobic pendant. High CS-unit substitutions into the glycol chain provided PFONs (200–400 nm) that were more intense and more red-shifted toward the NIR. The better penetration of these materials through the skin and the spectral correlation with the detection window of common NIR imaging equipment have been claimed as being appropriate for cell (HeLa) and *in vivo* imaging. Another system that warrants attention is the carbohydrate AIE-based PFONs (**$PhNH_2$–OA–Glu**) reported by Zhang *et al*.,[110a] which were prepared by using a one-pot ring-opening reaction at room temperature and in an air atmosphere, without the need for catalysts and initiators. The PFONs had uniform morphology (100–200 nm spherical nanoparticles), high water dispersibility, strong red-fluorescence and excellent biocompatibility, as evaluated in cell imaging studies (A549 cells). Interstingly, the same aggregation-induced emission dye (**$PhNH_2$**) was used by these authors to confirm that only the hydrophilic carboxyl groups created in the simple and mild one-step polymerization are suitable for the assembly of biocompatible spherical PFONs (100–200 nm diameter) in water. It was also proposed that targeting agents could be further integrated into the AIE-based FONs due to the presence of these reactive groups.[110h]

A different approach involves the incorporation of ionic bolaamphiphilic groups such as ammonium[112b] or pyridinium[113b, 117b, 117c, 117e, 128, 134] salts as hydrophilic entities for different purposes. On the one hand, endcaping of the flexible tails can provide versatile self-assemblies in aqueous solution. Thus, a concentration-dependent formation of monomolecular layered lamellas and helical nanofibers was reported by Jin *et al*.[113b] Interestingly, *Z/E*-isomerization upon irradiation allowed the morphology[117c] or dimensions[113b] of the nanoaggregates to be modified. On the other hand, ionic-CSs are appropriate for host-guest

complexation through molecular recognition. For example, monosubtituted-CSs such as those designed by Xing *et al*.[117c] form multi- or unilamellar vesicles at low concentrations but nanobelts at high concentrations. Furthemore, non-emissive vesicles were triggered by photoisomerization of colloidal solutions and, in addition, CS paired with cucurbit[7]uril (**CB[7]**). Interestingly, **CB[7]** binds the CS-molecule and suppresses the TICT state to turn on the fluorescence of the supramolecular system with remarkable hypochromicity and the emission could be further enhanced by photoisomerization (Figure 11A) Similarly, host−guest recognition between an amphiphilic-CS and a pillar[5]arene (**WP5**) (Figure 11B) formed the basis of the NIR-FONs described by Huang and co-workers.[112b] Attractively, neat CS forms nanoribbons in water that have fairly weak NIR emission at low concentrations. However, the addition of an equimolar amount of host transforms the aggregates into spherical particles with stronger NIR emission, pH responsiveness and suitability for living cell imaging.

With a rather different molecular design, compound **ASCP**[117b] with the appropriate combination of the CS-motif to form the AIE skeleton, a diphenylamino group to act as a strong electron-donating group to obtain red emission, and the salt motif as a mitochondrion-targeting moiety, afforded a dual-color organelle-specific probe with the AIE feature emitting at 450 nm for mitochondria (orange) but red for nucleolus (emission at 560 nm). The material had excellent biocompatibility (HeLa cells) and photostability (Figure 12C). Alternatively, on using a parent salt (**DPA-SCP**) Yu *et al*.[128] reported the first mitochondrion-anchoring photosensitizer that specifically generates singlet oxygen ($^1O_2$) in mitochondria under white light irradiation. The authors proposed the system to be a highly effective radiosensitizer that may trigger cancer cells to ionizing radiation without killing the cancer cells. $^1O_2$ is highly cytotoxic and it causes oxidative destruction of the cells in which it has been generated and damages the cell membrane and internal organelles. The authors claimed a supra-additive synergistic effect of ‘0+1>1’ by aggregation in the mitochondia. Remarkable ‘DPA-SCP +

white light' led to a high SER10 value (1.62), which is much higher than that of the most commonly used radiosensitizers such as gold nanoparticles (1.19) or paclitaxel (1.32). Testing with A549 lung carcinoma cells and HCT116 colonrectal cells revealed that this AIEgen-based photosensitizer with white light does not lead to apoptosis/death of cancer cells, whereas it does provide an elevated $^1O_2$ environment in the mitochondria.

In addition to the above unique examples, the incorporation of ethylene glycol-based blocks (EO or PEG-fragments) has clearly been the most commonly used tool to achieve amphiphilic features. Hirose *et al*.[112e] prepared a hexa(ethylene glycol)-based CS (labelled compound **2**) that showed a hierarchical fiber-like aggregation with a lamellar molecular arrangement, as shown by XRD. Due to the presence of the EO-segment, this compound exhibited a lower critical solution temperature (LCST) transition in water, which was determined to be 60 °C. The AIEE effect was almost completely diminished just below the LCST, which suggests that this system could be used as a sensitive probe for microscopic environmental changes. Short EO blocks have also been used to prepare amphiphilic **CNMBE-** and **CNTFMBE-**based compounds that form micelle-like FONs in water.[114b, 116f] Shin *et al*. reported that **12EO-CNTFMBE** formed stable rod-like 1D nanorods with diameter/length ratios of around 4.5.[114b] Fluorescence intensities in the blue-green region were enhanced by nanoaggregation, with QY up to 0.11 depending on the EO-length. The FONs of 1**2EO-CNTFMBE** are capable of cell uptake (HeLa cells) and this gives intense self-signaling fluorescence from cytoplasmic regions with its own spectral mark. Interestingly, nanorods could be formed even with the encapsulation of guest molecules such as hydrophobic Nile Red. Importantly, it was found that the nanorod transport significantly increased intracellular Nile Red signals. **EO-CNTFMBE**-based micelles reported by Wang *et al*.[116f] with a green fluorescence (λ_{max} = 544 nm) from AIE were employed as a platform for the construction of a FRET-based ratiometric sensor supported by excess amounts of the donor CS-amphiphile (Figure 13A). Interestingly, the incorporation of a very short EO-terminal chain led to the first organic

fluorophore-based nanoaggregates fabricated for bioimaging in the NIR region using 3PE, as referenced above.[110c]

Alternatively, the incorporation of very long PEG blocks has been the option towards a variety of CS-PEGylated PFONs. PEG45 was used to develop a novel method for the fabrication of main-chain copolymers (**PhNH2-OA-PEG**) through a one-pot ring-opening polymerization and condensation reaction at room temperature and in air, without the need for catalysts or initiators. These compounds assemble to form spherical PFONs (about 100 nm) with high water dispersibility, strong fluorescence at 600 nm and excellent biocompatibility with adenocarcinoma epitelial (A549) cells.[135] Similarly, Ma *et al*.[110i] prepared a cross-linked fluorescent DCS-polymer (**PhE-ITA-PEG**) by radical polymerization. The amphiphilic polymer assembled in water (CMC 0.012 mg mL^{-1}) to form spherical PFONs with diameters ranging from 50 to 80 nm and they had intense yellow fluorescence (QY 0.38) and excellent biocompatibility. Alternatively, long PEG tails as side-chains is an alternative to provide spherical PFONs with a low critical micelle concentration (CMC 0.004 mg mL^{-1}), uniform size (60–120 nm), excellent water dispersibility, strong fluorescence and outstanding biocompatibility. These materials have nanotheranostics potential as nanoprobes for cell imaging (HeLa) and they were loaded with *cis*-platin, as reported by Wan *et al*.[110f] Likewise, a PEGylated-aldehyde was used for the rapid preparation of AIE-active PFONs of **mPEG-CHO-Phe-NH_2-DEP** in a 'one-pot' microwave-assisted solvent- and catalyst-free Kabachnik–Fields reaction in an air atmosphere.[136] The spherical aggregates, which had a uniform size (200 nm) and rather narrow distribution, exhibited strong luminescence and excellent biocompatibility (HeLa) and they were internalized by endocytosis cells, mainly disseminated in the cytoplasm. Interestingly, only a low fluorescence intensity change was reported after these PFONs were irradiated with UV lamp for 2 hours. Alternatively, CSs units have been easily covalently coupled to a polyethylene–polypropylene glycol polymer

(Pluronic F127) to prepare ultrabright 555 nm-emissive, well-dispersed and biocompatible PFONs of **F127-TAMC-PhNH$_2$**.[137]

A different low-cost synthetic strategy was employed for the encapsulation of CS-emissive molecules within PEG-containing amphiphilic compounds, including Pluronics, for the successful self-assembly of CSs into micelles, vesicles and other structures in aqueous solutions. These structures provided environments for the aggregation of hydrophobic organic substances.

Thus, Wang *et al*.[116c] reported polymeric nanomicelles of PEGylated phospholipids doped with a CS (**StCN**) in water. The FONs had a small size (<30 nm), high monodispersity, excellent chemical stability and showed AIEE. **StCN@PEG** nanomicelles for the *in vitro* staining of HeLa cells and their biological uptake by tumor cells were confirmed by fluorescence microscopy. Furthermore, **StCN@PEG** nanomicelles conjugated with arginine-glycine-aspartic acid (RGD) peptides were suitable for *in vivo* tumor targeting. Likewise, on using **DSPE-PEG-Mal** as a matrix, Gao *et al*.[110d] embedded two novel FR/NIR AIE-active diketopyrrolopyrrole-based compounds (**DPPs**). The spherical micelles showed good water dispersibility and, by surface functionalization with cell penetration peptides (CCP), the authors achieved active nanoparticles for cell imaging and two-photon blood vasculature imaging with a cell viability close to 100% (MCF-7 breast cancer cells).

Furthermore, this kind of phospholipid (PE-PEGx) was used as the amphiphilic shell to obtain lipid coating semiconducting polymer dots (Pdots). By combining **CN-PPV** Pdots with **mTHPC** (meso-tetrahydroxyphenylchlorin) as a photosensitizer, Haupt *et al.*[129] prepared nanocomposites in which the fluorescence peak of the Pdots overlaps with the absorption band of **mTHPC**. These materials were suitable for use as a D-A pair as to show high efficiency generation of singlet oxygen ($^1O_2$) by FRET from the Pdots. Hence it was claimed that this nanomaterial would be useful for photodynamic therapy, the relatively new selective method in cancer treatment where a photosensitizer compound, under illumination at the

required wavelength, generates singlet oxygen ($^1O_2$) as well as other radical species (Figure 13B).

Amphiphilic polymers have been used as surfactants. For example, Pluronic-F68 was used by Maurin *et al.* [116b] to cloud a TPA-distyrylbenzene-derivative (a 2PA-excited dye) to afford colloidal FONs (20–100 nm) that exhibited, despite having a ten-times smaller mass, the same efficiency as Rhodamin B-Dextran for local tumor blood volume measurements during tumor growth and follow-up antiangiogenic therapies. Rapid movement of the fluorescence signal along lymphatic vessels was clearly detected using a digital imaging system. The researchers have claimed minor effects on blood viscosity and hemodynamics after injection of Pluronic nanomicelles (100 μL containing 1 mg Pluronic) in comparison to Dextran dyes (100 μL containing 10 mg Dextrans) without modifying the observation depth. Alternatively, Pluronic-F127 has recently been selected to compress different CS-based dyes in order to prepare FONs for *in vitro* and *in vivo* NIR bioimaging applications. The results were either efficient aggregated-state emissions ranging from the orange to FR/NIR regions (QY up to 0.22) and with potential for sentinel lymph node (SLN) mapping,[122b] (Figure 12B) or FONs with a combination of the unique photonic features of the NIR AIE-active **DPA-CN-PPV** (a low-bandgap conjugated polymer) and intraparticle energy relay from BODIPY (an energy gap-bridging molecule), which facilitates inflammatory H_2O_2-responsive chemical excitation of **DPA-CN-PPV** [126b] (Figure 12D).

A different approach that warrants comment is the clever use of AIE fluorogen-based nanoplatforms designed and prepared by Wang *et al*. by induced assembly of proteins.[110g] Bright-emission supramolecular FONs identified as **HSA-PhENH2-PPy-PTX-cRGD** should be highlighted due to their easy fabrication, excellent fluorescence properties, long-term circulation, specific tumor targeting ability (U87MG tumors) and outstanding chemo-photothermal combination therapy efficiency.

In addition to the above examples, other surfactant-assisted self-assemblies in water can be mentioned. For example, simple CSs have been favored to aggeragate in aqueous media with common cationic (cetyltrimethyl ammonium bromide (CTAB)),[116d, 116e, 116g] anionic (sodium dodecyl sulfate (SDS),[116e, 116g] sodium cholate (NaCh)[115b]) or neutral (polyethylene glycol *tert*-octylphenyl ether (Triton-X 100)) surfactants.[116g] The amphiphilic additive drives the formation of self-assembled structures of nanoscale dimensions with distinctive colors at, above and below the CMC of the surfactants, which makes these CSs fluorescence probes for CMC determinations. Interestingly, as was the case for a cholesterol-cyanostilbene derivative,[115b] the presence of a sodium cholate (**NaCh**) matrix (Figure 10A) led to self-assembly in aqueous conditions to give organized nanostructures with a different morphology to that induced when a non-cholesterol-tethered CS was used, but also far from the unilamellar vesicles reported for the cholesterol-appended fluorogen association alone.[115c] Finally, surfactant-stabilized water-dispersed cyanovinylene-backboned polymer dots (cvPDs) were directly synthesized by an *in situ* colloidal Knoevenagel polymerization, using a liquid surfactant (Tween 80) in the aqueous phase and avoiding the use of harmful organic solvents[116a] (Figure 12A). cvPDs showed bright emission, colloidal/chemical stability and a mesoscopic size range.

All of the reports outlined above highlight an attractive variety of surfactant-assisted nanoassembled CSs that lead to different sizes and nanoparticle morphologies, which in some cases are interconvertible under external stimuli. However, it should also be noted that much less attention has been paid to systematic research on the luminogen-aggregation abilities of a single compound in solution by simply changing the assembly conditions, such as adjusting the type and concentration of surfactants, aging time, temperature, mechanical stirring and freeze–thawing.

- *Towards self-assembly in a nonaqueous environment:* Motivated by a number of applications, diverse proposals that consider the dispersion of FONs in non-aqueous environments have been explored. In this respect, different authors have evaluated the *in situ* production of organic nanoparticles on different solid matrices through a variety of procedures. For example, Sanz *et al*. showed early on the role played by silicate matrices on the polymorphism of crystalline aggregates grown in the pores of dense sol-gel media when compared to solutions.[118a] The fluorescence efficiency of all the nanocomposite gel-glasses studied confirmed the formation of dye-nanocrystals in the bulk of amorphous matrices, since the **CMONS** used were only luminescent in their crystalline form. This methodology was proposed and also proved useful to obtain crystals that were simultaneously strongly active in second harmonic generation (SHG) and two-photon induced fluorescence due to the stabilization of a particular polymorph of the CS.[138]

However, PMMA solutions have been the common choice for a number of targets.[59b, 114a, 118c, 139] The variety and interesting nature of the results reported by Park's group[139b] are remarkable, with studies focussed on the *in-situ* generation of FONs of **Py-CN-MBE** on PMMA films. A simple, rapid, and reliable method based on vapor-driven self-assembly (VDSA) and patternwise photoacid generation was proposed by the authors, who fabricated photopatterned nanoaggregated arrays on solid surfaces and avoided the difficulties of transferring preformed colloidal nanoparticles onto fixed locations on substrates.[118a, 139b] Focussing on laser applications, **CN-MBE** was also successfully aggregated in PMMA during the ongoing radical polymerization of an MMA monomer and **CN-MBE** blend, which was subsequently spin-coated just before completion of the reaction to provide a post-annealing as the polymerization of the film finished.[139c] The doped film showed fluorescence over 400–600 nm and spectrally narrowed emission at 430 nm upon pumping with a nanosecond pulsed laser at a wavelength of 355 nm. DFB laser waveguides were successfully fabricated with composite **CN-MBE:PMMA** and the lasing wavelength was over 430 to 490 nm. Likewise,

so-called chameleon FONs that consisted of a photochromic CS (**BP-BTE**) in combination with luminescent organic CS and DCS (**CN-MBE**, **TPS-CNMBE**, **TPA-2CNMBE**) dipersed in PMMA films furnished multicomponent organic materials that combine FRET and photochromic switching capabilities in the system.[59b] Additionally, PMMA sheets that were loaded with high levels of size-tuned neat nanoparticles of a BTE-based CS were prepared by the reprecipitation method. These sheets were used by the same group for photo-rewritable fluorescence imaging by using UV (365 nm) and visible light (>500 nm).[139d]

As an alternative, polystyrene (PS) was preferred to produce efficient lasers by means of a rather different methodology. Wei *et al*.[140] selected an emulsion-solvent-evaporation method to construct highly flexible organic microdisk WGM resonators in a controlled way, through the dipersion of an efficient laser DCS-dye (**CNDPASDB**) in a PS matrix. The diameter of the microdisk can be finely tuned by altering the micelle size of the emulsion during the assembly process. The composite microdisks emitted uniform yellow fluorescence of **CNDPASDB** under UV excitation, which demonstrates the uniform doping of the dye in the PS matrix.

- *Other self-assembly mediated appplications:* The self-assembled systems reviewed so far have highlighted the wide-ranging attrative CS-based applications, which are mainly facilitated by the self-assembly into spherical-shaped nanoparticles, micelles or vesicles, either suspended in solvents or dispersed in appropriate matrices. Nevertheless, in addition to optical applications such as bioimaging and radiotherapy, lasing, tunable light emission and fluorescence writing or patterning already mentioned, further reports concern exceptional proposals inspired by precise tasks that will be discussed separately here, thus extending the panorama of practical uses of CSs.

In the the field of sensors the self-assembly mediated CSs represent a very attractive and highly appropriate strategy, especially concerning chemosensors in aqueous media, that

provides high selectivity or levels of sensitivity, as demonstrated in a range of reports. Fluorescent chemomonitors use weak supramolecular interactions, which are especially appropriate for the study of biological processes, signal transduction, and complicated environmental systems. Thus, CS-active motifs have been inserted into specific fundamental biopolymers. For example, special mention should be made of the few published DNA- and RNA-targeted assemblies that lead to bright emissive nanosystems. Reports proposed either a DCS-probe (**FcPy**) for the detection of nucleic acids due to the successful staining of the nucleus of HeLa cells, which was similar to commercial Hoechst 33258,[134b] or a fluorescent CS-agent (**Cy-Py-N_3**) for the detection of S-phase DNA synthesis and cell proliferation,[134c] with high brightness, photostability and tolerance to concentration change. This latter system provides remarkable alternatives to the commercial Alexa-azide dyes designed for this kind of mark. Likewise, it is worth highlighting chemodetectors for emissive sensing of glycosaminoglycans (GAGs) such as heparin (HEP), chondroitin 4-sulfate (ChS) and hyaluronic acid (HA), an important class of biopolymer that plays a key role in biofunctional regulation including cell growth and differentiation, angiogenesis, and immune response. On using two emissive DCS (**OPV-G1** and **OPV-G**2) with guanidinium groups to recognize specific ionic hydrogen bonding, a novel fluorescent sensing system by a binding mechanism, self-assembly and emissive response was designed by Noguchi *et al.*[141] The system exhibited an apparent 1:1 linear response toward the polyanion concentration and this is suitable for GAG sensing. Interestingly, self-assembly led to conventional HEP selectivity whereas unconventional discrimination for HA and detection of ChS was achieved by adjusting the pH of the medium.

In contrast to biomacromolecules, there are numerous active small biomolecules with crucial effects in living environments and the detection of these compounds is of great interest. This is the case of sodium houttuyfonate (SH), which has pharmaceutical and biological roles such as immunological enhancement and lysozyme function modulating activities both *in vitro* and

in vivo. However, highly sensitive, selective and real-time analytical methods for SH detection are scarce but are required. Yu *et al*.[115a] recently depicted a direct and highly selective fluorescence 'turn-on' assay method for SH *via* AIEE, using the CS-quaternary ammonium salt **CDB-DMA12**. In the presence of CS, SH – which has a negatively charged group – aggregates towards sheet, scroll and tube-shaped nanoobjects due to intermolecular electrostatic and hydrophobic interactions; as a result, the fluorescence of **CDB-DMA12** is switched on (558 nm). Another innovative proposal came from Park´s group, who succeeded in synthesizing a highly fluorescent supramolecular polymer based on cucurbit[8]uril (**CB[8]**), which acted as a linker of pyridinum-CS molecules.[134a] The host-guest polymer **Py^+-CN-MBE@CB[8]**, a unique combination of supramolecular polymer formation and bright fluorescence (λ_{em} = 516 nm, QY = 0.91), self-assembled to form rectangular nanoparticles and it was proposed as a very sensitive tryptophan sensor. The addition of L-tryptophan to **Py+-CN-MBE@CB[8]** polymerized water solution (10 μm) led to a dramatic decrease in the PL intensity of **Py+-CN-MBE@CB[8]** solution due to PL quenching by tryptophan. Hydrogen peroxide (H_2O_2) is a by-product of oxidative metabolism, it plays a significant role as a fundamental mediator in various redox-dependent cell-signaling pathways and it is abnormally overproduced above 10^{-6} M during the progress of inflammation. Consequently, sensitive H_2O_2-detectors have been actively pursued. It is worth noting the cholesterol-CS based system described by Xing *et al*.[115c] as this showed self-assembly and disassembly processes. After irradiation with UV light and treatment with H_2O_2, the fluorescence intensity of active CSC solutions showed a good selectivity and linear response to the molar equivalents of H_2O_2, which was reliably detected down to 10^{-9} M, i.e., far below the normal *in vivo* concentration of H_2O_2 (~10^{-7} M). In addition, it is worth mentioning the *in vivo* inflammation-responsive signaling based on the previously mentioned F127-micelles reported by Kim and co-workers,[126b] which combined the photonic features of NIR AIE-active **DPA-CN-PPV** and BODIPY-mediated intraparticle energy relay. These particles were successfully

used as H_2O_2 probes with a fairly high tissue penetration depth (>12 mm) in *ex vivo* conditions, which enabled deep imaging in a hair-covered mouse model of peritonitis (Figure 12D).

Fluorescence signals offer high selectivity, sensitivity, real-time detection, non-destructive determination, and low-cost instrumentation. As a consequence, a number of CS-based chemosensors have been developed to reveal certain cations, ranging from reversible pH fluorescence probes [112b, 142] to harmful cations such as Cr(IV)[143] but more commonly for Hg(II). Mercury and its ions, have long been identified as being amongst the most toxic heavy metal species and persistent contaminants. According to recent reports, the toxicity of Hg^{2+} can induce a variety of syndromes and harmful effects, such as DNA damage, disabling normal liver and kidney functions, and disruption of the immune system homeostasis, amongst others. Therefore, efficient monitoring of trace amounts of this cation is remarkably important for human health and this has attracted the interest of researchers. Highly sensitive and specific CS-based sensors for Hg^{2+} ions in aqueous media have been pursued, mainly via AIEE/AIE processes[114d, 144] but also in combination with FRET.[116f] In the latter case, the presence of two separate emission bands (I_{585} nm/I_{490}nm) demonstrates superior performance compared to the traditional 'turn-on/-off' type sensors, and these are highly selective for Hg^{2+} ion recognition versus a significant list of other cations (Li^+, Na^+, Cu^{2+}, Fe^{3+}, Co^{2+}, Al^{3+}, Pb^{2+}, Zn^{2+}, Fe^{2+}, Cd^{2+} and Mg^{2+}) (Figure 13A).

CSs have also been selected by different authors to develop a number of explosives-detectors (Picric acid),[145] antioxidant-detectors or enantioselective-sensors. For example, ascorbic acid (AA) is a natural antioxidant that is present in many biological processes, it is widely used as a food additive to prevent oxidation and it has recently shown potential in cancer therapy. As a result, AA-sensors with broad detection ranges and high sensitivity are a topic of current interest. With this target in mind, Nam *et al*.[110e] recently developed a unique strategy that combines a dual-quenching effect and bimodal spectral responses originating from the dual-

reactivity of the nitronyl-nitroxide moiety (**NN-CN-TFFP**). The probe showed fluorescence 'turn-on' and a diminished electron spin resonance signal upon AA addition. Either spherical FON suspensions or sensor papers responded over a broad concentration range of AA, from 1 μM to 2 mM, with excellent selectivity claimed over various antioxidants and acids. The attractive sensing ability of **NN-CN-TFFP** nanoparticles was maintained at pH values between 4 and 10, a characteristic that originates from the dual-features of the nitronyl-nitroxide group.

Chiral recognition through changes in fluorescence has attracted significant interest because it can provide time-efficient and sensitive enantiomer determination of a number of key chiral molecules (natural products, drugs, etc.). Concerning enantioselective sensors in which chiral CSs are used, it is worth noting results reported by Zheng and Hu [146] on a chiral tartaric acid-based CS, which covered for the first time the combination of AIE and chirality in an organic compound. A highly selective chiral recognition of the chiral tartaric-derivative with several chiral amines was achieved. For example, one amine enantiomer led to strong fluorescence and the other enantiomer showed weak or no fluorescence. Enantioselective assembly in aqueous ethanol could not only be visualized with the naked eye, but also quantified by fluorescence measurements. Additionally, on using analogous tartaric fluorophores it was shown that chirality could also affect molecular self-assembly because when nanofibers were formed, aggregates exhibited stronger emission intensity and longer absorption and emission wavelengths than when nanospheres were built.[111] In both cases a highly enantioselective self-assembly was demonstrated and a new method was claimed for the determination of chiral excess through changes in the fluorescence with high enantioselectivity. Likewise, by exploiting the self-assembly of a guanidinium-tethered DCSs (**OPV-G**), the structural information of dicarboxylates has been successfully translated into a characteristic fluorescent response. This system was used to discern the chirality difference between *L*- and *meso*-tartrate and to identify the geometrical difference between fumarates and maleates.[112g]

To conclude this CS-sensor overview, further detection systems can be highlighted, particularly for simplicity or applications that remain challenging. For example, chemical vapor detectors based on FONs of different DCSs deposited on TLC offered fast, reversible, highly sensitive, high contrast on/off responses in a dichloromethane vapor atmosphere.[7, 123b] Viscosity sensors warrant special mention.[117e, 147] Despite the fact that changes in biofluid viscosity are usually linked to perturbations and diseases in organisms, very few viscosity sensors in aqueous media has been developed by combining host-guest assembly and *Z*/*E*-isomerization. For this purspose the photo-lockable viscosity-sensitive behavior of CS-based FONs has been investigated using cyclodextrins (CD). The motion of a β-CD moiety acting as host around the *Z*-cyanostilbene structure (guest) is hindered by the steric effect of the aromatic rings in the photoisomerized *E*-isomer. Fluorescence emission and non-radiative decay, which are both environmental viscosity and fluid flow dependent, are then altered and this leads to the desired signal.

Particular emphasis should be placed on fibrillar emissive aggregations, rod-like particles or long fibers, which all have outstanding functions and potential, including through the formation of gels, which will be reviewed separately in the next section.

Intriguingly, assembly towards elongated aggregations is a common trend for a number of small CSs with CF_3 groups,[21, 22b, 112c, 112d] which are well-represented by the versatile **CN-TFMBE** (Figure 14), as first reported by Park's group.[112c] Sturdy π–π contacts between the aromatic segments, intermolecular interactions through the polar CF_3 unit, and the effects of the strongly dipolar CN groups all govern the fibrillar growth of the highly luminescent molecular self-assembly. Taking advantage of this feature, An *et al*.[21] developed a very easy method to produce large quantities of bright R,G,B,Y-color tuned nanofabrics consisting of extremely uniform emissive 1D-nanowires. The authors formulated a 2D-composite consisting of three layers of fibers of three different CS and DCSs, one each of CN-TFMBE (blue emission, ~20 μm thickness), THIO-Y (green emission, ~20 μm thickness) and DM-R

(red emission, ~30 μm thickness). The nanocomposite exhibited well-defined optical properties and excellent mechanical stability, which made the system suitable for nanoscale optoelectronics, sensors and biological devices (Figure 14).

Alternatively, **CN-TFMBE** was deposited by a simple vapor-phase process by the same group to self-assemble perpendicular organic nanoneedles (diameters in the range 250 to 500 nm, lengths up to 8 mm with rather sharp tips) on various substrates, thus providing superhydrophobic surfaces (Figure 14).[114a] Coated-glass, silicon, PMMA and perfluoropolymer substrates gave different wet angles. Furthermore, nanowires of **CN-TFMBE** were produced by using a micromolding in capillaries process,[148] which provides a procedure to manufacture nanoelectrical devices. The devices fabricated by patterning with an elastic stamp were reported to show a maximum electrical conductivity of 4.9×10^{-6} S cm^{1}. On the other hand, **CN-TFMBE** was likewise selected by Park's group to fabricate coaxial nanowires[149] by the deposition of a conductive polymer (**P3HT**) on the surface of **CN-TFMBE** nanowires, which led for the first time to the self-assembly of supramolecular nanofibrilar cores with an outer polymer shell (Figure 14). Devices based on these nanocables have been reported to show enhanced electrical conductivity (1.7 S cm^{-1}), chemically controlled charge accumulation and light-emitting properties. These coaxial nanocables were unique in having the coaxial D–A heterojunction macroscopically extended over the length of the coaxial nanocable. Nevertheless, the decay constant of the optical waveguided PL intensity was estimated to be about 0.21 micron^{-1} for the **CN-TFMBE** single nanowires, which is better than that of conventional organic nanowires and the **CN-TFMBE/P3HT** coaxial ones. This property is attributed to the charge transfer effect between the p-type shell (**P3HT**) and relatively n-type core (**CN-TFMBE**).[150]

6. Gels

Supramolecular gels formed by either low molecular mass organic gelators (LMOGs) or macromolecules have considerable potential not only because they represent a new class of assembled systems with unique architectures but they also have many practical applications such as in optoelectronics, sensors or for drug transfer and release.[151] LMOGs assemble into 3D networks and the driving forces for this process are weak intermolecular forces such as hydrogen bonding, van der Waals, π-stacking, electrostatic and charge-transfer interactions. This area has become a hot topic because stimuli-responsive units can be incorporated that lead to 'smart' or 'intelligent' gels and these respond to various stimuli such as temperature, pH, light, mechanical force, chemicals and electrical fields.

All of these appealing features of gels have attracted attention in the field of luminescent materials; however, most of these π-conjugated gelators lose their fluorescence through the assembly process (aggregation-caused quenching, ACQ). Nevertheless, CS-containing compounds stand out as suitable gelators for three main reasons. Firstly, the CS structure is easy to modify and this allows the introduction of well-known groups that favor gelation or units that are sensitive to pH or chemicals. Secondly, the assembly in the supramolecular gel usually produces strong fluorescence. Finally, such a motif is highly photoreactive, so the gel could respond to light and temperature, which would allow control of the fluorescence emission through two different stimuli (multi-stimuli gelators). However, it should be noted that the CS-based gels reported to date are limited.

Monocomponent gelators form the majority of the CS- or DCS-based gels, despite the fact that there are some precedents for multicomponent gels.[152] If we consider the fluid phase, a large number of organogels have been described that retain a wide variety of organic solvents and some aqueous mixtures, despite not forming a neat hydrogel. Liquid crystal gels have also been reported[153] and these generally lead to gels through fibrillar-morphology aggregation. The strategies used to design suitable gelators are diverse and range from the incorporation of long alkyl chains,[154] amide bonds,[152c, 152f, 155] polar groups such as nitro groups[152d, 152e, 156]

or previously mentioned –CF_3 groups,[22b, 112c, 112d, 152a, 152b, 153, 157] and tethering steroidal units.[158] Additionally, further rigid structures, such as benzimidazole,[152c, 152f, 155c] benzothiadiazole,[22b] benzoxazole[155i] or carbazole[156b] cores have been combined with a CS or DCS unit for different goals. Special mention should be made of the very simple structure of **β-DCS**,[159] a wholly π-conjugated aromatic DCS described in 2011 as an organogelator. The self-assembly of this compound was explained as being a consequence of the cooperative interplay of π-π stacking and secondary bonding interactions of strongly dipolar CN groups, with advantages claimed for the development of optoelectronic devices since long alkyl chains or steroidal groups present in other emissive gelators were inactive in terms of the desired optical absorption and charge transport.

Regarding applications, the main objective for this kind of soft assembled material has been to obtain fluorescent soft materials[22b, 112c, 112d, 152a, 152f, 154a, 155a, 155f, 155h, 155j, 156] that are almost non-fluorescent in the sol state but become much more emissive upon gel formation. Reports have revealed that the gel-sol transition through alternate heating and cooling processes could allow reversible switching between 'on and off' emissive states, which would be appropriate for temperature-controlled fluorescent switches. Thus, this class of thermoresponsive organogels has been proposed to have potential for use in optical devices, information storage, and biological applications.[5g]

In this area several different approachs can be found. For example, subtle molecular changes such as the position of the cyano group in the DCS backbone can be used to achieve gels with diverse emissive properties.[155j] More interestingly, the emission wavelength can be tuned by the solvent.[155a, 156a] Alternatively, more complex systems such as a nanocomposite polymer films composed of fluorescent fibers (DCS gelator) and a highly cross-linked polymer matrix have been evaluated. This system provided reversible thermochromism from orange (RT) to yellowish green emission (120 °C) as a consequence of the temporary disassembly of the fibers.[154b]

Likewise, fluorescence has also been explored in multi-component organogels[152d, 152e, 152g] because the gel properties can be tuned by altering the ratios and structures of the components[152d, 152e] or with additives, such as gel formation induced by the coordination of a CS derivative with a silver ion.[157] An interesting and novel approach was reported recently by Liu and co-workers[152g], who described fluorescent cogels that showed circularly polarized luminescence (Figure 15A). The chiral gelator **TMGE** assembled in a wide range solvents and this led to chiral natotubes that were suitable to confine some achiral CSs (**MeCNS**, and **BuCNS**) or DCSs (**α-DCS** and **β-DCS**) to provide a gamut of emission colors. Interestingly, nanotube chirality transfer to the guest dye aggregates was obtained and the guests emitted circularly polarized luminescence. It was claimed that these systems are highly interesting for applications such as optical displays, encrypted transmission and storage of information, chirooptical materials, and catalysts, amongst others.

Nevertheless, 'smart' multiresponsive organogels have received a great deal of attention due to their potential practical applications. Light-responsive gels have the possibility of combining both spatial and temporal control of input/output signals while avoiding physical contact. As mentioned previously, CS could act as a photoresponsive structure that shows both photoisomerization- and photocycloaddition-induced morphological changes, which in turn lead to fluorescence switching that has been successfully explored for different applications. Curiously, the first photoswitching properties of CS-based organogels were reported in 2009,[152b] with the known photochromic dopant **TFM-BTE** being the origin of the photoprocess rather than the CS-gelators. Examples of photoswitchable CS-based gels are rare [155g, 155k] and only photoisomerization has been surveyed, although the possibility of reversibility limiting practical applications has not been studied to date. Park and co-workers[155g] prepared and characterized the first CS-photosensitive gel. Gelator **PyG** (1 wt%) (Figure 15B) afforded a transparent and fluorescent organogel with cyclohexane that, due to weak intermolecular interactions between gelator molecules, allowed photoisomerization in

the aggregated state upon irradiation with 465 nm light. As a consequence, a gel-to-sol transition and a blue-shift in the fluorescence emission were produced, which could be exploited in fluorescence photopatterning. The second example was recently reported by Ma *et al*.[155k] who studied a V-shaped CS-diamide. This gelator formed AIE fluorescent organogels with aromatic solvents at low concentrations and, interestingly, this system showed dual-responsive behavior. Upon irradiation at 365 nm, CS-photoisomerization caused a gel-to-sol transition that switched off the fluorescence. Moreover, exposure of the gels to acid and base vapors (trifluoroacetic acid and triethylamine vapors) led to 'off/on' gel-sol transformations and the consequent fluorescent quenching, with the aim of achieving reversibility for chemical sensing.

In this area, and as in the case of self-assembled aggregates, vapor-sensing has also been addressed by using α-cyanostilbene emissive gels.[155c, 155i, 155k] Interestingly, the 3D-network of the gel provides a large surface area and a porous microstructure, which enhances the gas adsorption and allows changes in the fluorescence properties of the CS blocks. In this respect, Xu *et al*. designed a varierty of CS-based gelators for AIEE response that incorporated a benzoxazole unit as a responsive-binding site. Thus, compound **C12PhBPCP**[155i] formed fluorescent organogels in cyclohexane and this provided a xerogel that could act as a dual chemosensor. It was claimed that this system was suitable for the quantitative detection of organic amine vapors and volatile acids with fast reaction control and low limit sensoring (796 ppt and 25 ppb for gaseous aniline and trifluoroacetic acid, respectively).

CS-emissive gels have been proposed in the context of the notable development of ion chemo-sensors. For this purpose the sensing properties have been achieved by coupling two different structural motifs in the gelator. On the one hand there is the anion-binding zone (either amides or urea units) and on the other hand the use of a CS unit for signaling. Thus, fluoride sensors have been pursued by several authors, but the discrimination of F^- from $H_2PO_4^-$ and AcO^-, which have similar basicity, proved to be problematic. Nevertheless,

several CS- and DCS-gelators[155b, 155d, 155e] succeeded in discriminating the target, in some cases (e.g., **BPNIA**/DMSO gel)[155e] through a dual channel response since the presence of fluoride not only changed the color of the gel but also disrupted the 3D network to break up the gel.

Another benzimidazole-CS gelator described by Xue *et al*.[155c] provided, both as a gel and as a xerogel, logic gates that respond to chemical (F^-, OH^-, and H^+ ions in solution, and trifluoroacetic acid and NH_3 in the gaseous state) or light inputs and have multiple outputs (color, phase state, absorbance and emission intensity, etc.). In this way one chemical input could erase the effect of another chemical input (Figure 15C).

Further attractive examples for innovative applications have been developed to broaden the possibilities of CS-based gels. For example, Zhang *et al*.[158] proposed a phase-selective gelator for the separation and recovery of various aromatic solvents, and Xue *et al*.[152c] pursued photocurrent generation in a hybrid gel with C_{60}COOH, where the CS-gelator acted as an electron donor and the fullerene unit as acceptor.

Likewise, particular attention should be paid to the pioneering fluorescent liquid crystal gels described by Park's group, in which the versatile **CN-TFMBE**[153a] was used (Figure 16). In addition to the switching of optical transmittance due to the confined LC, the photoluminescence intensity of the gel could be repeatedly switched by an electric field. The discovery of electric-field-induced orientation of LCs to control and switch the photoluminescence emitted from fluorescent LC gels was claimed to open up new ways to explore the use of photoluminescence for display applications. Later on, using the same gelator, Zhao and Park[153b] prepared self-assembled LC gels in the form of micrometer-sized spherical droplets dispersed in aqueous solution, which led to circular and highly folded nanoscale fibers that contrasted with the extended ones formed in the bulk LC gel. In addition, the confinement also affected the electrooptical behavior of the LC gel.

7. Summary, conclusions and outlook

Functional organic materials constitute an extremely active and breakthrough research area in which, as this progress report illustrates, α-cyanostilbene (CS) structure and their self-assembly offer to the scientific community a variety of properties, effects and more importantly possibilities for practical applications, with different rational routes for the development of advanced functional materials. CS-based materials have yielded very attractive luminescent properties as they show bright fluorescence in condensed phases, with reports on AIEE or AIE behavior, and easy perturbation of the molecular packing, thus leading to an interesting fluorescence modulation. The photophysical properties of different CS self-assemblies have been successfully tuned in response to a variety of external stimuli, such as heat, light, pressure, solvents, pH or ions. Furthermore, CS-photochemical activity, through either *Z/E* isomerization or [2+2]-cycloaddition, induces changes in properties and this has evolved into an interesting topic for the development of novel multiresponsive systems, which have hardly been explored to date.

Despite the fact that some of these research topics are still in their infancy, substantial advances can be expected in view of the highligthed proposals and properties of the different CS self-assembled materials discussed here, with particular emphasis on crystalline polymorphs, liquid crystal phases, nanoaggregates and gels:

- CSs show excellent performance as fluorescent materials in powder form. A full color range and multicolor luminescence variations have been achieved with high QY and high contrast color changes due to the easy perturbation of the molecular arrangements by mechanical input (mechanoresponsive materials). Future interesting work should include the synthesis of ‘materials on demand’ based on more in-depth understanding of their aggregation/photophysical behavior.

Alternatively, single crystals of DCSs with high luminescence efficiency and high quality have been reported and they show great potential as the gain medium for solid state lasers

under one-photon and two-photon excitation (up-conversion lasers) and promise for electrically pumped lasers due to their excellent charge carrier mobilities.

Additionally, a wide variety of CS-based compounds have been processed as thin films (neat form or blends) for a variety of applications. Among them, remarkable results have been reported for films with multicolored emission and color switching for optical storage based on their known stimuli-responsive properties. Furthermore, extensive work has been carried out on optoelectronic applications such as OLEDs and solar cells (either dye-sensitized solar cells, DSSCs, or bulk-heterojunction, BHJ). Likewise, important results for CS-containing materials have been reported for thin film transistor (TFT) devices. Although this is a relatively unexplored field, DCS molecules show excellent properties as n-type semiconductors for OFETs due to advantages such as the low LUMO, the formation of high quality smooth films that facilitate contact with the electrodes and the possibility of thin film processing by thermal evaporation methods in a target orientation.

- Interestingly the CS-motif provides a good strategy to maintain the liquid crystalline and emitting properties and an attractive variety of mesophases such as nematic, smectic, columnar and, in recent years, the novel bent-core liquid crystalline phases have been achieved to date. Furthermore, as CS-based molecules are sensitive to different stimuli, additional responsive properties can be imparted to these liquid crystals. Nowadays these soft materials are attracting more interest and mesomorphic advanced functional materials that incorporate this structural motif are very appealing due to their special responses to external stimuli and electronic properties within an ordered assembly. The CS unit has been identified in the field of light-driven liquid crystalline materials as being suitable for photoresponsive systems due to the possibility of *Z*/*E* photoisomerization in a similar way to azobenzene-materials but, in contrast to these, the change occurs through an irreversible process. Remarkably, and also in contrast to azobenzene-LCs, a [2+2]-cycloaddition photoprocess is also possible although this is less commonly reported. Subsequent results on CS-LCs have

opened up new and attractive prospects for interesting applications for photonic band-edge laser or elastomer microactuators, amongst other uses. Nevertheless, taking into account the high photochemical activity imparted by the CS moiety in the liquid crystal state, in our opinion special care and confirmation in this respect is a prerequisite for reproducible results and the future implementation of CS-LC materials in devices.

- Materials and technologies based on size, controlled morphologies and structured organizations at nanodimensions have highlighted CS self-assembly and self-organization processes either in bulk, in the presence of solvents or on surfaces as an outstanding and versatile approach to functional nanostructures in recent years. Thus, a broad range of morphologies, with both micellar and vesicular character, and different ways to affect and control the size and shape of assemblies (temperature, the preparation procedure, changes in molecular design or external stimuli) have been achieved with CS-assemblies prepared by standard methodologies and remarkable attempts to innovate synthetic and preparative aspects can also be identified as an appealing future goal. Interestingly, by exploiting the emissive abilities of CS-blocks experimental methods (emission spectroscopy or fluorescence microscopy) could allow the observation and control of the assembly processes. CSs, DCSs and TPANs are applicable in the route to molecules with large two- or three-photon absorption cross-sections, which have been extensively explored for applications in three-dimensional fluorescence imaging, optical data storage, photodynamic therapy, optical power limiting, three-dimensional microfabrication and up-converted lasers. For example, CS-FONs have been successfully evaluated in the FR/NIR and the NIR-to-NIR ranges and these materials join the recently discovered new generation of nanoprobes for bioimaging and for tuning fluorescence emission spectra by FRET with a combination of two emitter systems. For these purposes numerous different plans for self-assembly in aqueous media have been evaluated on the road to emission-based applications in bioenvironments. All of these reports highlight attractive varieties of neat or surfactant-assisted nanoassembled CSs leading to

nanoparticles with different sizes and morphologies, which in some cases are interconvertible under external stimuli. However, it should also be noted that far less attention has been paid to systematic research on the luminogen-aggregation abilities of a single compound in solution by simply changing the assembly conditions, such as adjusting the type and concentration of surfactants, aging time, temperature, mechanical stirring and freeze–thawing. Alternatively, self-assembly in a nonaqueous environment by the *in situ* production of organic nanoparticles on different solid matrices has also been evaluated in a variety of procedures, although in some cases self-assembly has been mediated by the final appplications, such as for CS-based chemosensors or when fibrillar emissive aggregations, rod-like particles or long fibers were the final goal.

- Finally, CS-containing compounds stand out as suitable gelators because their structure is easy to modify, with the gel usually producing strong fluorescence and CSs being highly photoreactive through two different stimuli (multi-stimuli gelators). However, it should be noted that the CS-based gels reported to date are limited and mainly concern organogels, with neat hydrogels not reported to date. However, several reports have highlighted that the gel-sol transition shows a reversible switching between ‘on and off’ emissive states, with potential for use in optical devices, information storage, vapor- and chemo-sensing and biological applications.

Future work to address the aforementioned aspects as well as the continuous optimization of designs, preparation and properties required for the desired applications offer, in our opinion, very promising and attractive perspectives for the future judicious use of α-cyanostilbene structures and their molecular assemblies to explore and develop technological and biological applications for the next generations of functional materials.

Acknowledgements

This work was financially supported by MINECO-FEDER of Spain-UE (MAT2015-66208-C3-1-P) and the Aragón Government and FSE (Project E04).

Received: ((will be filled in by the editorial staff))
Revised: ((will be filled in by the editorial staff))
Published online: ((will be filled in by the editorial staff))

References

[1] a) I. D. W. Samuel, G. A. Turnbull, *Chem. Rev.* **2007**, *107*, 1272; b) S. W. Thomas, G. D. Joly, T. M. Swager, *Chem. Rev.* **2007**, *107*, 1339; c) H. Kobayashi, M. Ogawa, R. Alford, P. L. Choyke, Y. Urano, *Chem. Rev.* **2010**, *110*, 2620; d) H. N. Kim, Z. Guo, W. Zhu, J. Yoon, H. Tian, *Chem. Soc. Rev.* **2011**, *40*, 79; e) O. Ostroverkhova, Ed. *Handbook of Organic Materials for Optical and (Opto)electronic Devices*, Woodhead Publishing, Cambridge (UK) 2013; f) W. Hu, Ed. *Organic Optoelectronics*, Wiley-VCH, Weinheim 2013; g) B. Daly, J. Ling, A. P. de Silva, *Chem. Soc. Rev.* **2015**, *44*, 4203.

[2] a) J. B. Birks, Ed. *Photophysics of Aromatic Molecules*, Wiley, London 1970; b) C.-T. Chen, *Chem. Mater.* **2004**, *16*, 4389.

[3] F. Würthner, T. E. Kaiser, C. R. Saha-Möller, *Angew. Chem. Int. Ed.* **2011**, *50*, 3376.

[4] a) B.-K. An, J. Gierschner, S. Y. Park, *Acc. Chem. Res.* **2012**, *45*, 544; b) J. Gierschner, S. Y. Park, *J. Mater. Chem. C* **2013**, *1*, 5818; c) L. Zhu, Y. Zhao, *J. Mater. Chem. C* **2013**, *1*, 1059; d) C. Hang, H.-W. Wu, L.-L. Zhu, *Chin. Chem. Lett.* **2016**, *27*, 1155.

[5] a) Y. Hong, J. W. Y. Lam, B. Z. Tang, *Chem. Soc. Rev.* **2011**, *40*, 5361; b) L. Maggini, D. Bonifazi, *Chem. Soc. Rev.* **2012**, *41*, 211; c) Z. Zhao, J. W. Y. Lam, B. Z. Tang, *Soft Matter* **2013**, *9*, 4564; d) R. Hu, N. L. C. Leung, B. Z. Tang, *Chem. Soc. Rev.* **2014**, *43*, 4494; e) J. Mei, Y. Hong, J. W. Y. Lam, A. Qin, Y. Tang, B. Z. Tang, *Adv. Mater.* **2014**, *26*, 5429; f) Z. Ma, Z. Wang, M. Teng, Z. Xu, X. Jia, *ChemPhysChem* **2015**, *16*, 1811; g) J. Mei, N. L. C. Leung, R. T. K. Kwok, J. W. Y. Lam, B. Z. Tang, *Chem. Rev.* **2015**, *115*, 11718; h) Y. Sagara, S. Yamane, M. Mitani, C. Weder, T. Kato, *Adv. Mater.* **2016**, *28*, 1073; i) S. Xue, X. Qiu, Q. Sun, W. Yang, *J. Mater. Chem. C* **2016**, *4*, 1568. j) R. Zhan, Y. Pan, P. N. Manghnani, B. Liu, *Macromol. Biosci.* **2017**, *17*, 1600433. k) Q. Li, Z. Li, *Adv. Sci.* **2017**, 4, 1600484.

[6] H. Detert, D. Schollmeyer, E. Sugiono, *Eur. J. Org. Chem.* **2001**, *2001*, 2927.

[7] B. K. An, S. K. Kwon, S. D. Jung, S. Y. Park, *J. Am. Chem. Soc.* **2002**, *124*, 14410.

[8] J. Luo, Z. Xie, J. W. Y. Lam, L. Cheng, H. Chen, C. Qiu, H. S. Kwok, X. Zhan, Y. Liu, D. Zhu, B. Z. Tang, *Chem. Commun.* **2001**, 1740.

[9] X. Yao, T. Li, J. Wang, X. Ma, H. Tian, *Adv. Opt. Mat.* **2016**, *4*, 1322.

[10] C. Löwe, C. Weder, *Synthesis* **2002**, *2002*, 1185.

[11] a) C. Löwe, C. Weder, *Adv. Mater.* **2002**, *14*, 1625; b) B. R. Crenshaw, C. Weder, *Chem. Mater.* **2003**, *15*, 4717.

[12] J. Kunzelman, M. Kinami, B. R. Crenshaw, J. D. Protasiewicz, C. Weder, *Adv. Mater.* **2008**, *20*, 119.

[13] a) Y. Sagara, T. Kato, *Nat. Chem.* **2009**, *1*, 605; b) J. Xu, Z. Chi, Eds., *Mechanochromic Fluorescent Materials: Phenomena, Materials and Applications*, The Royal Society of Chemistry, Cambridge (UK) 2014; c) C. Calvino, L. Neumann, C. Weder, S. Schrettl, *J. Polym. Sci., Part A: Polym. Chem.* **2017**, *55*, 640.

[14] a) S.-J. Yoon, J. W. Chung, J. Gierschner, K. S. Kim, M.-G. Choi, D. Kim, S. Y. Park, *J. Am. Chem. Soc.* **2010**, *132*, 13675; b) H. Lu, S. Zhang, A. Ding, M. Yuan, G. Zhang, W. Xu, G. Zhang, X.-. Wang, L. Qiu, J. Yang, *New J. Chem.* **2014**, *38*, 3429; c) S. Jeon, J. P. Lee, J.-M. Kim, *J. Mater. Chem. C* **2015**, *3*, 2732; d) M. Martinez-Abadia, S. Varghese, R. Gimenez, M. B. Ros, *J. Mater. Chem. C* **2016**, *4*, 2886.

[15] a) J. L. X. Hou, N. Arulsamy and J. Huo, *Mater. Sci. Appl.* **2013**, *4*, 331; b) J. Huo, S. Yan, X. Hou, Y. Li, L. Yin, N. Arulsamy, *J. Mol. Struct.* **2015**, *1099*, 239.

[16] a) S. J. Yoon, S. Park, *J. Mater. Chem.* **2011**, *21*, 8338; b) Y. Xu, Z. Xie, H. Zhang, F. Shen, Y. Ma, *CrystEngComm* **2016**, *18*, 6824.

[17] Y. Xu, K. Wang, Y. Zhang, Z. Xie, B. Zou, Y. Ma, *J. Mater. Chem. C* **2016**, *4*, 1257.

[18] Y. Sagara, A. Lavrenova, A. Crochet, Y. C. Simon, K. M. Fromm, C. Weder, *Chem. Eur. J.* **2016**, *22*, 4374.

[19] Y. Sagara, K. Kubo, T. Nakamura, N. Tamaoki, C. Weder, *Chem. Mater.* **2017**, *29*, 1273.

[20] A. Lavrenova, D. W. R. Balkenende, Y. Sagara, S. Schrettl, Y. C. Simon, C. Weder, *J. Am. Chem. Soc.* **2017**, *139*, 4302.

[21] B. K. An, S. H. Gihm, J. W. Chung, C. R. Park, S. K. Kwon, S. Y. Park, *J. Am. Chem. Soc.* **2009**, *131*, 3950.

[22] a) C. Dou, L. Han, S. Zhao, H. Zhang, Y. Wang, *J. Phys. Chem. Lett.* **2011**, *2*, 666; b) C. Dou, D. Chen, J. Iqbal, Y. Yuan, H. Zhang, Y. Wang, *Langmuir* **2011**, *27*, 6323; c) X. Zhang, Z. Ma, Y. Yang, X. Zhang, X. Jia, Y. Wei, *J. Mater. Chem. C* **2014**, *2*, 8932.

[23] a) J. W. Chung, Y. You, H. S. Huh, B.-K. An, S.-J. Yoon, S. H. Kim, S. W. Lee, S. Y. Park, *J. Am. Chem. Soc.* **2009**, *131*, 8163; b) M. S. Kwon, J. Gierschner, S.-J. Yoon, S. Y. Park, *Adv. Mater.* **2012**, *24*, 5487; c) M. S. Kwon, J. Gierschner, J. Seo, S. Y. Park, *J. Mater. Chem. C* **2014**, *2*, 2552.

[24] a) C. Ma, X. Zhang, Y. Yang, Z. Ma, L. Yang, Y. Wu, H. Liu, X. Jia, Y. Wei, *Dyes Pigments* **2016**, *129*, 141; b) C. Ma, X. Zhang, L. Yang, Y. Li, H. Liu, Y. Yang, G. Xie, Y.-C. Ou, Y. Wei, *Dyes Pigments* **2017**, *136*, 85.

[25] Y. Lim, I. Choi, H. Lee, I. W. Kim, J. Y. Chang, *J. Mater. Chem. C* **2014**, *2*, 5963.

[26] a) Y. Zhang, J. Sun, G. Bian, Y. Chen, M. Ouyang, B. Hu, C. Zhang, *Photochem. Photobiol. Sci.* **2012**, *11*, 1414; b) Y. Zhang, J. Sun, X. Lv, M. Ouyang, F. Cao, G. Pan, L. Pan, G. Fan, W. Yu, C. He, S. Zheng, F. Zhang, W. Wang, C. Zhang, *CrystEngComm* **2013**, *15*, 8998; c) Y. Zhang, G. Zhuang, M. Ouyang, B. Hu, Q. Song, J. Sun, C. Zhang, C. Gu, Y. Xu, Y. Ma, *Dyes Pigments* **2013**, *98*, 486.

[27] M. Ouyang, L. Zhan, X. Lv, F. Cao, W. Li, Y. Zhang, K. Wang, C. Zhang, *RSC Adv.* **2016**, *6*, 1188.

[28] Y. Zhang, K. Wang, G. Zhuang, Z. Xie, C. Zhang, F. Cao, G. Pan, H. Chen, B. Zou, Y. Ma, *Chem. Eur. J.* **2015**, *21*, 2474.

[29] a) J. Sun, X. Lv, P. Wang, Y. Zhang, Y. Dai, Q. Wu, M. Ouyang, C. Zhang, *J. Mater. Chem. C* **2014**, *2*, 5365; b) J. Sun, Y. Dai, M. Ouyang, Y. Zhang, L. Zhan, C. Zhang, *J. Mater. Chem. C* **2015**, *3*, 3356.

[30] C. Feng, K. Wang, Y. Xu, L. Liu, B. Zou, P. Lu, *Chem. Commun.* **2016**, *52*, 3836.

[31] Y. Zhang, Q. Song, K. Wang, W. Mao, F. Cao, J. Sun, L. Zhan, Y. Lv, Y. Ma, B. Zou, C. Zhang, *J. Mater. Chem. C* **2015**, *3*, 3049.

[32] P. Zhang, W. Dou, Z. Ju, X. Tang, W. Liu, C. Chen, B. Wang, W. Liu, *Adv. Mater.* **2013**, *25*, 6112.

[33] a) W. Z. Yuan, Y. Tan, Y. Gong, P. Lu, J. W. Y. Lam, X. Y. Shen, C. Feng, H. H. Y. Sung, Y. Lu, I. D. Williams, J. Z. Sun, Y. Zhang, B. Z. Tang, *Adv. Mater.* **2013**, *25*, 2837; b) Y. Gong, Y. Tan, J. Liu, P. Lu, C. Feng, W. Z. Yuan, Y. Lu, J. Z. Sun, G. He, Y. Zhang, *Chem. Commun.* **2013**, *49*, 4009; c) Y. Gong, Y. Zhang, W. Z. Yuan, J. Z. Sun, Y. Zhang, *J. Phys. Chem. C* **2014**, *118*, 10998.

[34] Z. Ma, Y. Ji, Z. Wang, G. Kuang, X. Jia, *J. Mater. Chem. C* **2016**, *4*, 10914.

[35] Y. Gong, J. Liu, Y. Zhang, G. He, Y. Lu, W. B. Fan, W. Z. Yuan, J. Z. Sun, Y. Zhang, *J. Mater. Chem. C* **2014**, *2*, 7552.

[36] a) Y. Lu, Y. Tan, Y. Gong, H. Li, W. Yuan, Y. Zhang, B. Z. Tang, *Chin. Sci. Bull.* **2013**, *58*, 2719; b) Y. Zhan, P. Gong, P. Yang, Z. Jin, Y. Bao, Y. Li, Y. Xu, *RSC Adv.* **2016**, *6*, 32697.

[37] a) H. Zhao, Y. Wang, S. Harrington, L. Ma, S. Hu, X. Wu, H. Tang, M. Xuea, Y. Wanga, *RSC Adv.* **2016**, 66477; b) S. Li, J. Sun, M. Qile, F. Cao, Y. Zhang, Q. Song, *ChemPhysChem* **2017**, *18*, 1481.

[38] T. Jadhav, B. Dhokale, S. M. Mobin, R. Misra, *J. Mater. Chem. C* **2015**, *3*, 9981.

[39] Q. Lu, X. Li, J. Li, Z. Yang, B. Xu, Z. Chi, J. Xu, Y. Zhang, *J. Mater. Chem. C* **2015**, *3*, 1225.

[40] Y. Zhang, H. Li, G. Zhang, X. Xu, L. Kong, X. Tao, Y. Tian, J. Yang, *J. Mater. Chem. C* **2016**, *4*, 2971.

[41] Y. Li, F. Li, H. Zhang, Z. Xie, W. Xie, H. Xu, B. Li, F. Shen, L. Ye, M. Hanif, D. Ma, Y. Ma, *Chem. Commun.* **2007**, 231.

[42] W. Xie, Y. Li, F. Li, F. Shen, Y. Ma, *Appl. Phys. Lett.* **2007**, *90*, 141110.

[43] H. Wang, F. Li, I. Ravia, B. Gao, Y. Li, V. Medvedev, H. Sun, N. Tessler, Y. Ma, *Adv. Funct. Mater.* **2011**, *21*, 3770.

[44] X. Li, Y. Xu, F. Li, Y. Ma, *Org. Electron.* **2012**, *13*, 762.

[45] Y. Xu, H. Zhang, F. Li, F. Shen, H. Wang, X. Li, Y. Yu, Y. Ma, *J. Mater. Chem.* **2012**, *22*, 1592.

[46] a) J. Deng, J. Tang, Y. Xu, L. Liu, Y. Wang, Z. Xie, Y. Ma, *Phys. Chem. Chem. Phys.* **2015**, *17*, 3421; b) J. Deng, Y. Xu, L. Liu, C. Feng, J. Tang, Y. Gao, Y. Wang, B. Yang, P. Lu, W. Yang, Y. Ma, *Chem. Commun.* **2016**, *52*, 2370.

[47] a) Y. Li, F. Shen, H. Wang, F. He, Z. Xie, H. Zhang, Z. Wang, L. Liu, F. Li, M. Hanif, L. Ye, Y. Ma, *Chem. Mater.* **2008**, *20*, 7312; b) H.-H. Fang, Q.-D. Chen, J. Yang, L. Wang, Y. Jiang, H. Xia, J. Feng, Y.-G. Ma, H.-Y. Wang, H.-B. Sun, *Appl. Phys. Lett.* **2010**, *96*, 103508; c) X. Li, N. Gao, Y. Xu, F. Li, Y. Ma, *Appl. Phys. Lett.* **2012**, *101*, 063301.

[48] a) H.-H. Fang, J. Yang, R. Ding, Q.-D. Chen, L. Wang, H. Xia, J. Feng, Y.-G. Ma, H.-B. Sun, *Appl. Phys. Lett.* **2010**, *97*, 101101; b) H.-H. Fang, Q.-D. Chen, J. Yang, H. Xia, Y.-G. Ma, H.-Y. Wang, H.-B. Sun, *Opt. Lett.* **2010**, *35*, 441.

[49] H.-H. Fang, Q.-D. Chen, J. Yang, H. Xia, B.-R. Gao, J. Feng, Y.-G. Ma, H.-B. Sun, *J. Phys. Chem. C* **2010**, *114*, 11958.

[50] a) S. J. Yoon, S. Varghese, S. K. Park, R. Wannemacher, J. Gierschner, S. Y. Park, *Adv. Opt. Mat.* **2013**, *1*, 232; b) S. Varghese, S.-J. Yoon, S. Casado, R. C. Fischer, R. Wannemacher, S. Y. Park, J. Gierschner, *Adv. Opt. Mat.* **2014**, *2*, 542.

[51] S. Varghese, S. J. Yoon, E. M. Calzado, S. Casado, P. G. Boj, M. A. Díaz-García, R. Resel, R. Fischer, B. Milián-Medina, R. Wannemacher, S. Y. Park, J. Gierschner, *Adv. Mater.* **2012**, *24*, 6473.

[52] M. Kim, D. R. Whang, J. Gierschner, S. Y. Park, *J. Mater. Chem. C* **2015**, *3*, 231.

[53] S. Varghese, S. K. Park, S. Casado, R. Resel, R. Wannemacher, L. Lüer, S. Y. Park, J. Gierschner, *Adv. Funct. Mater.* **2016**, *26*, 2349.

[54] S. K. Park, J. H. Kim, S.-J. Yoon, O. K. Kwon, B.-K. An, S. Y. Park, *Chem. Mater.* **2012**, *24*, 3263.

[55] M. Wykes, S. K. Park, S. Bhattacharyya, S. Varghese, J. E. Kwon, D. R. Whang, I. Cho, R. Wannemacher, L. Lüer, S. Y. Park, J. Gierschner, *J. Phys. Chem. Lett.* **2015**, *6*, 3682.

[56] a) S. K. Park, S. Varghese, J. H. Kim, S.-J. Yoon, O. K. Kwon, B.-K. An, J. Gierschner, S. Y. Park, *J. Am. Chem. Soc.* **2013**, *135*, 4757; b) S. K. Park, J. H. Kim, T. Ohto, R. Yamada, A. O. F. Jones, D. R. Whang, I. Cho, S. Oh, S. H. Hong, J. E. Kwon, J. H. Kim, Y. Olivier, R. Fischer, R. Resel, J. Gierschner, H. Tada, S. Y. Park, *Adv. Mater.* **2017**, 1701346.

[57] J. H. Kim, S. K. Park, J. H. Kim, D. R. Whang, W. S. Yoon, S. Y. Park, *Adv. Mater.* **2016**, *28*, 6011.

[58] a) S. G. Jo, D. H. Park, B.-G. Kim, S. Seo, S. J. Lee, J. Kim, J. Kim, J. Joo, *J. Mater. Chem. C* **2014**, *2*, 6077; b) H. J. Park, S. G. Jo, J. Kim, J. Joo, *Synth. Met.* **2016**, *216*, 59.

[59] a) J. Lott, C. Ryan, B. Valle, J. R. Johnson, D. A. Schiraldi, J. Shan, K. D. Singer, C. Weder, *Adv. Mater.* **2011**, *23*, 2425; b) S. Kim, S.-J. Yoon, S. Y. Park, *J. Am. Chem. Soc.* **2012**, *134*, 12091; c) J. H. Kim, B.-K. An, S.-J. Yoon, S. K. Park, J. E. Kwon, C.-K. Lim, S. Y. Park, *Adv. Funct. Mater.* **2014**, *24*, 2746; d) H.-J. Kim, D. R. Whang, J. Gierschner, C. H. Lee, S. Y. Park, *Angew. Chem. Int. Ed.* **2015**, *54*, 4330.

[60] J. H. Burroughes, D. D. C. Bradley, A. R. Brown, R. N. Marks, K. Mackay, R. H. Friend, P. L. Burns, A. B. Holmes, *Nature* **1990**, *347*, 539.

[61] N. C. Greenham, S. C. Moratti, D. D. C. Bradley, R. H. Friend, A. B. Holmes, *Nature* **1993**, *365*, 628.

[62] a) D. Oelkrug, A. Tompert, H. J. Egelhaaf, M. Hanack, E. Steinhuber, M. Hohloch, H. Meier, U. Stalmach, *Synth. Met.* **1996**, *83*, 231; b) R. E. Gill, A. Hilberer, P. F. van Hutten, G. Berentschot, M. P. L. Werts, A. Meetsma, J.-C. Wittmann, G. Hadziioannou, *Synth. Met.* **1997**, *84*, 637; c) D. Oelkrug, A. Tompert, J. Gierschner, H. J. Egelhaaf, M. Hanack, M. Hohloch, E. Steinhuber, *J. Phys. Chem. B* **1998**, *102*, 1902; d) P. F. van Hutten, H.-J. Brouwer, V. V. Krasnikov, L. Ouali, U. Stalmach, G. Hadziioannou, *Synth. Met.* **1999**, *102*, 1443; e) P. F. Van Hutten, V. V. Krasnikov, G. Hadziioannou, *Acc. Chem. Res.* **1999**, *32*, 257; f) P. F. van Hutten, V. V. Krasnikov, H. J. Brouwer, G. Hadziioannou, *Chem. Phys.* **1999**, *241*, 139; g) A. Cirpan, H. P. Rathnayake, G. Gunbas, P. M. Lahti, F. E. Karasz, *Synth. Met.* **2006**, *156*, 282; h) Z. I. Niazimbetova, H. Y. Christian, Y. J. Bhandari, F. L. Beyer, M. E. Galvin, *J. Phys. Chem. B* **2004**, *108*, 8673; i) J. Gierschner, D. Oelkrug, in *Encyclopedia of Nanoscience and Nanotechnology*, Vol. 8 (Ed: H. Nalwa), American Scientific Publishers, 2004, 219.

[63] X. W. Zhan, S. Wang, Y. Q. Liu, X. Wu, D. B. Zhu, *Chem. Mater.* **2003**, *15*, 1963.

[64] M. G. Murali, U. Dalimba, V. Yadav, R. Srivastava, *Polym. Eng. Sci.* **2013**, *53*, 1161.

[65] W. Jia, P. Yang, J. Li, Z. Yin, L. Kong, H. Lu, Z. Ge, Y. Wu, X. Hao, J. Yang, *Polym. Chem.* **2014**, *5*, 2282.

[66] E. Ravindran, E. Varathan, V. Subramanian, N. Somanathan, *J. Mater. Chem. C* **2016**, *4*, 8027.

[67] a) R. Freudenmann, B. Behnisch, F. Lange, M. Hanack, *Synth. Met.* **2000**, *111–112*, 441; b) R. Freudenmann, B. Behnisch, M. Hanack, *J. Mater. Chem.* **2001**, *11*, 1618.

[68] a) J.-W. Park, J.-H. Lee, H.-S. Lee, D.-Y. Kang, T.-W. Kim, *Thin Solid Films* **2000**, *363*, 90; b) H. Ryu, L. R. Subramanian, M. Hanack, *Tetrahedron* **2006**, *62*, 6236; c) B. Wang, Y. Wang, J. Hua, Y. Jiang, J. Huang, S. Qian, H. Tian, *Chem. Eur. J.* **2011**, *17*, 2647.

[69] a) D. U. Kim, S. H. Paik, S.-H. Kim, T. Tsutsui, *Synth. Met.* **2001**, *123*, 43; b) S. Liu, F. Li, Q. Diao, Y. Ma, *Org. Electron.* **2010**, *11*, 613; c) W. Z. Yuan, Y. Gong, S. Chen, X. Y. Shen, J. W. Y. Lam, P. Lu, Y. Lu, Z. Wang, R. Hu, N. Xie, H. S. Kwok, Y. Zhang, J. Z. Sun, B. Z. Tang, *Chem. Mater.* **2012**, *24*, 1518; d) Z. Jiang, Z. Zhong, S. Xue, Y. Zhou, Y. Meng, Z. Hu, N. Ai, J. Wang, L. Wang, J. Peng, Y. Ma, J. Pei, J. Wang, Y. Cao, *ACS Appl. Mater. Interfaces* **2014**, *6*, 8345; e) C. Li, M. Hanif, X. Li, S. Zhang, Z. Xie, L. Liu, B. Yang, S. Su, Y. Ma, *J. Mater. Chem. C* **2016**, *4*, 7478.

[70] a) S. H. Lim, G. Y. Ryu, G. Y. Kim, J. H. Seo, Y. K. Kim, D. M. Shin, *Mol. Cryst. Liq. Cryst.* **2008**, *491*, 40; b) S. H. Lim, G. Y. Ryu, J. H. Seo, J. H. Park, S. W. Youn, Y. K. Kim, D. M. Shin, *Ultramicroscopy* **2008**, *108*, 1251; c) J. H. Park, J. H. Seo, S. H. Lim, G. Y. Ryu, D. M. Shin, Y. K. Kim, *J. Phys. Chem. Solids* **2008**, *69*, 1314; d) S. E. Shin, J. H. Seo, S. G. Lee, J. S. Park, G. Y. Ryu, Y. K. Kim, D. M. Shin, *Mol. Cryst. Liq. Cryst.* **2009**, *504*, 76; e) G. Y. Ryu, S. G. Lee, S. E. Shin, J. J. Park, S. Park, D. M. Shin, *J. Nanosci. Nanotechnol.* **2010**, *10*, 6805; f) N. R. Park, G. Y. Ryu, S. J. Moon, J. H. Seo, Y. K. Kim, D. M. Shin, *Mol. Cryst. Liq. Cryst.* **2011**, *538*, 75; g) G. Y. Ryu, S. E. Shin, J. H. Seo, J. S. Park, H. M. Chang, S. Shin, Y. K. Kim, D. M. Shin, *J. Nanosci. Nanotechnol.* **2011**, *11*, 4430; h) N. R. Park, G. Y. Ryu, D. H. Lim, S. J. Lee, Y. K. Kim, D. M. Shin, *Mol. Cryst. Liq. Cryst.* **2012**, *567*, 117; i) G. Y. Ryu, N. R. Park, D. M. Shin, *J. Nanosci. Nanotechnol.* **2012**, *12*, 4142; j) S. N. Lee, S. J. Lee, Y. K. Kim, D. M. Shin, *Mol. Cryst. Liq. Cryst.* **2013**, *581*, 59; k) S. N. Lee, S. J. Lee, Y. K. Kim, D. M. Shin, *J. Nanosci. Nanotechnol.* **2014**, *14*, 6185; l) N. R. Park, G. Y. Ryu, D. H. Lim, S. J. Lee, Y. K. Kim, D. M. Shin, *J. Nanosci. Nanotechnol.* **2014**, *14*, 5109.

[71] T. Malinauskas, J. Stumbraite, V. Getautis, V. Gaidelis, V. Jankauskas, G. Juška, K. Arlauskas, K. Kazlauskas, *Dyes Pigments* **2009**, *81*, 131.

[72] J. A. Mikroyannidis, D. V. Tsagkournos, P. Balraju, G. D. Sharma, *Org. Electron.* **2010**, *11*, 1242.

[73] J. A. Mikroyannidis, A. Kabanakis, P. Balraju, G. D. Sharma, *J. Phys. Chem. C* **2010**, *114*, 12355.

[74] J. A. Mikroyannidis, G. Charalambidis, A. G. Coutsolelos, P. Balraju, G. D. Sharma, *J. Power Sources* **2011**, *196*, 6622.

[75] S. P. Singh, M. S. Roy, K. R. J. Thomas, S. Balaiah, K. Bhanuprakash, G. D. Sharma, *J. Phys. Chem. C* **2012**, *116*, 5941.

[76] G. D. Sharma, K. R. Patel, M. S. Roy, R. Misra, *Org. Electron.* **2014**, *15*, 1780.

[77] S. Ramkumar, S. Manoharan, S. Anandan, *Dyes Pigments* **2012**, *94*, 503.

[78] a) J. A. Mikroyannidis, A. N. Kabanakis, S. S. Sharma, G. D. Sharma, *Adv. Funct. Mater.* **2011**, *21*, 746; b) J. A. Mikroyannidis, A. N. Kabanakis, P. Suresh, G. D. Sharma, *J. Phys. Chem. C* **2011**, *115*, 7056.

[79] G. D. Sharma, T. S. Shanap, K. R. Patel, M. K. El-Mansy, *Materials Science-Poland* **2012**, *30*, 10.

[80] S. P. Singh, C. H. P. Kumar, G. D. Sharma, R. Kurchania, M. S. Roy, *Adv. Funct. Mater.* **2012**, *22*, 4087.

[81] B. Kim, H. R. Yeom, W.-Y. Choi, J. Y. Kim, C. Yang, *Tetrahedron* **2012**, *68*, 6696.

[82] Y. Zhao, G. Xu, X. Guo, Y. Xia, C. Cui, M. Zhang, B. Song, Y. Li, Y. Li, *J. Mater. Chem. A* **2015**, *3*, 17991.

[83] P. Nagarjuna, A. Bagui, J. Hou, S. P. Singh, *J. Phys. Chem. C* **2016**, *120*, 13390.

[84] J.-H. Kim, H. U. Kim, W. S. Shin, S.-J. Moon, S. C. Yoon, D.-H. Hwang, *Sol. Energy Mater. Sol. Cells* **2012**, *101*, 131.

[85] H. J. Wang, Y. P. Chen, Y. C. Chen, C. P. Chen, R. H. Lee, L. H. Chan, R. J. Jeng, *Polymer (United Kingdom)* **2012**, *53*, 4091.

[86] J. A. Mikroyannidis, A. N. Kabanakis, S. S. Sharma, A. Kumar, G. D. Sharma, *Org. Electron.* **2010**, *11*, 1631.

[87] a) J. A. Mikroyannidis, A. N. Kabanakis, S. S. Sharma, G. D. Sharma, *Org. Electron.* **2011**, *12*, 774; b) T. Jia, Z. Peng, Q. Li, Y. Xie, Q. Hou, L. Hou, *Synth. Met.* **2015**, *199*, 14.

[88] J. A. Mikroyannidis, D. V. Tsagkournos, S. S. Sharma, Y. K. Vijay, G. D. Sharma, *J. Mater. Chem.* **2011**, *21*, 4679.

[89] G. D. Sharma, J. A. Mikroyannidis, R. Kurchania, K. R. J. Thomas, *J. Mater. Chem.* **2012**, *22*, 13986.

[90] G. D. Sharma, J. A. Mikroyannidis, S. S. Sharma, K. R. Justin Thomas, *Dyes Pigments* **2012**, *94*, 320.

[91] G. D. Sharma, J. A. Mikroyannidis, S. S. Sharma, M. S. Roy, K. R. Justin Thomas, *Org. Electron.* **2012**, *13*, 652.

[92] a) S. Zeng, L. Yin, X. Jiang, Y. Li, K. Li, *Dyes Pigments* **2012**, *95*, 229; b) C. Ji, L. Yin, L. Wang, T. Jia, S. Meng, Y. Sun, Y. Li, *J. Mater. Chem. C* **2014**, *2*, 4019; c) L. Wang, L. Yin, C. Ji, Y. Li, *Dyes Pigments* **2015**, *118*, 37; d) C. Ji, L. Yin, B. Xie, X. Wang, X. Li, J.-J. Zhang, J. Ni, Y. Li, *Synth. Met.* **2016**, *220*, 448.

[93] T. Z. Oo, N. Mathews, T. L. Tam, G. C. Xing, T. C. Sum, A. Sellinger, L. H. Wong, S. G. Mhaisalkar, *Thin Solid Films* **2010**, *518*, 5292.

[94] O. K. Kwon, J.-H. Park, D. W. Kim, S. K. Park, S. Y. Park, *Adv. Mater.* **2015**, *27*, 1951.

[95] a) O. K. Kwon, J.-H. Park, S. K. Park, S. Y. Park, *Adv. Energy Mat.* **2015**, *5*, 1400929; b) O. K. Kwon, J.-H. Park, S. Y. Park, *Org. Electron.* **2016**, *30*, 105; c) O. K. Kwon, M. A. Uddin, J.-H. Park, S. K. Park, T. L. Nguyen, H. Y. Woo, S. Y. Park, *Adv. Mater.* **2016**, *28*, 910.

[96] a) S. Nagamatsu, T. Moriguchi, T. Nagase, S. Oku, K. Kuramoto, W. Takashima, T. Okauchi, K. Mizoguchi, S. Hayase, K. Kaneto, *Appl. Phys. Express* **2009**, *2*, 101502; b) K. Shoji, J.-i. Nishida, D. Kumaki, S. Tokito, Y. Yamashita, *J. Mater. Chem.* **2010**, *20*, 6472; c) S. W. Yun, J. H. Kim, S. Shin, H. Yang, B.-K. An, L. Yang, S. Y. Park, *Adv. Mater.* **2012**, *24*,

911; d) S. Nagamatsu, S. Oku, K. Kuramoto, T. Moriguchi, W. Takashima, T. Okauchi, S. Hayase, *ACS Appl. Mater. Interfaces* **2014**, *6*, 3847.

[97] J. W. Goodby, P. J. Collings, T. Kato, C. Tschierske, H. Gleeson, P. Raynes, Eds., *Handbook of Liquid Crystals*, Wiley-VCH, Weinheim 2014.

[98] a) T. Geelhaar, K. Griesar, B. Reckmann, *Angew. Chem. Int. Ed.* **2013**, *52*, 8798; b) Q. Li, Ed. *Liquid crystals beyond displays, Chemistry, Physics, and Applications.* , Wiley-VCH, 2013.

[99] a) M. O'Neill, S. M. Kelly, *Adv. Mater.* **2011**, *23*, 566; b) S. Yamane, K. Tanabe, Y. Sagara, T. Kato, *Top. Curr. Chem.* **2012**, *318*, 395; c) Y. Wang, J. Shi, J. Chen, W. Zhu, E. Baranoff, *J. Mater. Chem. C* **2015**, *3*, 7993.

[100] a) B. Umanskii, N. Novoseletskii, S. Torgova, G. Dorozhkina, *Mol. Cryst. Liq. Cryst.* **2004**, *412*, 313; b) R. Wei, Y. He, X. Wang, P. Keller, *Macromol. Rapid Commun.* **2014**, *35*, 1571; c) J. Li, Z. Zhang, J. Tian, G. Li, J. Wei, J. Guo, *Adv. Opt. Mat.* **2017**, *5*, 1700014; d) H. Lu, C. Xu, Z. Li, G. Xia, S. Jing, X. Bai, J. Yang, L. Qiu, Y. Ding, *Liq. Cryst.* **2017**, DOI:10.1080/02678292.2017.1292007.

[101] a) M. J. Holm, F. B. Zienty, M. A. Terpstra, *J. Chem. Eng. Data* **1968**, *13*, 70; b) F. Hardouin, G. Sigaud, M. F. Achard, H. Gasparoux, *Solid State Commun.* **1979**, *30*, 265; c) N. Koide, K. Iimura, *Mol. cryst. liq. cryst. inc. nonlinear opt.* **1987**, *153*, 73; d) A. M. Ahmed, W. J. Feast, J. Tsibouklis, *Polymer* **1993**, *34*, 1297; e) J. Tsibouklis, P. H. Richardson, A. M. Ahmed, R. W. Richards, W. J. Feast, S. J. Martin, D. D. C. Bradley, M. Warner, *Synth. Met.* **1993**, *61*, 159; f) E. I. Rjumtse, M. A. Osipov, T. A. Rotinyan, N. P. Yevlampieva, *Liq. Cryst.* **1995**, *18*, 87; g) H. Aoki, T. Mihara, N. Koide, *Mol. Cryst. Liq. Cryst.* **2004**, *408*, 53; h) S. Bronnikov, V. Zuev, *Soft Mater.* **2008**, *6*, 15; i) V. V. Zuev, S. V. Kostromin, S. V. Bronnikov, *Russ. J. Gen. Chem.* **2007**, *77*, 2091; j) J. H. Lee, N. Kawatsuki, *Mol. Cryst. Liq. Cryst.* **2009**, *498*, 59; k) R. Bao, M. Pan, J. J. Qiu, C. M. Liu, *Chin. Chem. Lett.* **2010**, *21*, 682; l) R. Bao, M. Pan, Y. Zhou, J. J. Qiu, H. Q. Tang, C. M. Liu, *Synth. Commun.* **2012**, *42*, 1661;

m) W. Mao, K. Chen, M. Ouyang, J. Sun, Y. Zhou, Q. Song, C. Zhang, *Acta Chim. Sinica* **2013**, *71*, 613; n) S. M. Morris, M. M. Qasim, D. J. Gardiner, P. J. W. Hands, F. Castles, G. Tu, W. T. S. Huck, R. H. Friend, H. J. Coles, *Opt. Mater.* **2013**, *35*, 837; o) M. Kondo, T. Nakanishi, T. Matsushita, N. Kawatsuki, *Macromol. Chem. Phys.* **2016**, *218*, 1600321.

[102] a) V. Percec, A. De Souza Gomes, M. Lee, *J. Polym. Sci., Part A: Polym. Chem.* **1991**, *29*, 1615; b) J. W. Chung, S.-J. Yoon, B.-K. An, S. Y. Park, *J. Phys. Chem. C* **2013**, *117*, 11285; c) H. Lu, S. Wu, J. Hu, L. Qiu, X. Wang, G. Zhang, J. Hu, G. Lv, J. Yang, *Dyes Pigments* **2015**, *121*, 147; d) M. Martínez-Abadía, S. Varghese, P. Romero, J. Gierschner, R. Giménez, M. B. Ros, *Adv. Opt. Mat.* **2017**, *5*, 1600860.

[103] a) S.-J. Yoon, J. H. Kim, K. S. Kim, J. W. Chung, B. Heinrich, F. Mathevet, P. Kim, B. Donnio, A.-J. Attias, D. Kim, S. Y. Park, *Adv. Funct. Mater.* **2012**, *22*, 61; b) J. W. Park, S. Nagano, S.-J. Yoon, T. Dohi, J. Seo, T. Seki, S. Y. Park, *Adv. Mater.* **2014**, *26*, 1354; c) L. Lin, H. Guo, X. Fang, F. Yang, *RSC Adv.* **2017**, *7*, 20172.

[104] J. Lee, S. Matsuda, N. Kawatsuki, *Mol. Cryst. Liq. Cryst.* **2010**, *529*, 20.

[105] N. Kawatsuki, R. Ando, R. Ishida, M. Kondo, Y. Minami, *Macromol. Chem. Phys.* **2010**, *211*, 1741.

[106] a) H. Lu, L. Qiu, G. Zhang, A. Ding, W. Xu, G. Zhang, X. Wang, L. Kong, Y. Tian, J. Yang, *J. Mater. Chem. C* **2014**, *2*, 1386; b) H. Lu, S. Wu, C. Zhang, L. Qiu, X. Wang, G. Zhang, J. Hu, J. Yang, *Dyes Pigments* **2016**, *128*, 289.

[107] M. Martinez-Abadia, B. Robles-Hernandez, B. Villacampa, M. R. de la Fuente, R. Gimenez, M. B. Ros, *J. Mater. Chem. C* **2015**, *3*, 3038.

[108] a) M. Martinez-Abadia, S. Varghese, B. Milian-Medina, J. Gierschner, R. Gimenez, M. B. Ros, *Phys. Chem. Chem. Phys.* **2015**, *17*, 11715; b) M. Martínez-Abadía, B. Robles-Hernández, M. R. de la Fuente, R. Giménez, M. B. Ros, *Adv. Mater.* **2016**, *28*, 6586.

[109] H. K. Bisoyi, Q. Li, *Chem. Rev.* **2016**, *116*, 15089.

[110] a) X. Zhang, X. Zhang, B. Yang, L. Liu, F. Deng, J. Hui, M. Liu, Y. Chen, Y. Wei, *RSC Adv.* **2014**, *4*, 24189; b) W. Huang, F. Tang, B. Li, J. Su, H. Tian, *J. Mater. Chem. C* **2014**, *2*, 1141; c) A. K. Mandal, S. Sreejith, T. He, S. K. Maji, X.-J. Wang, S. L. Ong, J. Joseph, H. Sun, Y. Zhao, *ACS Nano* **2015**, *9*, 4796; d) Y. Gao, G. Feng, T. Jiang, C. Goh, L. Ng, B. Liu, B. Li, L. Yang, J. Hua, H. Tian, *Adv. Funct. Mater.* **2015**, *25*, 2857; e) H. Nam, J. E. Kwon, M.-W. Choi, J. Seo, S. Shin, S. Kim, S. Y. Park, *ACS Sensors* **2016**, *1*, 392; f) Q. Wan, G. Zeng, Z. He, L. Mao, M. Liu, H. Huang, F. Deng, X. Zhang, Y. Wei, *J. Mater. Chem. B* **2016**, *4*, 5692; g) K. Wang, X. Fan, L. Zhao, X. Zhang, X. Zhang, Z. Li, Q. Yuan, Q. Zhang, Z. Huang, W. Xie, Y. Zhang, Y. Wei, *Small* **2016**, *12*, 6568; h) X. Zhang, X. Zhang, B. Yang, J. Hui, M. Liu, Z. Chi, S. Liu, J. Xu, Y. Wei, *Polym. Chem.* **2014**, *5*, 318; i) C. Ma, X. Zhang, K. Wang, X. Zhang, Y. Zhou, H. Liu, Y. Wei, *Polym. Chem.* **2015**, *6*, 3634; j) M. Paramasivam, S. Kanvah, *J. Phys. Chem. C* **2016**, *120*, 10757; k) A.-X. Ding, H.-J. Hao, Y.-G. Gao, Y.-D. Shi, Q. Tang, Z.-L. Lu, *J. Mater. Chem. C* **2016**, *4*, 5379.

[111] D.-M. Li, Y.-S. Zheng, *J. Org. Chem.* **2011**, *76*, 1100.

[112] a) J. Sun, X. Lv, M. Ouyang, Q. Wu, C. Zhang, *Integr. Ferroelectr.* **2014**, *153*, 42; b) B. Shi, K. Jie, Y. Zhou, J. Zhou, D. Xia, F. Huang, *J. Am. Chem. Soc.* **2016**, *138*, 80; c) B. K. An, D. S. Lee, J. S. Lee, Y. S. Park, H. S. Song, S. Y. Park, *J. Am. Chem. Soc.* **2004**, *126*, 10232; d) J. W. Chung, B. K. An, S. Y. Park, *Chem. Mater.* **2008**, *20*, 6750; e) T. Hirose, K. Matsuda, *Chem. Commun.* **2009**, 5832; f) T. Hirose, K. Higashiguchi, K. Matsuda, *Chem. Asian J.* **2011**, *6*, 1057; g) T. Noguchi, B. Roy, D. Yoshihara, Y. Tsuchiya, T. Yamamoto, S. Shinkai, *Chem. Eur. J.* **2014**, *20*, 13938.

[113] a) X. Li, L. Zhu, S. Duan, Y. Zhao, H. Agren, *Phys. Chem. Chem. Phys.* **2014**, *16*, 23854; b) Y. Jin, Y. Xia, S. Wang, L. Yan, Y. Zhou, J. Fan, B. Song, *Soft Matter* **2015**, *11*, 798; c) L. Zhu, X. Li, Q. Zhang, X. Ma, M. Li, H. Zhang, Z. Luo, H. Agren, Y. Zhao, *J. Am. Chem. Soc.* **2013**, *135*, 5175.

[114] a) J. W. Chung, B.-K. An, J. W. Kim, J.-J. Kim, S. Y. Park, *Chem. Commun.* **2008**, 2998; b) S. Shin, S. H. Gihm, C. R. Park, S. Kim, S. Y. Park, *Chem. Mater.* **2013**, *25*, 3288; c) G. Tian, N. Xiang, H. Zhou, Y. Li, B. Li, Q. Wang, J. Su, *Tetrahedron* **2016**, *72*, 298; d) W. Fang, G. Zhang, J. Chen, L. Kong, L. Yang, H. Bi, J. Yang, *Sens. Actuator B-Chem.* **2016**, *229*, 338.

[115] a) F. Yu, Y. Yang, A. Wang, B. Hu, X. Luo, R. Sheng, Y. Dong, W. Fan, *New J. Chem.* **2015**, *39*, 9743; b) V. Palakollu, S. Kanvah, *RSC Adv.* **2015**, *5*, 33049; c) P. Xing, H. Chen, L. Bai, Y. Zhao, *Chem. Commun.* **2015**, *51*, 9309.

[116] a) S. Kim, C.-K. Lim, J. Na, Y.-D. Lee, K. Kim, K. Choi, J. F. Leary, I. C. Kwon, *Chem. Commun.* **2010**, *46*, 1617; b) M. Maurin, O. Stéphan, J.-C. Vial, S. R. Marder, B. van der Sanden, *BIOMEDO* **2011**, *16*, 036001; c) D. Wang, J. Qian, S. He, J. S. Park, K.-S. Lee, S. Han, Y. Mu, *Biomaterials* **2011**, *32*, 5880; d) A. M. Asiri, S. A. El-Daly, K. A. Alamry, M. N. Arshad, M. Pannipara, *J. Mol. Struct.* **2015**, *1098*, 153; e) M. Pannipara, A. M. Asiri, K. A. Alamry, I. A. Salem, S. A. El-Daly, *J. Lumin.* **2015**, *157*, 163; f) X. Wang, Z. Gao, J. Zhu, Z. Gao, F. Wang, *Polym. Chem.* **2016**, *7*, 5217; g) V. Palakollu, A. K. Vasu, V. Thiruvenkatam, S. Kanvah, *New J. Chem.* **2016**, *40*, 4588.

[117] a) F. J. M. Hoeben, I. O. Shklyarevskiy, M. J. Pouderoijen, H. Engelkamp, A. P. H. J. Schenning, P. C. M. Christianen, J. C. Maan, E. W. Meijer, *Angew. Chem. Int. Ed.* **2006**, *45*, 1232; b) C. Y. Y. Yu, W. Zhang, R. T. K. Kwok, C. W. T. Leung, J. W. Y. Lam, B. Z. Tang, *J. Mater. Chem. B* **2016**, *4*, 2614; c) P. Xing, H. Chen, M. Ma, X. Xu, A. Hao, Y. Zhao, *Nanoscale* **2016**, *8*, 1892; d) M. Yang, P. Xing, M. Ma, Y. Zhang, Y. Wang, A. Hao, *Soft Matter* **2016**, *12*, 6038; e) L.-L. Zhu, D.-H. Qu, D. Zhang, Z.-F. Chen, Q.-C. Wang, H. Tian, *Tetrahedron* **2010**, *66*, 1254.

[118] a) N. Sanz, P. L. Baldeck, J.-F. Nicoud, Y. Le Fur, A. Ibanez, *Solid State Sciences* **2001**, *3*, 867; b) K. A. N. Upamali, L. A. Estrada, P. K. De, X. Cai, J. A. Krause, D. C.

Neekers, *Langmuir* **2011**, *27*, 1573; c) L. Zhu, C. Y. Ang, X. Li, N. Kim Truc, S. Y. Tan, H. Agren, Y. Zhao, *Adv. Mater.* **2012**, *24*, 4020.

[119] X. Zhang, X. Zhang, B. Yang, Y. Yang, Y. Wei, *Polym. Chem.* **2014**, *5*, 5885.

[120] F. Ito, J.-i. Fujimori, N. Oka, M. Sliwa, C. Ruckebusch, S. Ito, H. Miyasaka, *Faraday Discuss.* **2017**, *196*, 231.

[121] V. L. Tran, V. Genot, J.-F. Audibert, Y. Prokazov, E. Turbin, W. Zuschratter, H.-J. Kim, J. Jung, S. Y. Park, R. B. Pansu, *New J. Chem.* **2016**, *40*, 4601.

[122] a) Z.-Q. Yan, Z.-Y. Yang, H. Wang, A.-W. Li, L.-P. Wang, H. Yang, B.-R. Gao, *Spectrochim. Acta Mol. Biomol. Spectrosc.* **2011**, *78*, 1640; b) H. Lu, Y. Zheng, X. Zhao, L. Wang, S. Ma, X. Han, B. Xu, W. Tian, H. Gao, *Angew. Chem. Int. Ed.* **2016**, *55*, 155.

[123] a) C. Ma, X. Zhang, Y. Yang, Z. Ma, L. Yang, Y. Wu, H. Liu, X. Jia, Y. Wei, *J. Mater. Chem. C* **2016**, *4*, 4786; b) B.-K. An, S.-K. Kwon, S. Y. Park, *Bull. Korean Chem. Soc* **2005**, *26*, 1555.

[124] a) J. S. Park, R. H. Kim, N. S. Cho, H.-K. Shim, K.-S. Lee, *J. Nanosci. Nanotechnol.* **2008**, *8*, 4793; b) Y. Liu, M. Kong, Q. Zhang, Z. Zhang, H. Zhou, S. Zhang, S. Li, J. Wu, Y. Tian, *J. Mater. Chem. B* **2014**, *2*, 5430.

[125] a) W. Huang, H. Zhou, B. Li, J. Su, *RSC Adv.* **2013**, *3*, 3038; b) S. B. Noh, R. H. Kim, W. J. Kim, S. Kim, K.-S. Lee, N. S. Cho, H.-K. Shim, H. E. Pudavar, P. N. Prasad, *J. Mater. Chem.* **2010**, *20*, 7422; c) H. Zhou, W. Huang, L. Ding, S. Cai, X. Li, B. Li, J. Su, *Tetrahedron* **2014**, *70*, 7050; d) T. Jiang, D. Li, Y. Hang, Y. Gao, H. Zhang, X. Zhao, X. Li, B. Li, J. Qian, J. Hua, *Dyes Pigments* **2016**, *133*, 201.

[126] a) C.-K. Lim, S. Kim, I. C. Kwon, C.-H. Ahn, S. Y. Park, *Chem. Mater.* **2009**, *21*, 5819; b) Y. H. Seo, A. Singh, H.-J. Cho, Y. Kim, J. Heo, C.-K. Lim, S. Y. Park, W.-D. Jang, S. Kim, *Biomaterials* **2016**, *84*, 111.

[127] R. Guan, H. Wang, Q. Zhang, J. Wu, Y. Tian, *Dyes Pigments* **2017**, *136*, 473.

[128] C. Y. Y. Yu, H. Xu, S. Ji, R. T. K. Kwok, J. W. Y. Lam, X. Li, S. Krishnan, D. Ding, B. Z. Tang, *Adv. Mater.* **2017**, 1606167.

[129] S. Haupt, I. Lazar, H. Weitman, M. O. Senge, B. Ehrenberg, *Phys. Chem. Chem. Phys.* **2015**, *17*, 11412.

[130] F. Wang, X. Li, S. Wang, C.-P. Li, H. Dong, X. Ma, S.-H. Kim, D.-R. Cao, *Chin. Chem. Lett.* **2016**, *27*, 1592.

[131] G. A. Sherwood, R. Cheng, K. Chacon-Madrid, T. M. Smith, L. A. Peteanu, J. Wildeman, *J. Phys. Chem. C* **2010**, *114*, 12078.

[132] C. H. Chen, S. L. Lee, T. S. Lim, C. H. Chen, T. Y. Luh, *Polym. Chem.* **2011**, *2*, 2850.

[133] Z. Qiu, T. Han, R. T. K. Kwok, J. W. Y. Lam, B. Z. Tang, *Macromolecules* **2016**, *49*, 8888.

[134] a) H.-J. Kim, D. R. Whang, J. Gierschner, S. Y. Park, *Angew. Chem. Int. Ed.* **2016**, *55*, 15915; b) X. Xu, S. Yan, Y. Zhou, R. Huang, Y. Chen, J. Wang, X. Weng, X. Zhou, *Bioorg. Med. Chem. Lett.* **2014**, *24*, 1654; c) Y. Zhao, C. Y. Y. Yu, R. T. K. Kwok, Y. Chen, S. Chen, J. W. Y. Lam, B. Z. Tang, *J. Mater. Chem. B* **2015**, *3*, 4993.

[135] X. Zhang, X. Zhang, B. Yang, J. Hui, M. Liu, W. Liu, Y. Chen, Y. Wei, *Polym. Chem.* **2014**, *5*, 689.

[136] Z. Long, M. Liu, Q. Wan, L. Mao, H. Huang, G. Zeng, Y. Wan, F. Deng, X. Zhang, Y. Wei, *Macromol. Rapid Commun.* **2016**, *37*, 1754.

[137] Z. Long, M. Liu, K. Wang, F. Deng, D. Xu, L. Liu, Y. Wan, X. Zhang, Y. Wei, *Mater. Sci. Eng., C* **2016**, *66*, 215.

[138] F. Treussart, E. Botzung-Appert, N.-T. Ha-Duong, A. Ibanez, J.-F. Roch, R. Pansu, *ChemPhysChem* **2003**, *4*, 757.

[139] a) C.-W. Chang, C. J. Bhongale, C.-S. Lee, W.-K. Huang, C.-S. Hsu, E. W.-G. Diau, *J. Phys. Chem. C* **2012**, *116*, 15146; b) B.-K. An, S.-K. Kwon, S. Y. Park, *Angew. Chem. Int. Ed.* **2007**, *46*, 1978; c) M. Tanaka, Y. Oki, D. Nagano, B.-K. An, S. Y. Park, M. Maeda, *Mol.*

Cryst. Liq. Cryst. **2007**, *463*, 173/[455]; d) S.-J. Lim, B.-K. An, S. D. Jung, M.-A. Chung, S. Y. Park, *Angew. Chem. Int. Ed.* **2004**, *43*, 6346.

[140] C. Wei, S.-Y. Liu, C.-L. Zou, Y. Liu, J. Yao, Y. S. Zhao, *J. Am. Chem. Soc.* **2015**, *137*, 62.

[141] T. Noguchi, B. Roy, D. Yoshihara, J. Sakamoto, T. Yamamoto, S. Shinkai, *Angew. Chem. Int. Ed.* **2016**, *55*, 5708.

[142] V. Palakollu, S. Kanvah, *New J. Chem.* **2014**, *38*, 5736.

[143] K. A. N. Upamali, L. A. Estrada, D. C. Neckers, *Analytical Methods* **2011**, *3*, 2469.

[144] a) G. Zhang, A. Ding, Y. Zhang, L. Yang, L. Kong, X. Zhang, X. Tao, Y. Tian, J. Yang, *Sens. Actuator B-Chem.* **2014**, *202*, 209; b) A. Wang, Y. Yang, F. Yu, L. Xue, B. Hu, W. Fan, Y. Dong, *Talanta* **2015**, *132*, 864.

[145] A. Ding, L. Yang, Y. Zhang, G. Zhang, L. Kong, X. Zhang, Y. Tian, X. Tao, J. Yang, *Chem. Eur. J.* **2014**, *20*, 12215.

[146] Y.-S. Zheng, Y.-J. Hu, *J. Org. Chem.* **2009**, *74*, 5660.

[147] L. L. Zhu, X. Li, F.-Y. Ji, X. Ma, Q.-C. Wang, H. Tian, *Langmuir* **2009**, *25*, 3482.

[148] J. H. Kim, Y. Jung, J. W. Chung, B.-K. An, S. Y. Park, *Small* **2009**, *5*, 804.

[149] J. H. Kim, A. Watanabe, J. W. Chung, Y. Jung, B.-K. An, H. Tada, S. Y. Park, *J. Mater. Chem.* **2010**, *20*, 1062.

[150] Y. D. Han, J. H. Kim, J. W. Lee, H. Lee, J. H. Kim, J. Kim, S. Y. Park, J. Joo, *Synth. Met.* **2012**, *162*, 1299.

[151] a) S. S. Babu, V. K. Praveen, A. Ajayaghosh, *Chem. Rev.* **2014**, *114*, 1973; b) R. G. Weiss, *J. Am. Chem. Soc.* **2014**, *136*, 7519; c) C. D. Jones, J. W. Steed, *Chem. Soc. Rev.* **2016**, *45*, 6546.

[152] a) J. Seo, J. W. Chung, E.-H. Jo, S. Y. Park, *Chem. Commun.* **2008**, 2794; b) J. W. Chung, S.-J. Yoon, S.-J. Lim, B.-K. An, S. Y. Park, *Angew. Chem. Int. Ed.* **2009**, *48*, 7030; c) P. Xue, R. Lu, L. Zhao, D. Xu, X. Zhang, K. Li, Z. Song, X. Yang, M. Takafuji, H. Ihara,

Langmuir **2010**, *26*, 6669; d) D.-M. Li, H. Wang, Y.-S. Zheng, *Chem. Commun.* **2012**, *48*, 3176; e) Y.-C. Chen, H. Wang, D.-M. Li, Y.-S. Zheng, *Eur. J. Org. Chem.* **2013**, *2013*, 1521; f) P. Xue, R. Lu, P. Zhang, J. Jia, Q. Xu, T. Zhang, M. Takafuji, H. Ihara, *Langmuir* **2013**, *29*, 417; g) J. Han, J. You, X. Li, P. Duan, M. Liu, *Adv. Mater.* **2017**, *29*, 1606503.

[153] a) X. Tong, Y. Zhao, B. K. An, S. Y. Park, *Adv. Funct. Mater.* **2006**, *16*, 1799; b) X. Tong, J. W. Chung, S. Y. Park, Y. Zhao, *Langmuir* **2009**, *25*, 8532.

[154] a) H. Nam, B. Boury, S. Y. Park, *Chem. Mater.* **2006**, *18*, 5716; b) H. Kim, J. Y. Chang, *Langmuir* **2014**, *30*, 13673.

[155] a) P. Xue, R. Lu, X. Yang, L. Zhao, D. Xu, Y. Liu, H. Zhang, H. Nomoto, M. Takafuji, H. Ihara, *Chem. Eur. J.* **2009**, *15*, 9824; b) P. Xue, Y. Zhang, J. Jia, D. Xu, X. Zhang, X. Liu, H. Zhou, P. Zhang, R. Lu, M. Takafuji, H. Ihara, *Soft Matter* **2011**, *7*, 8296; c) P. Xue, R. Lu, J. Jia, M. Takafuji, H. Ihara, *Chem. Eur. J.* **2012**, *18*, 3549; d) P. Xue, J. Sun, Q. Xu, R. Lu, M. Takafuji, H. Ihara, *Org. Biomol. Chem.* **2013**, *11*, 1840; e) Y. Zhang, S. Jiang, *Org. Biomol. Chem.* **2012**, *10*, 6973; f) Y. Zhang, C. Liang, H. Shang, Y. Ma, S. Jiang, *J. Mater. Chem. C* **2013**, *1*, 4472; g) J. Seo, J. W. Chung, J. E. Kwon, S. Y. Park, *Chem. Sci.* **2014**, *5*, 4845; h) O. Simalou, R. Lu, P. Xue, P. Gong, T. Zhang, *Eur. J. Org. Chem.* **2014**, *2014*, 2907; i) P. Xue, B. Yao, P. Wang, P. Gong, Z. Zhang, R. Lu, *Chem. Eur. J.* **2015**, *21*, 17508; j) F. Aparicio, S. Cherumukkil, A. Ajayaghosh, L. Sánchez, *Langmuir* **2016**, *32*, 284; k) Y. Ma, M. Cametti, Z. Dzolic, S. Jiang, *J. Mater. Chem. C* **2016**, *4*, 10786.

[156] a) Y. Xu, P. Xue, D. Xu, X. Zhang, X. Liu, H. Zhou, J. Jia, X. Yang, F. Wang, R. Lu, *Org. Biomol. Chem.* **2010**, *8*, 4289; b) P. Xue, B. Yao, Y. Zhang, P. Chen, K. Li, B. Liu, R. Lu, *Org. Biomol. Chem.* **2014**, *12*, 7110; c) S. Wang, P. Xue, P. Wang, B. Yao, K. Li, B. Liu, *Dyes Pigments* **2015**, *122*, 302.

[157] J. Seo, J. W. Chung, I. Cho, S. Y. Park, *Soft Matter* **2012**, *8*, 7617.

[158] Y. Zhang, Y. Ma, M. Deng, H. Shang, C. Liang, S. Jiang, *Soft Matter* **2015**, *11*, 5095.

[159] S.-J. Yoon, J. H. Kim, J. W. Chung, S. Y. Park, *J. Mater. Chem.* **2011**, *21*, 18971.

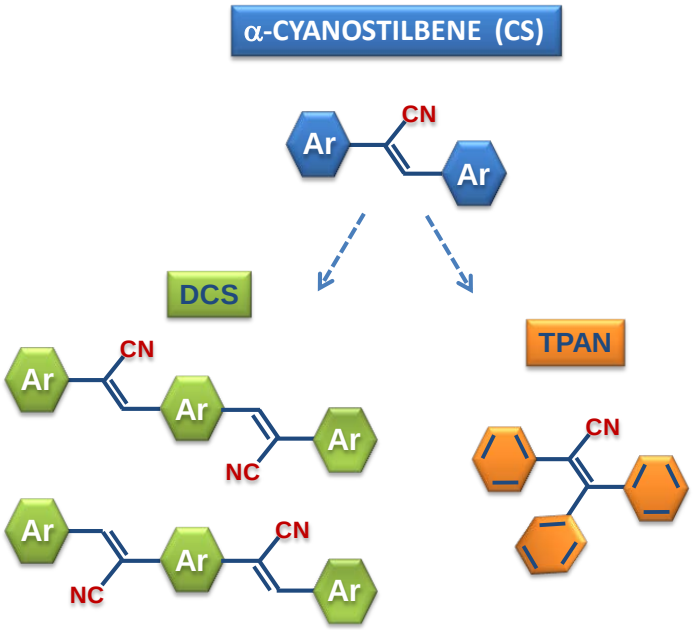

Figure 1. General structure of α-cyanostilbene (CS) and relevant subfamilies, dicyanodistyrylbenzene (DCS) and 2,3,3-triphenylacrylonitrile (TPAN). Ar stands for any aromatic ring.

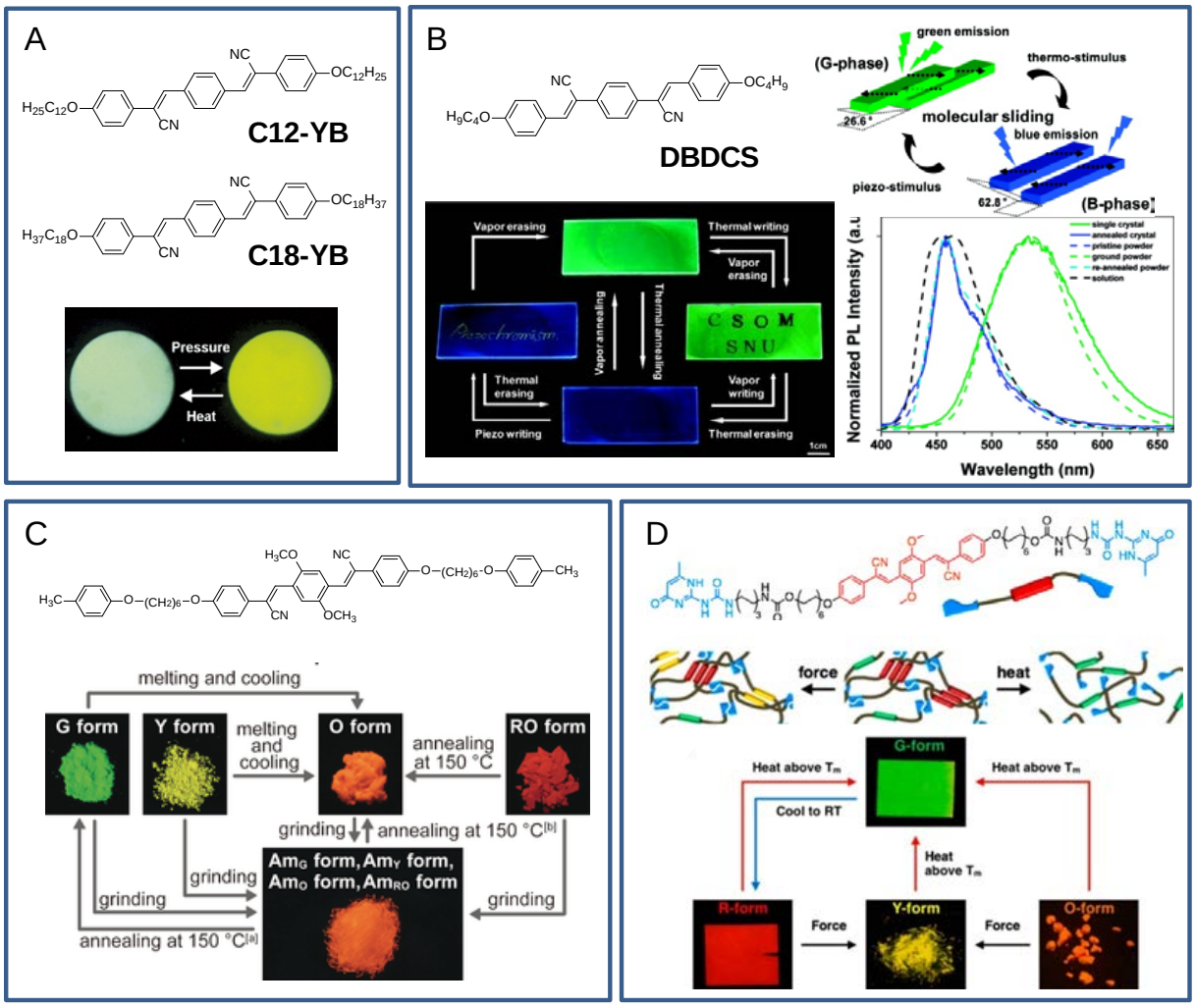

Figure 2. Selected alkoxy-substituted DCS compounds with mechanofluorochromic properties. **A:** Reproduced with permission.[12] Copyright 2008, Wiley-VCH. **B:** Adapted with permission.[14a] Copyright 2010, American Chemical Society. **C:** Reproduced with permission.[18] Copyright 2016, Wiley-VCH. **D:** Adapted with permission.[20] Copyright 2017, American Chemical Society.

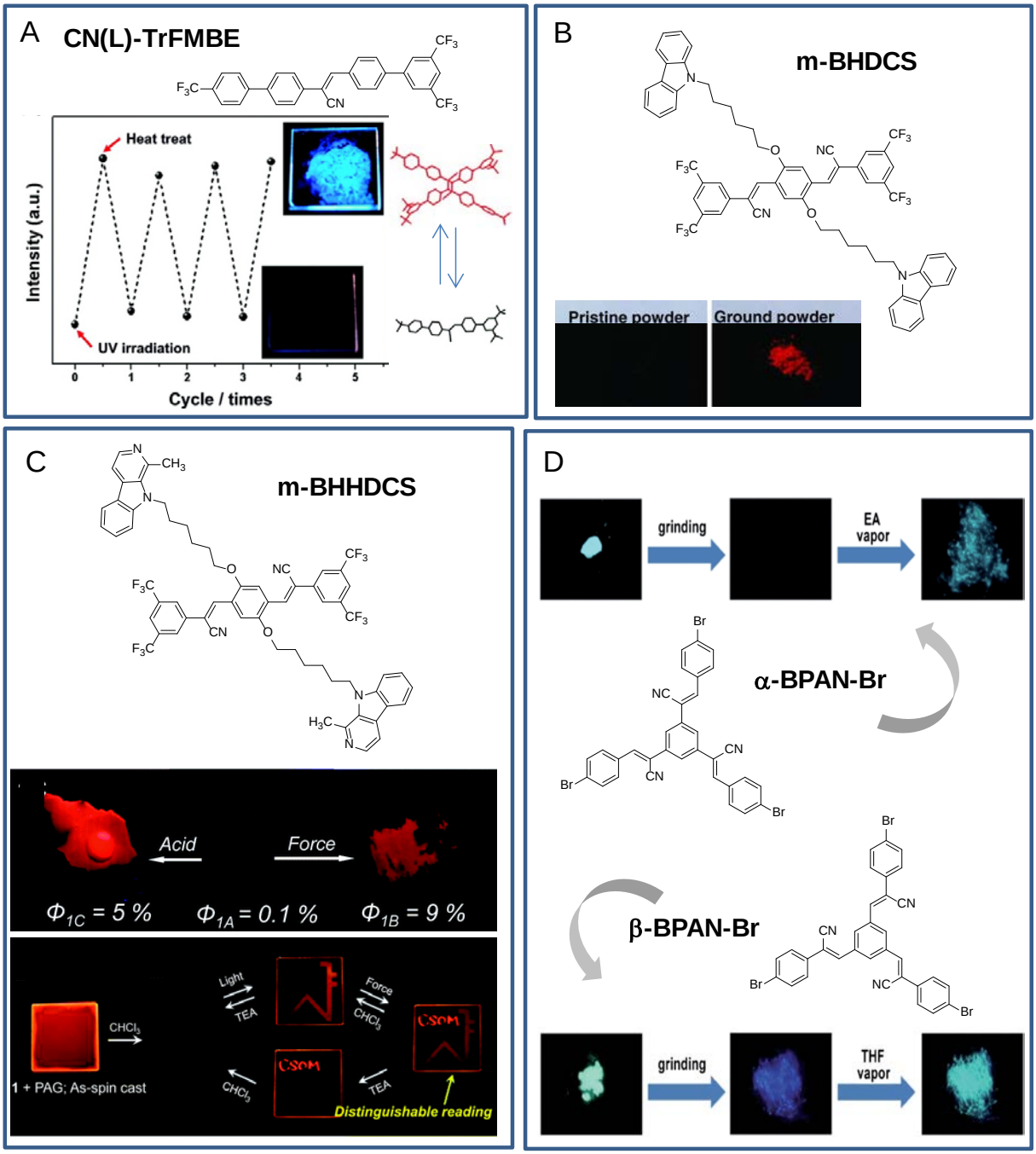

Figure 3. Selected CS materials with mechanically induced on/off fluorescence switching. **A:** Adapted with permission.[23a] Copyright 2009, American Chemical Society. **B:** Adapted with permission.[23b] Copyright 2012, Wiley-VCH. **C:** Adapted with permission.[23c] Copyright 2014, The Royal Society of Chemistry. **D:** Adapted with permission.[25] Copyright 2014, The Royal Society of Chemistry.

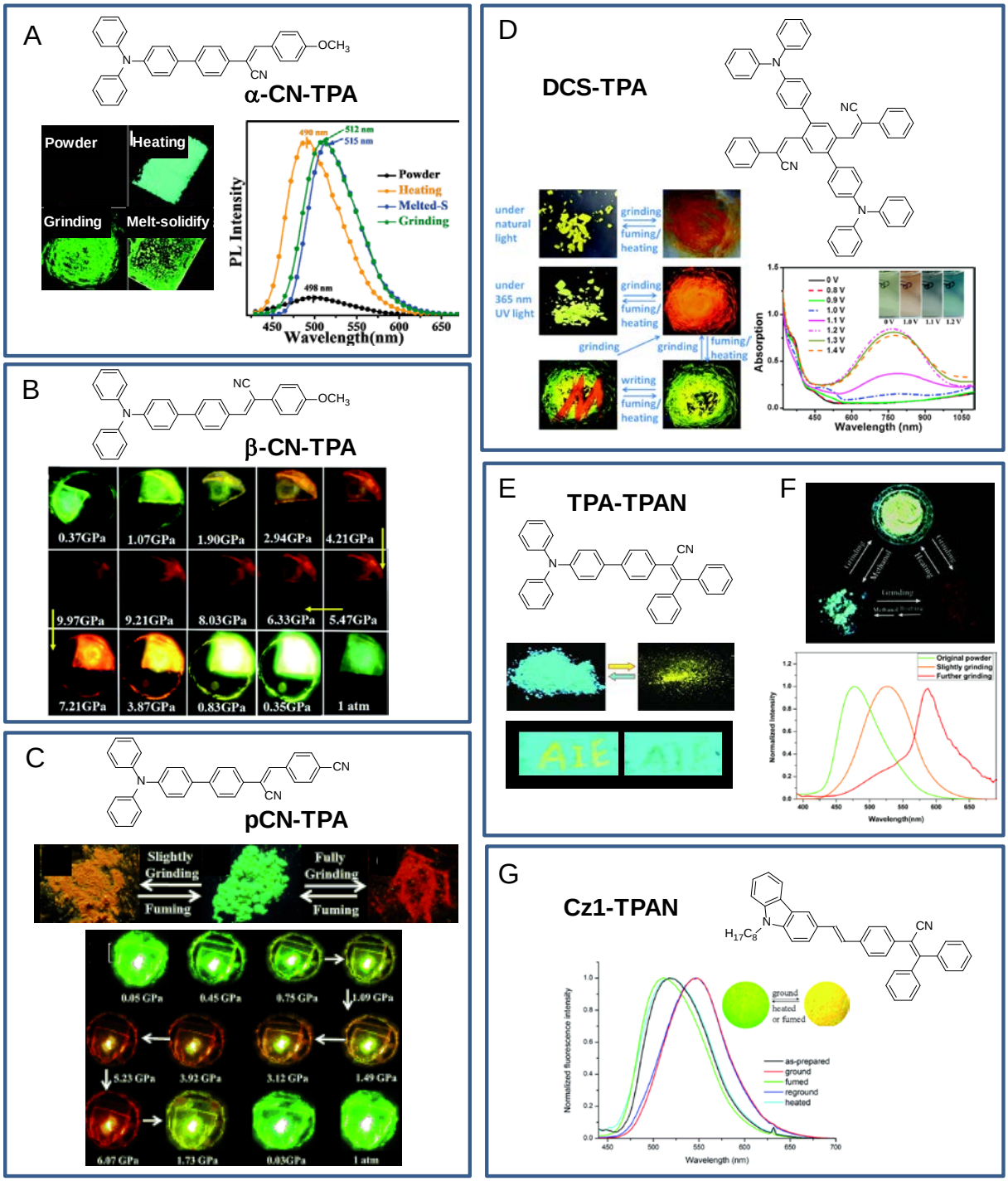

Figure 4. Selected triphenylamine and carbazole-containing CS compounds with mechanofluorochromic properties. **A:** Adapted with permission.[26b] Copyright 2013, The Royal Society of Chemistry. **B:** Reproduced with permission.[27] Copyright 2016, The Royal Society of Chemistry. **C:** Adapted with permission.[28] Copyright 2015, Wiley-VCH. **D:** Adapted with permission.[29b] Copyright 2015, The Royal Society of Chemistry. **E:** Adapted with permission.[33a] Copyright 2013, Wiley-VCH. **F:** Reproduced with permission.[34] Copyright 2016, The Royal Society of Chemistry. **G:** Reproduced with permission.[36b] Copyright 2016, The Royal Society of Chemistry.

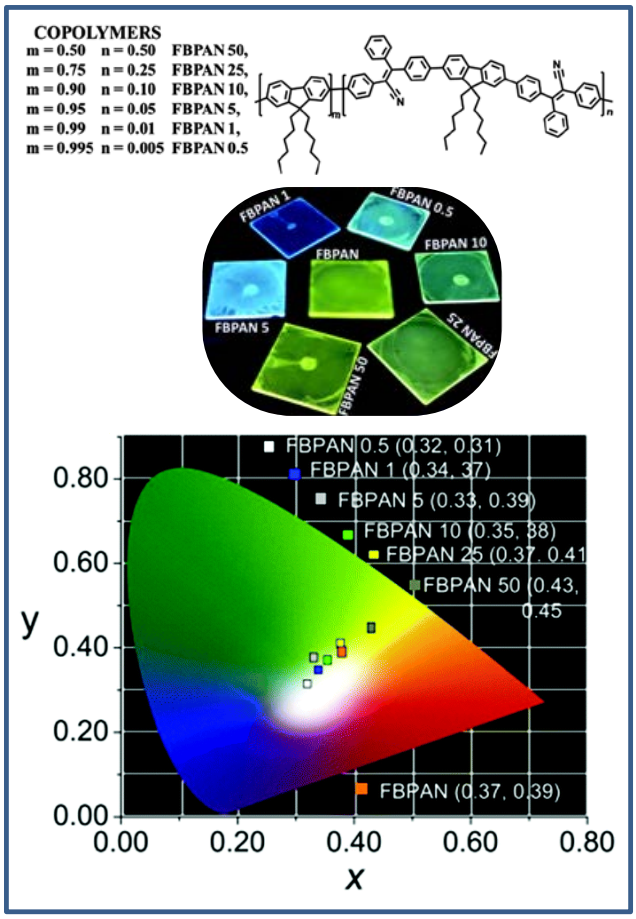

Figure 5. TPAN copolymers for WOLEDs. Adapted with permission.[66] Copyright 2016, The Royal Society of Chemistry.

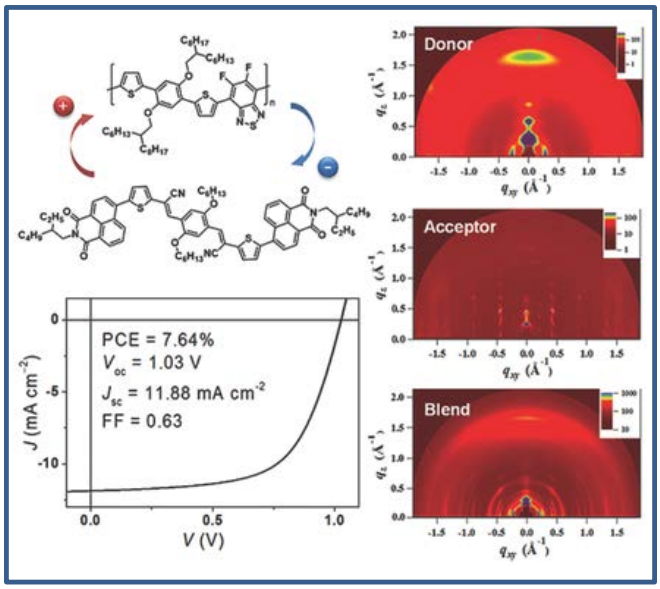

Figure 6. *J–V* curve of a BHJ device made from a blend of polymeric donor, PPDT2FBT, and a CS-naphthalimide acceptor, NIDCS-HO. GIWAXS patterns of the pure and blend films. Adapted with permission.[95c] Copyright 2014, Wiley-VCH.

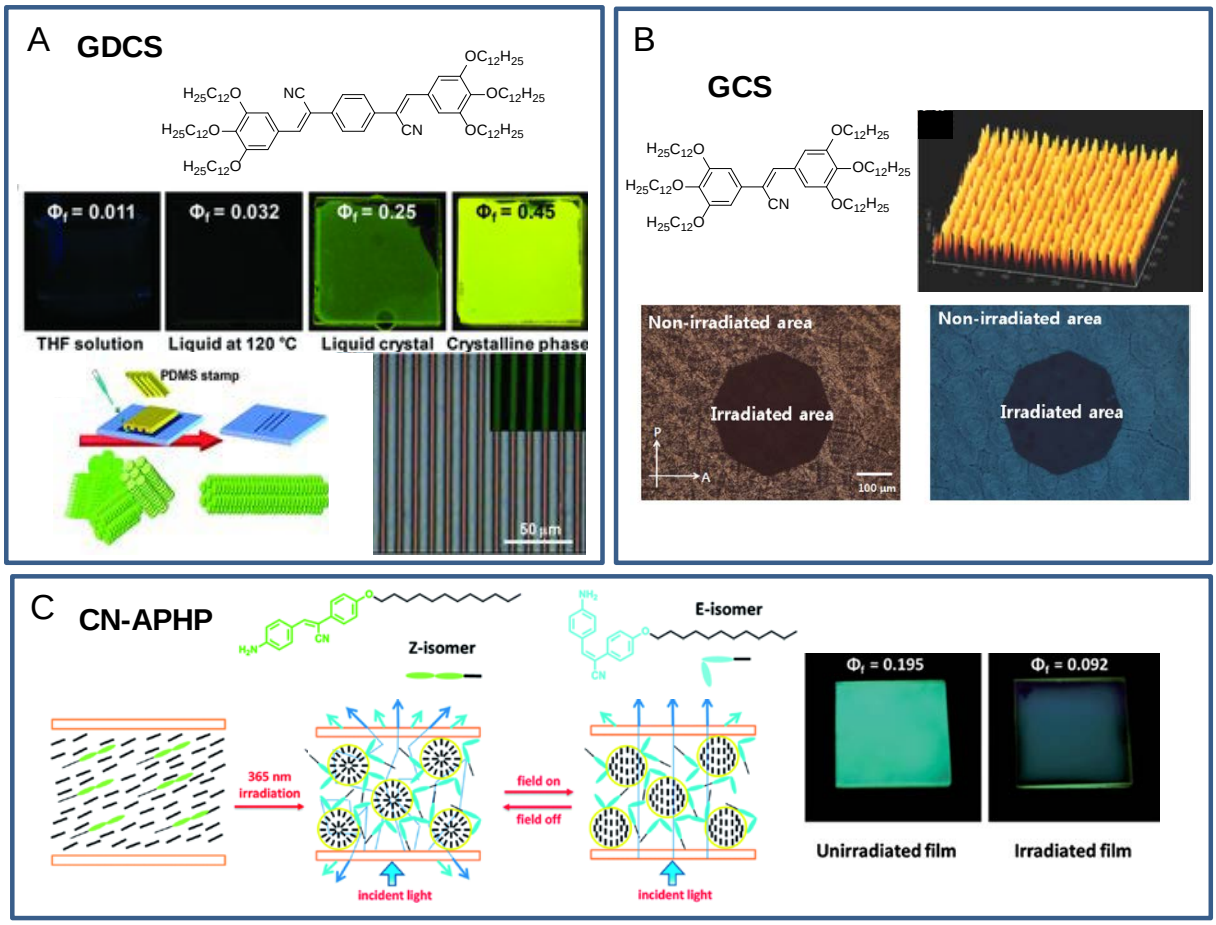

Figure 7. Selected liquid crystalline CS derivatives and their light-responsive properties. **A:** Luminescence thermochromism of GDCS and micromolding in capillaries for the alignment of the columnar mesophase. Adapted with permission.[103a] Copyright 2012, Wiley-VCH. **B:** 3D topological AFM image of surface relief formation and textural change and fluorescence change at the optical microscope under light irradiation of GCS. Adapted with permission.[103b] Copyright 2014, Wiley-VCH. **C:** *Z*/*E* photoisomerization of CN-APHP in polymer dispersed liquid crystals and luminescence change upon light irradiation of a thin film. Adapted with permission.[106a] Copyright 2014, The Royal Society of Chemistry.

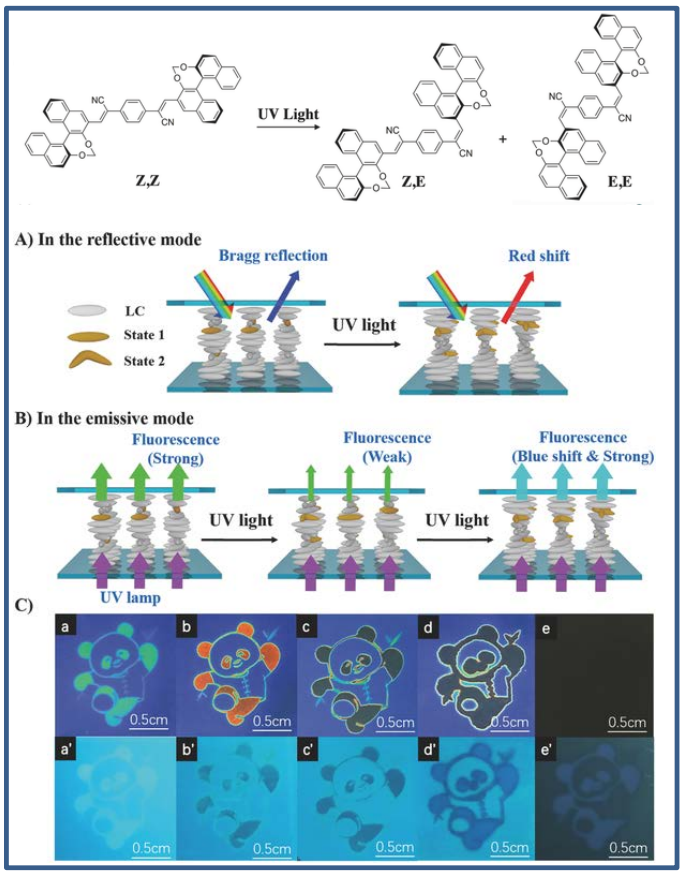

Figure 8. *Z*/*E* photoisomerization under light irradiation of a chiral fluorescent CS compound. Schematic diagrams of: **A:** reflective mode and **B:** emissive mode of cholesteric LC doped with chiral fluorescent photoswitches. **C:** Real cell images, in the reflective mode (a–e) and the corresponding fluorescent images (a'–e') of a 6-µm thick LC cell. The image was recorded in a planar state through a photomask using a 365-nm UV light for different irradiation times (a,a'–2 min; b,b'–4 min; c,c'–6 min; d,d'–25 min). e,e': the sample was irradiated with a 365-nm UV light for 25 min through a photomask and another 5 min without photomask. Adapted with permission.[100c] Copyright 2017, Wiley-VCH.

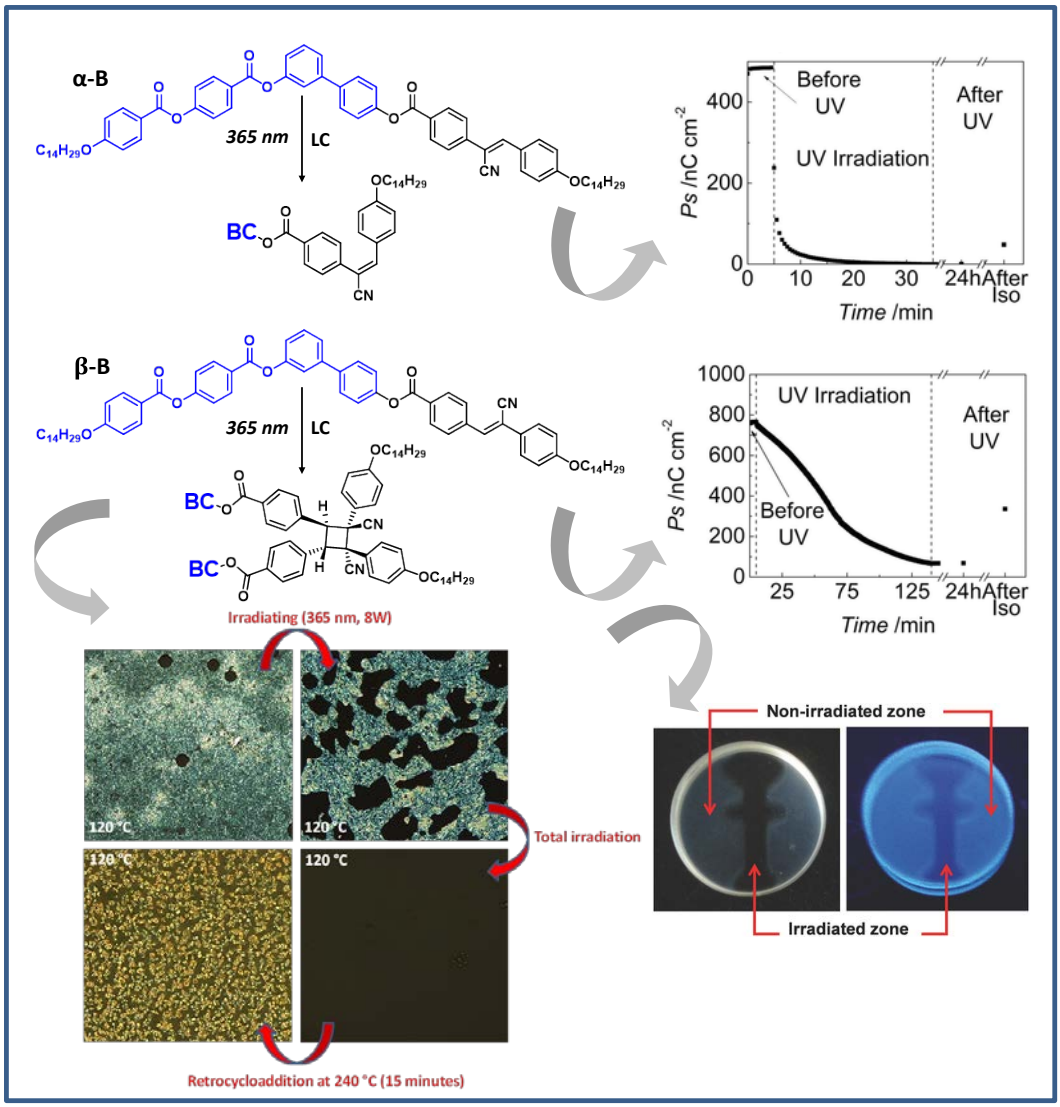

Figure 9. Photochemical reactions of α-B and β-B upon light irradiation and resulting spontaneous polarization drop, textural change of the LC mesophase, and opacity/luminescence changes. Adapted with permission.[108b] Copyright 2016, Wiley-VCH.

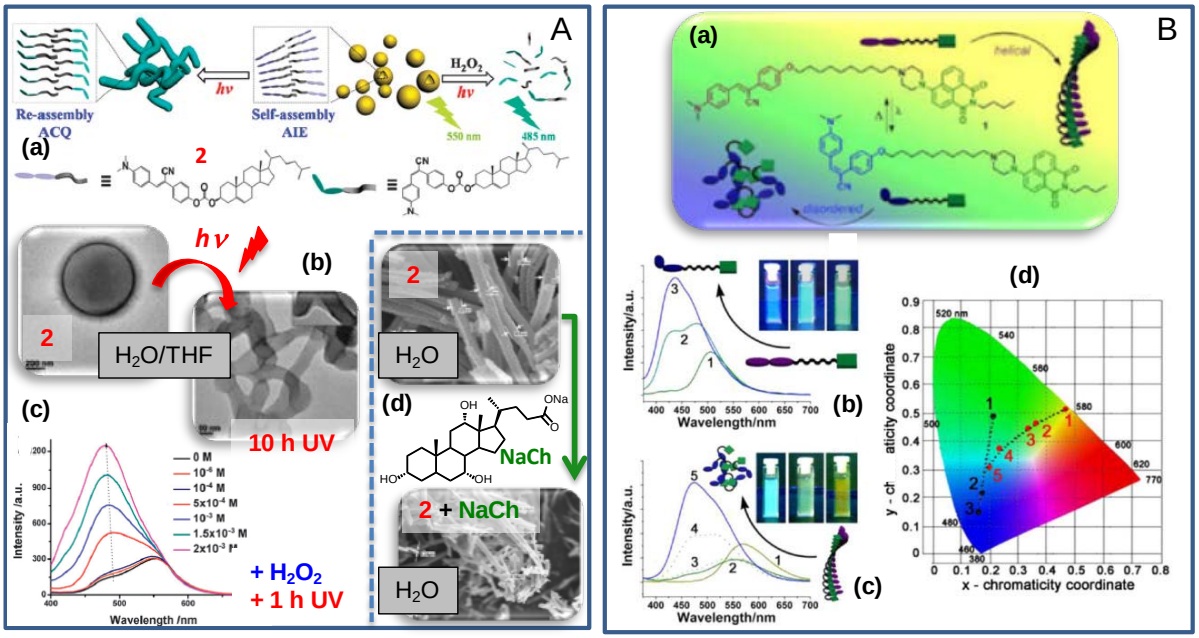

Figure 10. A: (a) Schematic representation of the controlled assembly of compound **2** by varying solvents as well as by UV light irradiation. (b) TEM images of aggregates of compound **2** in H_2O/dioxane (8/2, v/v), and in H_2O/THF (9/1, v/v) after 10 h of UV light irradiation. (c) Fluorescence intensity changes of compound **2** in H_2O/THF (9/1, v/v) upon addition of H_2O_2 with 1 h of UV light irradiation. (d) SEM images of the aggregates of compound **2** in H_2O without and with the addition of sodium cholate (NaCh). Adapted with permission.[115b-c] Copyright 2015, Royal Society of Chemistry. **B:** (a) Z/E isomerization of compound **1** and a schematic representation of the helical and disordered assemblies of the Z-isomer and E-isomer, assisted by the solvent. (b) Emission spectra (λ_{ex} = 365 nm) of compound **1** in THF at (1) initial state and after photoirradiation at 254 nm, (2) 3 h and (3) 6 h. Photos (right-to-left) of the corresponding states 1, 2, and 3 under a UV light (λ = 365 nm). (c) Emission spectra (λ_{ex} = 365 nm) of compound **1** in DMSO with 90% water at (1) initial state and after photoirradiation at 254 nm for (2) 2 h, (3) 3 h, (4) 5 h, and (5) 8 h. Photos (right-to-left) of the corresponding states 1, 2, and 5 under a UV light (λ = 365 nm). (d) CIE 1931 chromaticity diagram with the luminescent color coordinates for the diffrerent states. Adapted with permission.[113c] Copyright 2013, American Chemical Society.

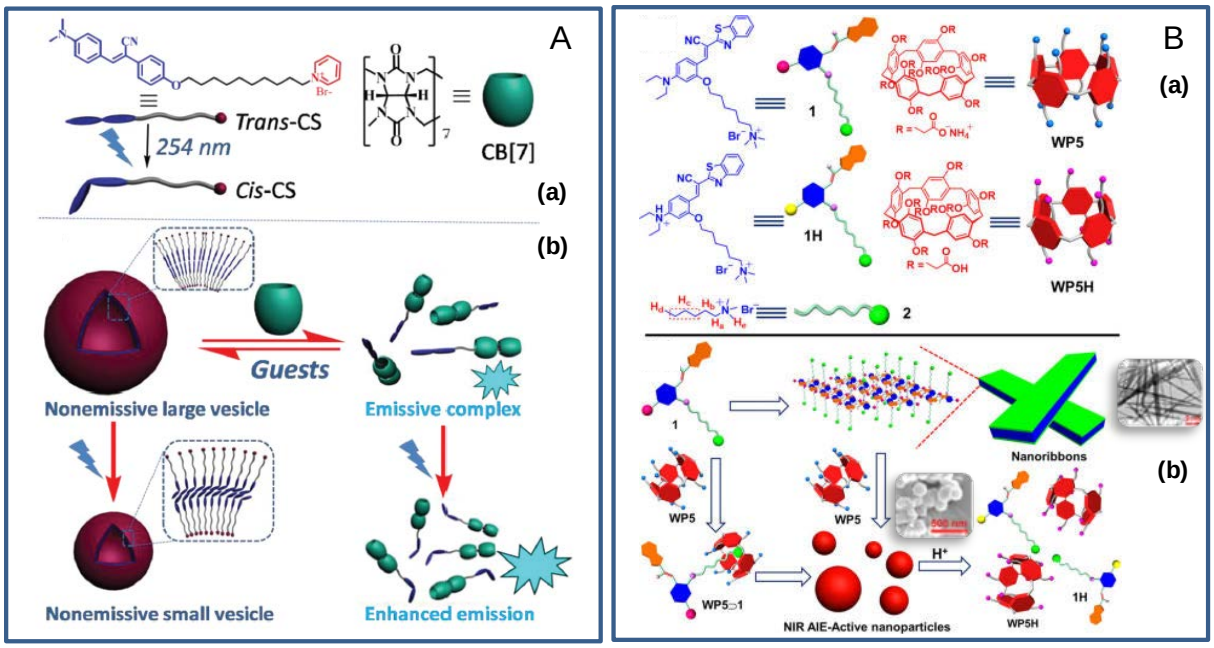

Figure 11. A: (a) Chemical structures of CS and CB[7]. (b) Schematic representation of the controllable self-assemblies of CS by adding CB[7] and under UV light irradiation. Reproduced with permission.[117c] Copyright 2016, Royal Society of Chemistry. **B:** (a) Structures and representations of studied compounds 1, 1H, 2, WP5, and WP5H, and (b) representations of self-assemblies of 1 and WP5⊃1 and pH responsiveness of nanoparticles prepared from WP5⊃1. TEM images of the nanoribbon aggregates of compound 1 and nanoparticles of WP5⊃1 in H_2O. Adapted with permission.[112b] Copyright 2016, American Chemical Society.

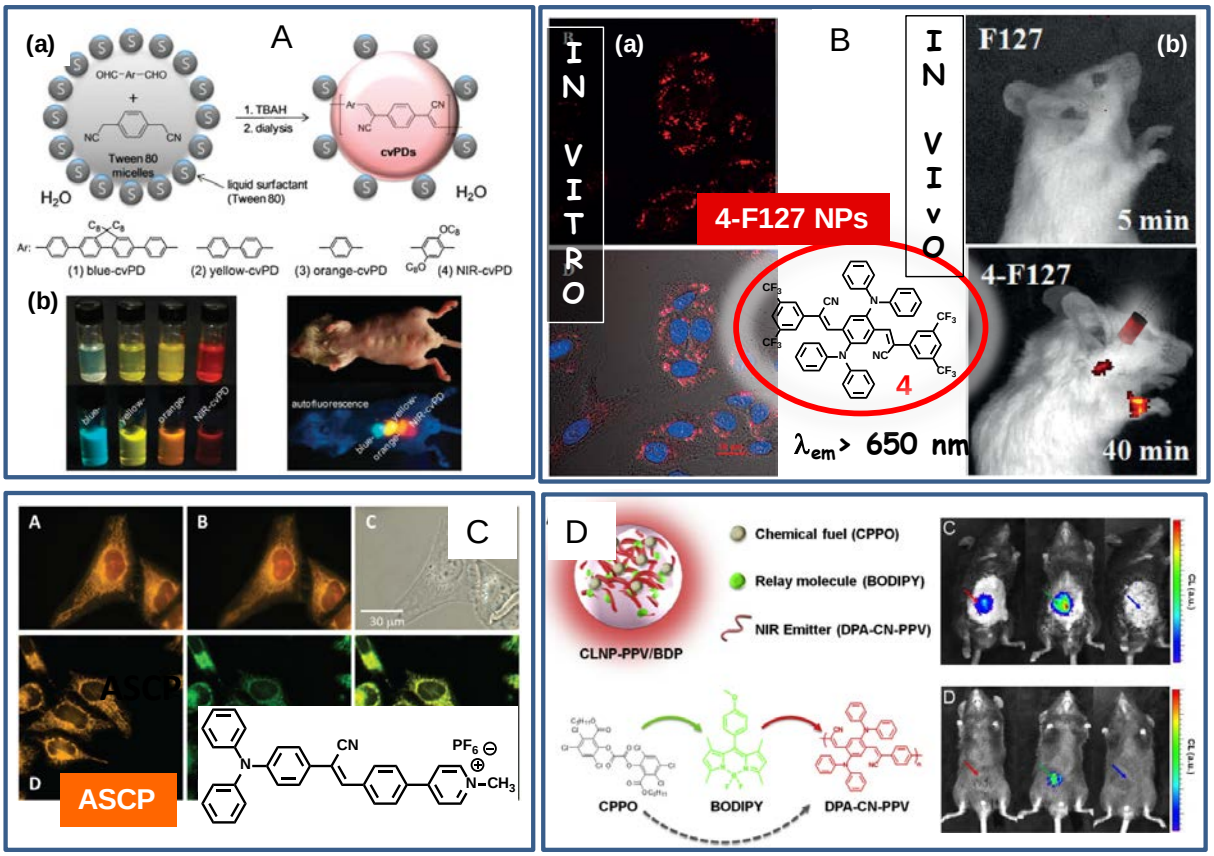

Figure 12. A: (a) Schematic diagram of colloidal synthesis of CS-polymer dots (cvPDs) through TBAH-catalyzed Knoevenagel condensation in solvent-free aqueous micelles. (b) Water-dispersed cvPDs (left) and a cvPD-injected live mouse (right) under ambient light (top) and UV excitation at 365 nm for fluorescence (bottom). Adapted with permission.[116a] Copyright 2010, Royal Society of Chemistry. **B:** Structure of the fluorophore **4** embedded in F127. (a) CLSM images of A549 cells incubated with 4-F127 NPs. (b) In vivo fluorescence images of mice with F127 and 4-F127 NPs at 40 min. Adapted with permission.[122b] Copyright 2016, Wiley-VCH. **C:** (A and B) Fluorescence and (C) bright-field images of HeLa cells stained with ASCP (5 mM) for 30 min with focus at mitochondria (A) and nucleolus (B), respectively. λ_{ex} = 460–490 nm. (D) Confocal images of HeLa cells stained with ASCP. Adapted with permission.[117b] Copyright 2016, Royal Society of Chemistry. **D:** (A) Schematic representation of the energy-relayed CLNP-PPV/BDP nanoparticle and intraparticle energy-relay between the encased molecules therein. Solid and dashed arrows indicate efficient and inefficient energy transfers, respectively. (B, C) In vivo imaging (left) and intensity plots (right) of CL signals generated by peritonitis in hair-shaved and unshaved mice, taken at 1 min after the intra-peritoneal probe injection: (red arrow/bar) inflamed, CLNP-PPV; (green arrow/bar) inflamed, CLNP-PPV/BDP; (blue arrow/bar) normal, CLNP-PPV/BDP. Adapted with permission.[126b] Copyright 2016, Elsevier Ltd.

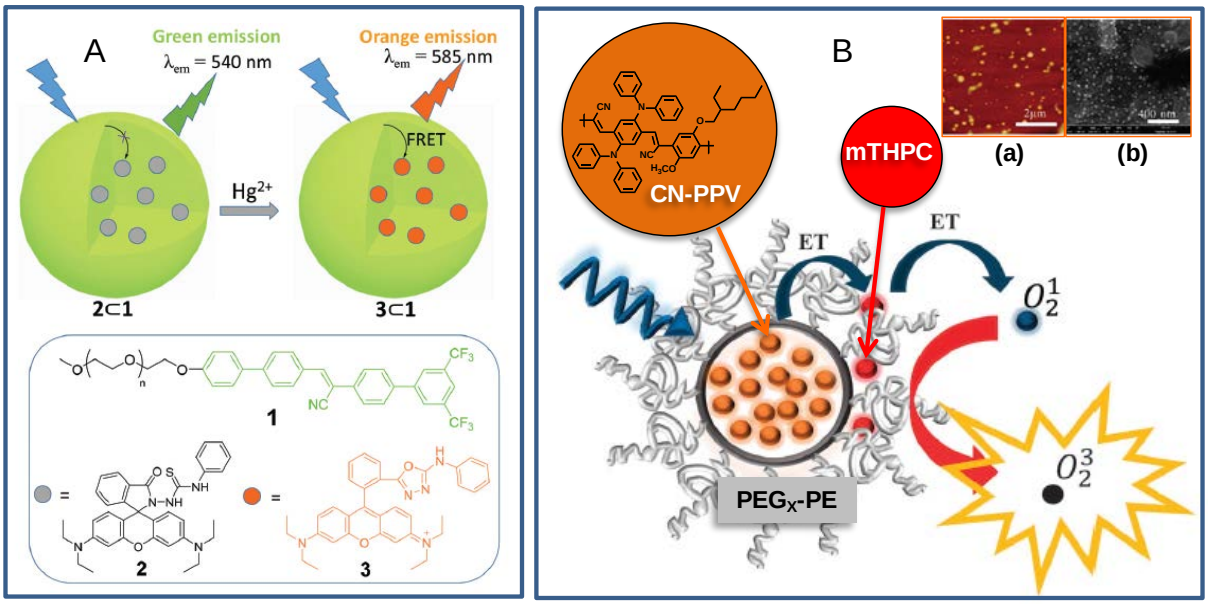

Figure 13. A: Schematic representation for the construction of the self-assembled AIE system with amphipilic-CS **1** for FRET-based ratiometric detection of Hg^{2+} ions. Reproduced with permission.[116f] Copyright 2016, Royal Society of Chemistry**. B:** Pdot nanoparticle based on CN-PPV enhance the singlet oxygen production by FRET to the photosensitizer. (a) AFM and (b) HR-SEM images of the Pdots with PEG350-PE coating. Adapted with permission.[129] Copyright 2015, PCCP Owner Societies.

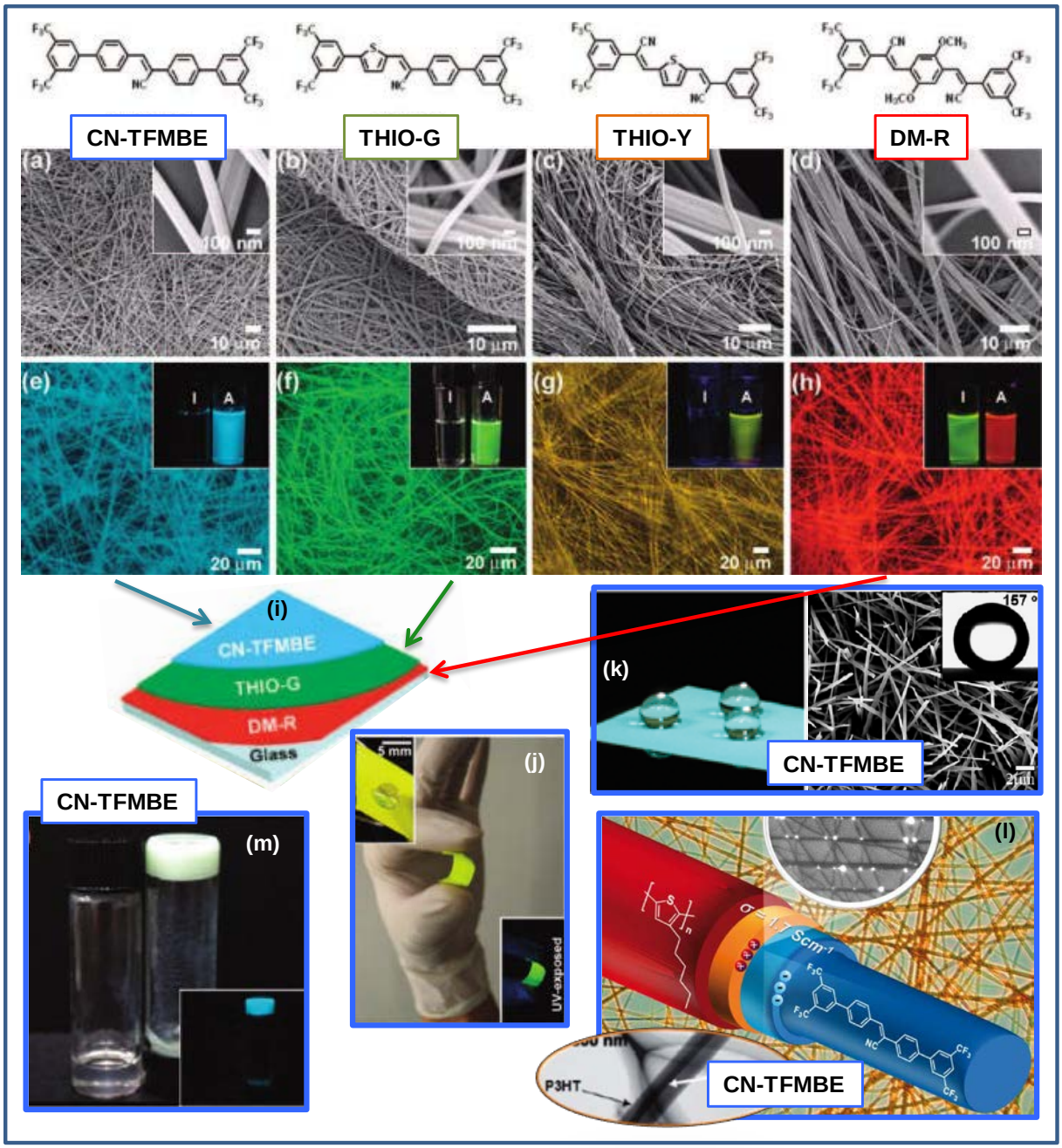

Figure 14. (a–d) SEM micrographs of fibers generated from 1,2-dichloroethane/methanol (9:1 v/v) solutions of different CSs and (e–h) their fluorescence microscopy images. Inset photos show the fluorescence colors of the isolated molecular state in THF solution (*I*) and the aggregated nanoparticle state in THF/water (1:4 v/v) (*A*), respectively. (i) Schema of color-tuned fluorescent nanofabrics obtained with these fibers deposited on glass substrates without wrinkling. (j) Flat (upper inset) and curved form of the THIO-G 2D-NFs (~100 μm) and fluorescence image of the curved form (lower inset). Adapted with permission.[21] Copyright 2009, American Chemical Society. (k) Water droplets on the vapor-deposited CN-TFMBE film (8.0 μm) and SEM images of the film surface. (l) Schema, optical microscopy and TEM images of a coaxial nanocable with interfacial charge-transfer layers formed by a CN-TFMBE core and P3HT shell. Adapted with permission.[114a, 149] Copyright 2008 and 2015, Royal Society of Chemistry. (m) Photo of CN-TFMBE (0.8 wt/vol %) dissolved in 1,2-dichloroethane at 60 °C (left vial) and the corresponding organogel at 20 °C (right vial). (inset) Fluorescence emission of the same samples under the UV light (365 nm). Adapted with permission.[112c] Copyright 2004, American Chemical Society,

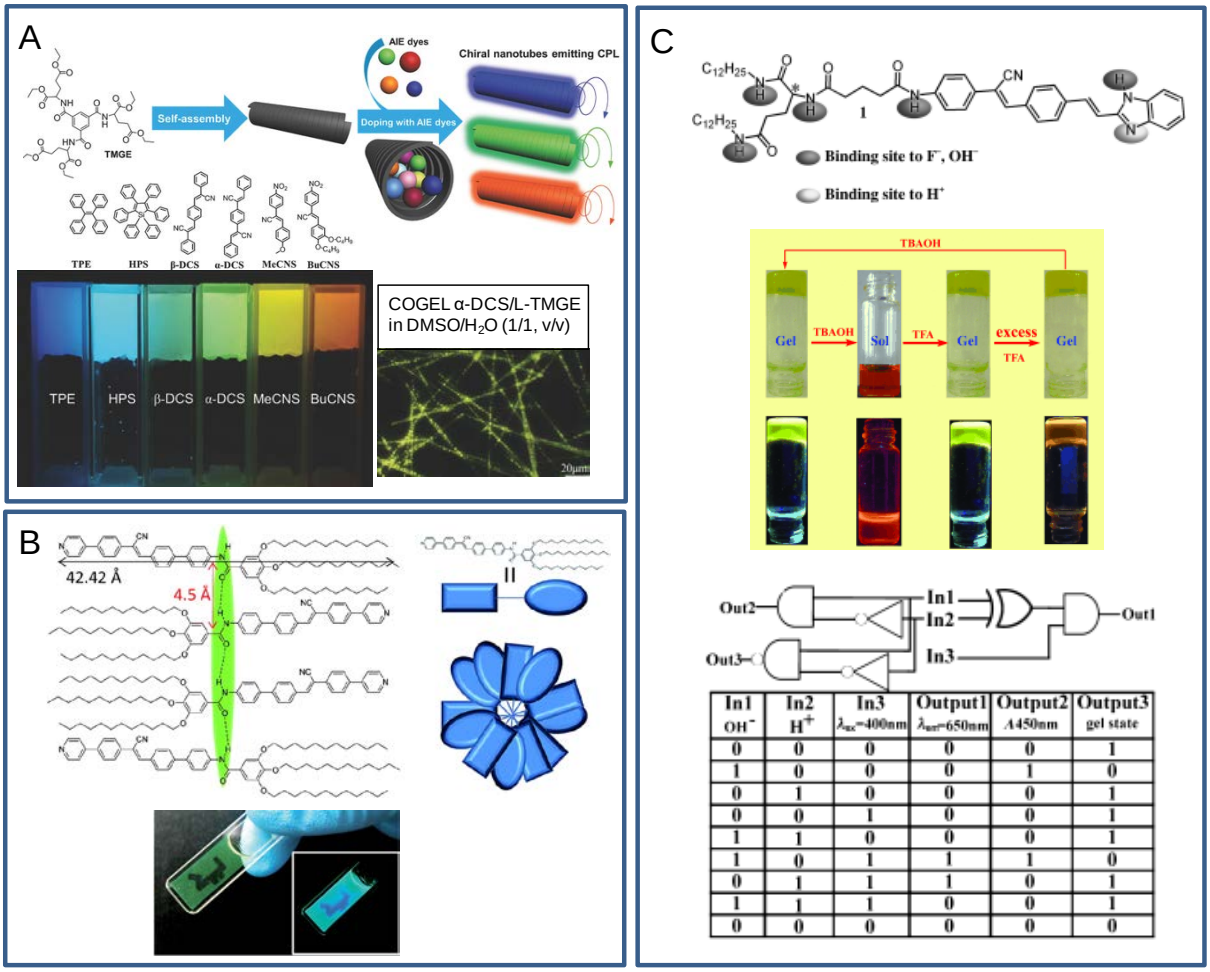

In1 OH^-	In2 H^+	In3 λ_{ex}=400nm	Output1 λ_{em}=650nm	Output2 A450nm	Output3 gel state
0	0	0	0	0	1
1	0	0	0	1	0
0	1	0	0	0	1
0	0	1	0	0	1
1	1	0	0	0	1
1	0	1	1	1	0
0	1	1	1	0	1
1	1	1	0	0	1
0	0	0	0	0	0

Figure 15. A: AIE-gen dyes encapsulated in chiral TMGE nanotubes yielding cogels that emit circularly polarized light (CPL), and fluorescence microscopy images showing nanotubes of a particular cogel composition. Adapted with permission.[152g] Copyright 2017, Wiley-VCH. **B:** Molecular structure of a CS gelator and arrangement in the gel and photograph of a photopatterning image in the gel state with a specific emblem, under ambient light. The fluorescence image is shown in the inset. Adapted with permission.[155g] Copyright 2014, The Royal Society of Chemistry. **C:** Molecular structure of a CS gelator, gel-to-sol transformation upon different chemical stimuli and truth table of a combination logic gate. Adapted with permission.[155c] Copyright 2012, Wiley-VCH.

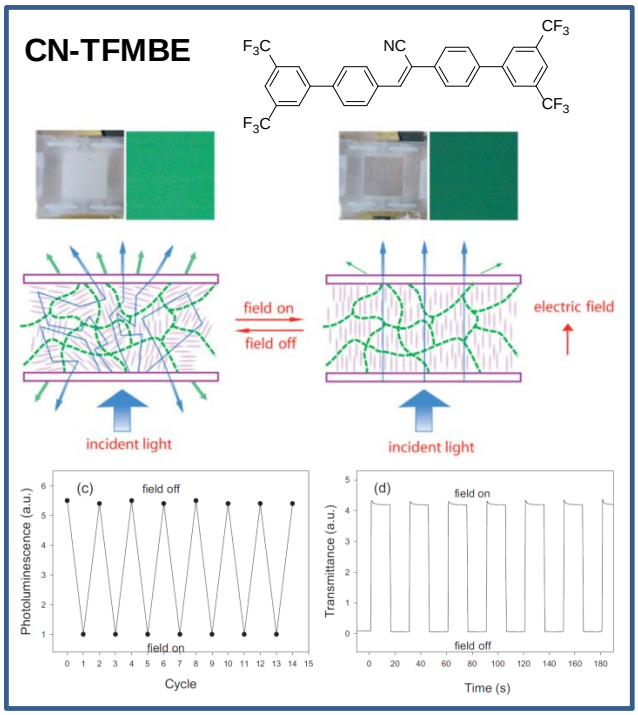

Figure 16. Nematic liquid crystal (LC) doped with CN-TFMBE gelator to obtain a fluorescent LC gel with electrically switchable photoluminescence. Differences in PL intensities at the field-off and field-on state are attributed to different numbers of gelator molecules excited by the incident light modulated by electric-field-induced orientation of LC molecules. Changes in transparency and in brightness of photoluminescence are shown by photos of the cell and by fluorescence microscopy images. Adapted with permission.[153a] Copyright 2006, Wiley-VCH.

Table 1. ASE properties and QY of DCS single crystals

Compound	QY	λ_{exc} (nm)	λ_{ASE} (nm)	Threshold (kW cm^{-2})	Ref
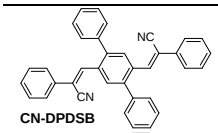 **CN-DPDSB**	0.70	355 470	470 470	39.5[42] 23.0[43]	[42] [43]
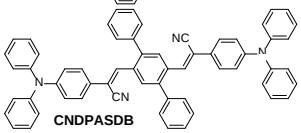 **CNDPASDB**	0.30	355 355 500 800	560 573 559 561	30.5 12.8 141.7 13x10^6	[47a] [47c] [47b] [48b]
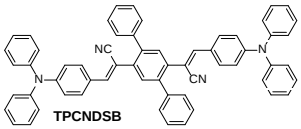 **TPCNDSB**	0.31	400 800	600 600	1.25x10^6 29x10^6	[49] [49]
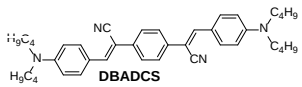 **DBADCS**	0.69	355 532	597 581 [a]	6x10^3 7x10^3	[51] [51]
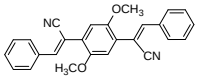 **α-MODCS**	0.66	355	495	7x10^3	[50a]
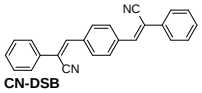 **CN-DSB**	-	355	482	36	[45]
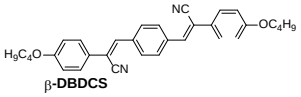 **β-DBDCS**	0.84	355 355	500 [b] 482 [a]	116 1.3	[50b] [50b]
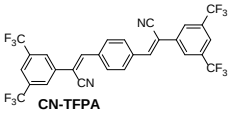 **CN-TFPA**	0.55	355	455 [b]	7x10^3	[53]

[a] Laser emission with a single crystal; [b] ASE in crystalline thin film

Table 2. Device characteristics of selected OLEDs containing thin film small molecule CS-based active layer.

Compound	Color (CIE)	L_{max} (cd m^2)	V_{on} (V)	EQE (%)	Device configuration [a)]	Ref
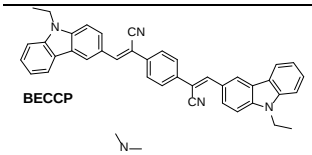 BECCP	Blue	50	8	-	ITO/BECCP/Al	[68a]
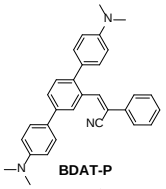 BDAT-P	Greenish-yellow	18300	-	3.83	ITO/NPB/MADN:BDAT-P(8%)/BPhen/Liq/Al	[70f]
	Warm white (0.36, 0.39)	26950	-	6.58	ITO/NPB/MADN:PFVtPh (8%)/CBP/CBP:Ir(pq)$_2$acac(8%)/CBP/MADN:BDAT-P(8%)/CBP/MADN:PFVtPh (8%)/TPBi/Liq/Al	[70k]
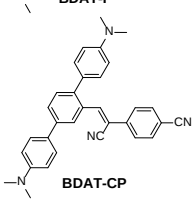 BDAT-CP	Yellow	14700	-	2.77	ITO/NPB/MADN:BDAT-CP(5%)/BPhen/Liq/Al	[70j]
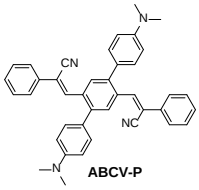 ABCV-P	Red	9784	-	3.19	ITO/NPB/MADN:ABCV-P(40%):NPB(10%):BAlq(10%)/BAlq/Liq/Al	[70l]
	White (0.284,0.396)	2500	-	2.45	ITO/NPB/mCP/mCP:FIrpic:ABCV-P(8%, 1%)/Bphen/Liq/Al	[70g]
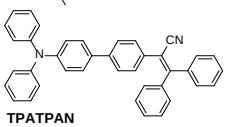 TPATPAN	Yellow	39419	3	3.47	ITO/NPB/TPATPAN/TPBi/LiF/Al	[33a]
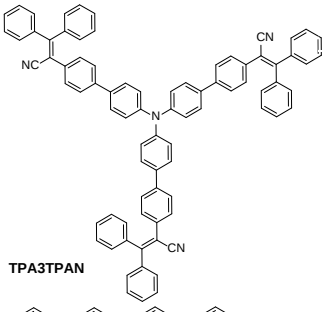 TPA3TPAN	Yellow	3101	7.4	2.18	ITO/TPA3TPAN/TPBi/LiF/Al	[69c]
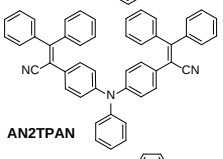 AN2TPAN	Yellow	11430	-	3.3	ITO/MeO−TPD/TCTA/AN2TPAN/Bphen/Liq/Al	[33c]
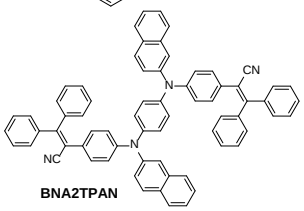 BNA2TPAN	Yellow	18820	-	4.2	ITO/MeO−TPD/TCTA/MADN:BNA2TPAN(3%)/Bphen/Liq/Al	[35]
	Orange (candle light)	2947	-	1.3	ITO/NPB/BNA2TPAN/Bphen/LiF/Al	[35]
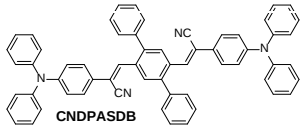 CNDPASDB	Orange	14667	5	-	ITO/NPB/CNDPADSB/TPBi/LiF/Al	[69b]
	White (0.36,0.38)	25350	3.5	-	ITO/NPB/TDPVBi/CNDPASDB/TPBi/LiF/Al	[69b]
	White (0.32,0.37)	22400	3.25	6.45	Solution processed: ITO/PEDOT:PSS/PVK/G0dendrimer:CNDPASDB/PFNR2:CsF/Ba/Al	[69d]
	Yellow	38828	3.1	5.3	ITO/HATCN/NPB/MADN:CNDPADSB(7%)/TPBi/LiF/Al	[69e]

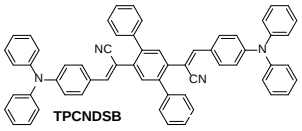 TPCNDSB	Green	23240	3.2	2	ITO/HATCN/NPB/MADN:TPCNDSB(7%)/TPBi/LiF/Al	[69e]

[a] Vacuum deposited films under otherwise noted. ITO (indium tin oxide), NPB (N,N′-bis(naphthalen-1-yl)-N,N′-bis(phenyl)benzidine), MADN (2-methyl-9,10-bis(naphthalen-2-yl)anthracene), BPhen (4,7-diphenyl-1,10-phenanthroline), Liq (8-quinolinolato lithium), PFVtPh (4′-[2-(2-diphenylamino-9,9-diethyl-9H-fluoren-7-yl)vinyl]-p-terphenyl), $Ir(pq)_2acac$ (Bis(2-phenylquinoline)(acetylactonate)iridium(III)), CBP (4,4′-Bis(9-carbazolyl)-1,1′-biphenyl), BAlq (Bis(8-hydroxy-2-methylquinoline)-(4-phenylphenoxy)aluminum), mCP (1,3-di(9*H*-carbazol-9-yl)benzene), FIrpic (bis[2-(4,6-difluorophenyl)pyridinato-C^2,*N*](picolinato)iridium(III)), TPBi (2,2′,2"-(1,3,5-Benzenetriyl)-tris(1-phenyl-1-*H*-benzimidazole)), MeO−TPD (*N*,*N*,*N*′,*N*′-Tetrakis(4-methoxyphenyl)benzidine), TCTA (Tris(4-carbazoyl-9-ylphenyl)amine), PEDOT:PSS (Poly(3,4-ethylenedioxythiophene)-poly(styrenesulfonate)), PVK (Poly(9-vinylcarbazole)), PFNR2 (poly[(9,9-bis(30-(N,N-dimethylamino)propyl)-2,7-fluorene)-alt-2,7-(9,9-dioctylfluorene)]), HATCN (1,4,5,8,9,11-hexaazatriphenylenehexacarbonitrile).

Table 3. Device characteristics of thin film transistors (TFTs) with DCS compounds.

Compound	Field effect electron mobility ($cm^2 V^{-1} cm^{-1}$)	On/off current ratio	Threshold voltage (V)	Ref
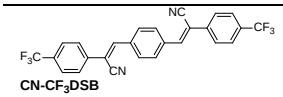 **CN-CF_3DSB**	0.068[b) c)] 0.127[b) c)] 0.016[d)] 0.04[b) e)]	6×10^5 - 8×10^5 1×10^5	38 - 48 29	[96a] [96d] [96b] [96b]
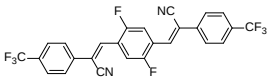 **CN-CF_3DSBF**	0.17[b)] 0.389[b) c)]	1×10^6 -	5 -	[96d] [96d]
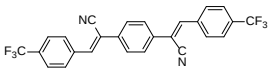 β-**CN-CF_3DSB**	$4.5\ 10^{-4}$ [d)] 0.13[b) e)] 0.30[b) f)]	2×10^5 2×10^5	36 21	[96b] [96b] [96b]
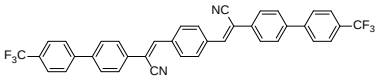 **CN-CF_3DPSB**	0.011[d)]	9×10^6	44	[96b]
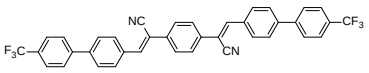 β-**CN-CF_3DPSB**	$9.2\ 10^{-4}$ [d) e)]	2×10^5	69	[96b]
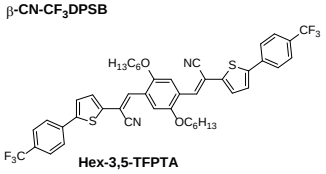 **Hex-3,5-TFPTA**	0.61[b) f)]	10^5-10^6	34	[96c]
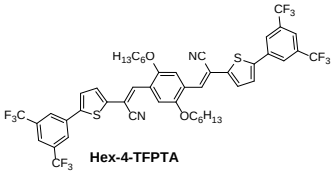 **Hex-4-TFPTA**	2.14[b) f)]	10^6-10^7	25	[96c]
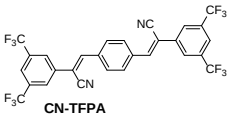 **CN-TFPA**	0.03 (G phase)[b) g)] 0.55 (B phase)[b) g)] 0.053[b) h)] 0.34[b)]	10^4 10^5 10^4-10^5 10^6	41 45 38 50	[54] [54] [54] [54]

[a)] Vacuum deposited films unless otherwise noted. [b)] Top contact configuration. [c)] Measurement under vacuum. [d)] Bottom contact configuration. [e)] HDMS treated surface. [f)] OTS treated. [g)] Layered crystalline films prepared by solvent evaporation crystal growth technique. [h)] Exfoliated B-phase layered film fabricated by mechanical cleavage method.

Table 4. Summary of two-photon (2PA) and three-photon (3PA) absorption parameters and properties evaluated for a selection of CS-based molecules.

Compound [a]	Cross-section [b] (2PA or 3PA, λ_{exc} nm)	SA / NSA [c] (solvent)	Applications	Ref
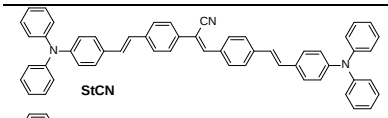 **StCN**	σ_2 : 2368 GM (2PA, 800 nm)	FON (50%w)	-	[124a]
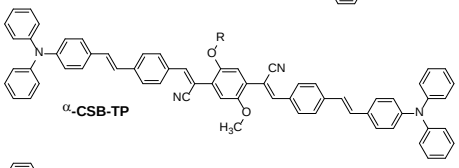 **α-CSB-TP**	σ_2 : 315 GM (2PA, 800 nm)	FON (90%w)		[125b]
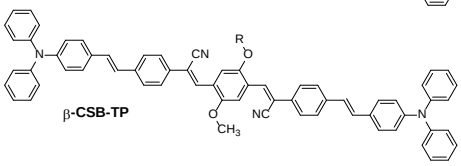 **β-CSB-TP**	σ_2 : 326 GM (2PA, 800 nm) σ_2 : 2500 GM (2PA, 800 nm)	FON (90%w) FON (water)	Blood plasma staining, and diffusion across the tumor vascular endothelium	[125b] [116b]
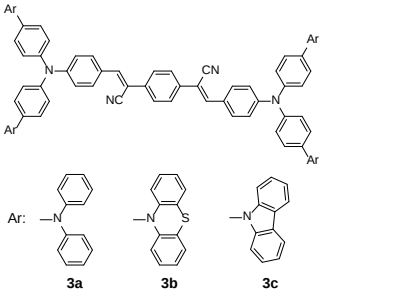 **3a** **3b** **3c**	σ_2 : 1016 GM σ_2 : 1484 GM σ_2 : 814 GM (2PA, 800 nm)	FON (90%w)		[68c]
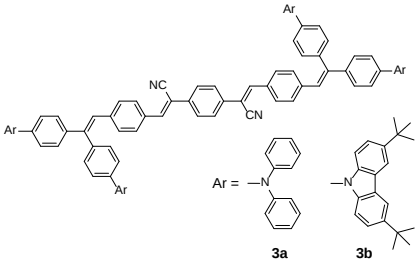 **3a** **3b**	σ_2 : 1363 GM σ_2 : 413 GM (2PA, 800 nm)	FON (90%w)		[110b]
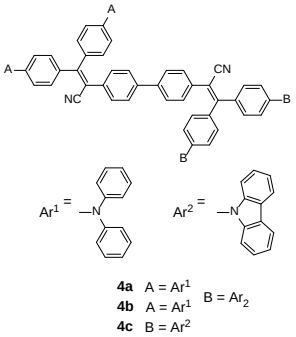 **4a** A = Ar^1 B = Ar_2 **4b** A = Ar^1 **4c** B = Ar^2	σ_2 : 511 GM σ_2 : 257 GM σ_2 : 180 GM (2PA, 800 nm)	FON (70%w)		[125a]
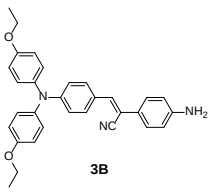 **3B**	σ_2 : 394 GM (2PA, 680-1050 nm)	MS (ethyl-acetate)	Cell imaging labeling the cytoplasm and actin regulatory protein in live cells (HepG2 Cells)	[124b]

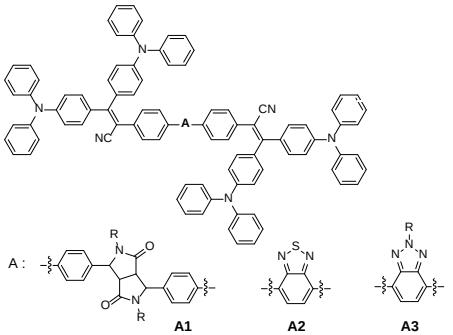	σ_2 : 702 GM σ_2 : 603 GM σ_2 : 293 GM (2PA, 800 nm)	FON (50-90%w)		[125c]
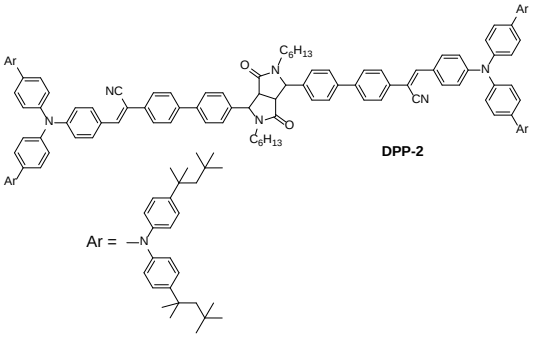	σ_2 : 8100 GM (2PA, 800 nm)	FON (90%w)	cell imaging and two-photon blood vasculature imaging (MCF7 Cells) Red/NIR emissive	[110d]
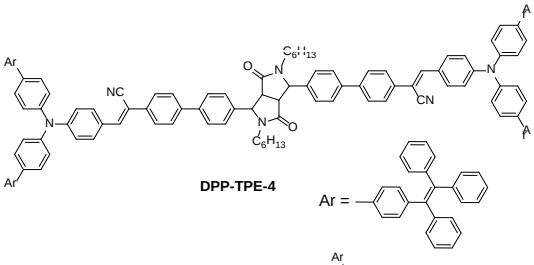	σ_2 : 1016 GM (2PA, 800 nm)	FON (70%w)		[125d]
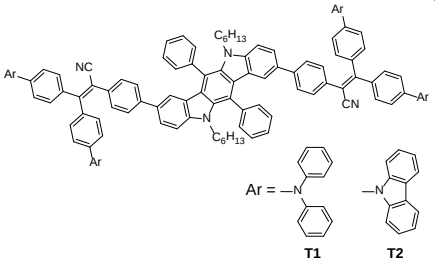	σ_2 : 867 GM σ_2 : 1300 GM (2PA, 800 nm)	MS (chloroform)	TPA-FONs: T1: deep yellow emission (50%w). T2: strong yellow emission (90%)	[114c]
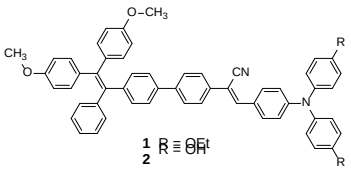	σ_2 : 4230 GM σ_2 : 4004 GM (2PA, 700-860 nm)	MS (toluene)	Cell imaging (HepG2 and U2OS Cells)	[123a]
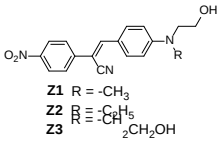	σ_2 : 1045 GM σ_2 : 3951 GM σ_2 : 7581 GM (2PA, 710 nm)	MS (DMF)		[127]
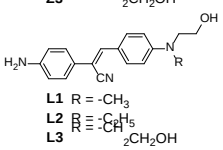	σ_2 : 890 GM σ_2 : 936 GM σ_2 : 3790 GM (2PA, 710 nm)	MS (DMF)	mitochondria-specific imaging (HepG2 Cells)	[127]

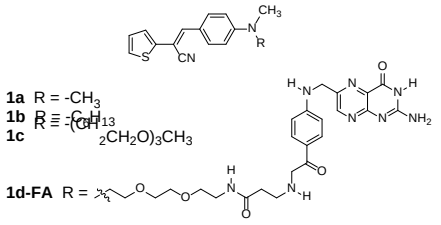 **1a** R = -CH_3 **1b** R ≡ -C_6H_{13} **1c** R = -$(CH_2CH_2O)_3CH_3$ **1d-FA** R =	σ_3 : 1.3 10^{-80} cm^6 s^2 $photon^{-2}$ □□□□□□□□σ_3 : 4.0 10^{-80} cm^6 s^2 $photon^{-2}$ □□□ σ_3 : 5.0 10^{-80} cm^6 s^2 $photon^{-2}$ σ_3 : 6.0 10^{-80} cm^6 s^2 $photon^{-2}$ (3PA, 1300 nm)	FON (DMSO/ w)	Cell imaging (HEK293 and MCF7 Cells) Enhanced targeting 1d-FA(FON) to HeLa cancer cells	[110c]

[a] Original labeling; [b] 2PA or 3PA cross-section parameter under excitation wavelength (λ_{exc}). [c] Cross-section parameter for self-assembled nanoparticle solutions [FON] or molecular solutions [MS] (solvent or aqueous mixtures).